Title
Discovery and Development of Small Molecule Sarcospan Enhancers for Duchenne Muscular Dystrophy

Author
Shu, Cynthia

Publication Date
2020

Peer reviewed|Thesis/dissertation

UNIVERSITY OF CALIFORNIA

Los Angeles

Discovery and Development of Small Molecule Sarcospan Enhancers for Duchenne Muscular Dystrophy

A dissertation submitted in partial satisfaction of the

requirements for the degree of Doctor of Philosophy

in Molecular Biology

by

Cynthia Shu

2020

ABSTRACT OF THE DISSERTATION

Discovery and Development of Small Molecule Sarcospan Enhancers

for Duchenne Muscular Dystrophy

by

Cynthia Shu

Doctor of Philosophy in Molecular Biology

University of California, Los Angeles, 2020

Professor Rachelle H. Crosbie, Chair

Duchenne muscular dystrophy (DMD) is a progressive muscle wasting disorder that affects 1 in every 5,700 males. Individuals with DMD experience muscle degeneration beginning in early childhood, wheelchair reliance by age 10-12, and succumb to cardiac or respiratory failure by the third decade of life. DMD is caused by mutations in the gene encoding for the dystrophin protein, which normally connects the muscle cell membrane to the extracellular matrix (ECM). Loss of this connection renders the membrane vulnerable to contraction-induced damage, resulting in muscle inflammation and degeneration. Restoring the adhesion between the cell and the ECM is a critical target in the development of urgently needed therapies for DMD.

The Crosbie group previously established that transgenic overexpression of the integral membrane protein sarcospan (SSPN) in murine models of DMD prevents muscle disease by increasing membrane localization of adhesion complexes that compensate for dystrophin. In this

thesis work, we describe the identification and development of chemical modulators of SSPN for the treatment of DMD. To develop a platform to efficiently screen large chemical libraries, we first created fluorescent and luminescent reporter cell lines to quantify SSPN gene activation. We created high-throughput cell-based assays and conducted a proof-of-concept screen on FDA approved drugs. The assay is capable of identifying drugs that increase SSPN gene and protein expression in dystrophin-deficient murine muscle cells. To identify compounds that could be developed into new chemical entities, we screened over 200,000 small molecules from curated libraries of lead-like drugs. We identified lead compounds that increased SSPN gene and protein expression in both dystrophin-deficient mouse and human DMD myotubes. The lead compound OT-9 improved *in vitro* membrane stability of dystrophin-deficient mouse and human myotubes. Knockdown of SSPN reduced the ability of OT-9 to increase membrane stability, demonstrating that OT-9 improved membrane stability through SSPN. *In vivo* studies revealed that OT-9 increased SSPN gene expression in the muscle of the murine model of DMD, indicating its therapeutic potential in a relevant animal model. Optimization of the lead compounds through structure-activity relationship analysis resulted in the creation of new chemical entities with improved solubility and activity. Future studies will focus on target identification and further optimization of the new chemical entities. In summary, this thesis work sets the path for the development of pharmacological modulators of SSPN for the treatment of DMD.

The dissertation of Cynthia Shu is approved.

Linda G. Baum

Michael F. Carey

M. Carrie Miceli

Melissa J. Spencer

Rachelle H. Crosbie, Committee Chair

University of California, Los Angeles

2020

Dedication

To my mother Ohn Chen Shu (1955-2004), whose admirable state of harmony and motivation to be a great mother, wife, daughter, and sister remained strong while she lived with muscular dystrophy.

To my family who has been there since day one and who I am grateful to share this lifetime with.

To my partner Daniel Kaplan who encourages me to always aim high and who is truly a pillar in my life.

To the brilliant and kind-hearted individuals who I am lucky to have as friends.

Table of Contents

List of Figures and Tables

Chapter 1: Introduction

Chapter 2: Development of a high-throughput screen to identify small molecule enhancers of sarcospan for the treatment of Duchenne muscular dystrophy

Chapter 4: Second generation new chemical entity enhancers of sarcospan improve solubility and activity

Acknowledgements

Thank you to Dr. Rachelle Crosbie for providing exceptional mentorship and continuously pushing me to grow and improve throughout this incredible experience of obtaining a Ph.D. Thank you to my committee members Dr. Melissa Spencer, Dr. Linda Baum, Dr. Carrie Miceli, and Dr. Michael Carey for their direction and pushing me to deepen my research. Thank you to all the current and past members of the Crosbie Lab for their support.

Thank you to Robert Damoiseaux for guiding assay design and providing core services at the Molecular Screening Shared Source (MSSR) and to MSSR staff members Bobby Tofig, Bryan France, Constance Au, and David Austin. Thank you to Liubov Parfenova, Ekaterina Mokhonova, Judd R. Collado, and Ariana N. Kaxon-Rupp for their essential roles in the drug discovery team. Thank you to Varghese John, Jesus Campagna, and Barbara Jagodzinska of the Drug Discovery Lab for providing the medicinal chemistry and chemical engineering expertise we needed to balance our biology team. Thank you to members of the Center for Duchenne Muscular Dystrophy for both their guidance and friendship throughout the years. Thank you to the Muscle Cell Biology, Pathogenesis, and Therapeutics Training Grant (NIH T32 AR065972) for continuous support of my work throughout my Ph.D.

Chapter 2 was originally published in Skeletal Muscle: Shu C, Kaxon-Rupp AN, Collado JR, Damoiseaux R, Crosbie RH. Development of a high-throughput screen to identify small molecule enhancers of sarcospan for the treatment of Duchenne muscular dystrophy. *Skel. Muscle.* (2019) 9:32. doi: 10.1186/s13395-019-0218-x. C.S. designed the screening assays, including creation of stable cell lines. C.S. performed all experiments including high-throughput screening and *in vitro* studies with assistance from A.N.R. during cell culture and imaging. C.S. conducted all data analysis, prepared all figures and wrote the manuscript. A.N.R. and J.R.C. performed

immunofluorescence, imaging, and image analysis for fusion index. R.D. designed assays, screening cascade, and provided core services for screening. R.H.C. conceived of the project and consulted on all experiments, data analysis, figures, and manuscript drafting.

Chapter 3 is currently undergoing peer review and contains work performed by Cynthia Shu, Liubov Parfenova, Ekaterina Mokhonova, Judd R. Collado, Robert Damoiseaux, Jesus Campagna, Varghese John, and Rachelle H. Crosbie.

Chapter 4 is currently unpublished and reflects work performed by Cynthia Shu, Liubov Parfenova, Ekaterina Mokhonova, Judd R. Collado, Jesus Campagna, Barbara Jagodzinska, Varghese John, and Rachelle H. Crosbie.

Support for this work was provided by the Muscle Cell Biology, Pathogenesis, and Therapeutics Training Grant (NIH T32 AR065972), Pilot and Feasibility Seed Grant program (NIH/NIAMS P30 AR057230), UCLA Department of Integrative Biology & Physiology Eureka Scholarship, Muscular Dystrophy Association (MDA 274143; Venture Philanthropy Program), NIH/NIAMS (R01 AR048179), and NIH NHLBI (R01 HL126204).

Curriculum Vitae

Education

2006-10 B.S. in Developmental and Cell Biology from the University of California, Irvine

Professional Research

2011-14 FutureCeuticals (Irvine, CA)

Research Support

2018-20 Muscular Dystrophy Association Venture Philanthropy Program
2018-19 Eureka Scholarship
2016-19 NIH T32 "Muscle Cell Biology, Pathogenesis, and Therapeutics Grant"
2015-16 NIH T32 "Virology and Gene Therapy Training Grant"

Patents

3/1/2018 Crosbie RH, **Shu C**, John V, Alam MP. "Small molecule therapy for Duchenne muscular dystrophy". Invention disclosure, case number: 2018-598.

Publications

1. **Shu C**, Kaxon-Rupp AN, Collado JR, Damoiseaux R, Crosbie RH. Development of a high-throughput screen to identify small molecule enhancers of sarcospan for the treatment of Duchenne muscular dystrophy. *Skel. Muscle.* (2019) 9:32.
2. Phan AQ, Lee J, Oei M, Flath C, Hwe C, Mariano R, Vu T, **Shu C**, Dinh A, Simkin J, Muneoka K, Bryant SV, Gardiner DM. (2015) "Positional information in axolotl and mouse limb extracellular matrix is mediated via heparan sulfate and fibroblast growth factor during limb regeneration in the axolotl (Ambystoma mexicanum)" Regeneration. 2(4):182-201.
3. *Reyes-Izquierdo T, Pietrzkowski Z, Argumedo R,* ***Shu C****, Nemzer B, Wybraniec S.* (2014). Betalain-rich red beet concentrate improves reduced knee discomfort and joint function: a double blind, placebo-controlled pilot clinical study**.** *Nutr. Diet. Suppl.* 6:9-13.
4. *Reyes-Izquierdo T, Phelan MJ, Keller R,* ***Shu C****, Argumedo R, Pietrzkowski Z.* (2014). Short-Term efficacy of a combination of glucosamine and chondroitin sulfate compared to a combination of glucosamine, chondroitin sulfate and calcium fructoborate (CFB) on improvement of knee discomfort in healthy subjects. A comparative, double-blind, placebo controlled acute clinical study. *J. Aging. Res. Clin. Practice* 3(4): 223-228.
5. Pietrzkowski Z, Phelan MJ, Keller R, **Shu C**, Argumedo R, Reyes-Izquierdo T. (2014). Short-term efficacy of calcium fructoborate on subjects with knee discomfort: a comparative, double-blind, placebo-controlled clinical study. *Clin. Interv. Aging.* 9:895-9.
6. Reyes-Izquierdo T, Nemzer B, Argumedo R, **Shu C**, Hunyh L, Pietrzkowski Z. (2013). Dermaval inhibits glucose-induced neutrophil elastase activity in healthy subjects. *Nutr. Diet. Suppl.* 6: 1-7.
7. Reyes-Izquierdo T, Nemzer B, Argumedo R, **Shu C**, Hunyh L, Pietrzkowski Z. (2013). Effect of the Dietary Supplement elevATP on Blood ATP Level: An Acute Pilot Clinical Study. *J. Aging. Res. Clin. Practice* 2(2): 178-184.
8. Reyes-Izquierdo T, Argumedo R, **Shu C**, Nemzer B, Pietrzkowski Z. (2013). Stimulatory Effect of Whole Coffee Fruit Concentrate Powder on Plasma Levels of Total and Exosomal

Brain-Derived Neurotrophic Factor in Healthy Subjects: An Acute Within-Subject Clinical Study. *Food and Nutr. Sci.* 4(19): 984-990.

9. Reyes-Izquierdo T, Nemzer B, **Shu C**, Hunyh L, Argumedo R, Keller R, Pietrzkowski Z. (2012). Modulatory effect of coffee fruit extract on plasma levels of brain-derived neurotrophic factor in healthy subjects. *Brit. J. of Nutr.* 110(3): 420-425.

10. Reyes-Izquierdo T, Nemzer B, Gonzalez AE, Zhou Q, Argumedo R, **Shu C**, Pietrzkowski Z. (2011). Short-term Intake of Calcium Fructoborate Improves WOMAC and McGill Scores and Beneficially Modulates Biomarkers Associated with Knee Osteoarthritis: A Pilot Clinical Double-blinded Placebo-controlled Study. *Am. J. Biomed. Sci*. 4(2): 111-122.

11. Reyes-Izquierdo T, Nemzer B, Zhou Q, Argumedo R, **Shu C**, Jimenez R, Pietrzkowski Z. (2011). Acute Effect of MCRC on Selected Blood Parameters – A Placebo-controlled Acute Clinical Study. *Am. J. Biomed. Sci*. 4(1): 36-49.

12. Sun L, Chen M, Yang H, Wang T, Liu B, **Shu C**, Gardiner DM. (2011). Large scale gene expression profiling during intestine and body wall regeneration in the sea cucumber Apostichopus japonicus. *Comp. Biochem. Physiol. Part D Genomics Proteomics* 6(2): 195-205.

13. Shu C. (2010). Inhibition of Regenerative Responses in the Salamander Limb by Extracellular Matrix. *Journal of Undergraduate Research in the Biological Sciences, 2009-2010.*

Select Presentations

1. Shu C, Parfenova L, Mokhonova K, Campagna J, Damoiseaux R, John V, Crosbie RH. (2020, February). "Small molecular enhancers of sarcospan for the treatment of Duchenne muscular dystrophy". Center for Duchenne Muscular Dystrophy Muscle Cell Biology and Disease Annual Scientific Retreat, Los Angeles, CA. Oral presentation.
2. Shu C, Damoiseaux R, Crosbie-Watson RH. (2018, June). "Development of a high-throughput screen to identify small molecule enhancers of sarcospan for the treatment of Duchenne muscular dystrophy". UCLA Biomedical/Life Science Innovation Day, Los Angeles, CA. Poster presentation.
3. Shu C, Damoiseaux R, Alam MP, John V, Crosbie-Watson RH. (2018, June). "High throughput screening reveals small molecule enhancers of sarcospan for the treatment of Duchenne muscular dystrophy". New Directions in Biology and Disease of Skeletal Muscle. New Orleans, LA. Poster presentation.
4. Shu C. (2017, May). *Developing a novel treatment for muscular dystrophies via pharmacological upregulation of the muscle adhesion protein sarcospan*. Seminar talk at the Molecular Biology Institute Student Seminar Series. University of California, Los Angeles.
5. Shu C. (2015, February). *Sarcospan overexpression as a novel approach to treat Duchenne muscular dystrophy.* Poster presentation at the Center for Duchenne Muscular Dystrophy Annual Scientific Retreat. University of California, Los Angeles.
6. Shu C. (2010, April). *Inhibition of Regenerative Responses in the Salamander Limb by Extracellular Matrix*. Oral presentation at the Excellence in Research Symposia. University of California, Irvine.

Chapter 1: Introduction

Duchenne muscular dystrophy

The muscular dystrophies are a group of genetic diseases characterized by progressive loss of muscle strength. The most common form in children is Duchenne muscular dystrophy (DMD). DMD is an X-linked condition that affects every 1 in 5,700 males and is considered the most common, fatal, inherited disease in children.[24] Patients with DMD experience progressive muscle weakness beginning in early childhood and become wheelchair reliant between age 10-12. Approximately 90% of patients develop cardiomyopathy and respiratory complications, resulting in premature death between age 20-30.[24, 25]

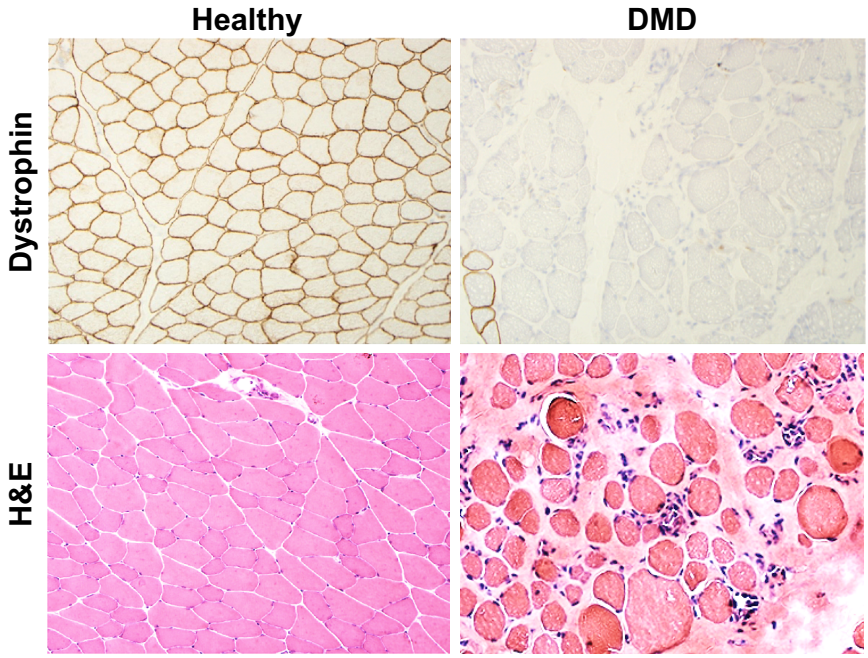

Figure 1-1. Skeletal muscle histopathology of DMD. Top left: In healthy muscle, dystrophin is distributed uniformly at the sarcolemma as seen by immunostaining of a muscle cross section. Top right: DMD muscle lacks dystrophin, except for revertant fibers as seen in the lower left-hand corner. Bottom left: Hematoxylin and eosin (H&E) staining of healthy muscle shows densely packed, uniformly sized myofibers. Bottom right: DMD muscle undergoes inflammation as indicated by the immune cell infiltrates. The myofibers go through asynchronous cycles of regeneration and degeneration leading to variable myofiber sizes. In the middle to late stages of the DMD, the muscle becomes fibrotic as seen with the increased endomysial area. Figure adapted from[10, 11].

DMD is caused by loss of the dystrophin protein, which stabilizes the cardiac and skeletal muscle cell membrane during contractions.[26] In healthy individuals, dystrophin localizes to the intracellular surface of myofibers (Figure 1-1, top left). In individuals with DMD, dystrophin is absent (Figure 1-1, top right) leading to contraction-induced damage, inflammation, degeneration, and fibrosis (Figure 1-1, bottom). In the early stages of DMD, satellite cells regenerate damaged myofibers leading to asynchronous cycles of regeneration and degeneration.[27] However, as the disease progresses, the population of satellite cells becomes depleted and the muscle loses its ability to regenerate, instead undergoing fibrosis and replacement with adipose tissue.

The adhesion complexes in muscle

The gene causative of DMD was identified in 1985 by Louis Kunkel at Harvard University.[28] Soon after, the 425 kDa protein product of the gene was identified as dystrophin and confirmed to be absent in muscle from DMD patients.[26] Since these early discoveries, dystrophin has been extensively studied to understand its basic function. The work of several groups demonstrated that dystrophin associates with numerous integral and peripheral membrane proteins to form the dystrophin-glycoprotein complex (DGC).[29, 30] The DGC provides a physical axis of connection between the actin cytoskeleton, muscle cell membrane (sarcolemma), and the extracellular matrix (ECM).[29, 30] This connection is critical to stabilize the membrane during muscle contractions. In DMD patients, both dystrophin and the DGC are absent at the sarcolemma, leading to contraction-induced membrane damage and subsequent muscle degeneration (Fig. 1-2).[31] Within the DGC, dystrophin interacts with the actin cytoskeleton at its N-terminus and the integral membrane protein β-dystroglycan (β-DG) at its C-terminus.[32] β-DG associates with α-DG, a peripheral protein that binds to laminin in the ECM. The transmembrane proteins sarcospan

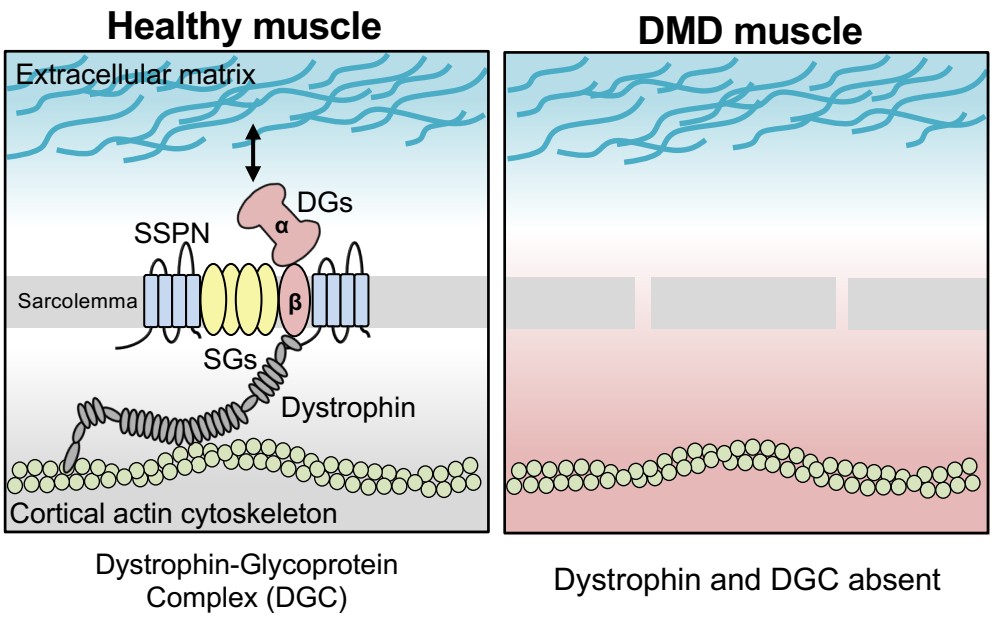

Figure 1-2. The dystrophin-glycoprotein complex is critical for membrane integrity. The dystrophin-glycoprotein complex (DGC) is composed of several proteins including dystrophin, sarcospan (SSPN), the sarcoglycans (SGs), and the dystroglycans (DGs). In healthy muscle, the DGC localizes to the sarcolemma and connects the actin cytoskeleton to the extracellular matrix to stabilize the muscle during contractions. In DMD muscle, the DGC does not localize to the membrane due to the lack of dystrophin, leading to contraction-induced damage and muscle degeneration. Figure adapted from[4].

and the sarcoglycans also contribute to the membrane stabilization provided by the DGC (Fig. 1-2).[33, 34]

In addition to the DGC, the utrophin-glycoprotein complex (UGC) and the α7β1D-integrin complex facilitate adhesion between the sarcolemma and ECM (Fig. 1-3).[35-37] The UGC is highly similar to the DGC, except that utrophin, the 395 kDa autosomal paralogue of dystrophin, takes the place of dystrophin. Another distinguishing feature is that while the DGC is expressed uniformly around the sarcolemma, the UGC is expressed at the neuromuscular and myotendinous junctions in healthy muscle.[38] In DMD muscle, the UGC is redistributed extra-synaptically across the sarcolemma, suggesting the existence of a naturally occurring compensatory mechanism in the absence of the DGC.[39] Kay Davies at the University of Oxford was the first to demonstrate rescue of the *mdx* murine of DMD through transgenic overexpression of utrophin. This discovery

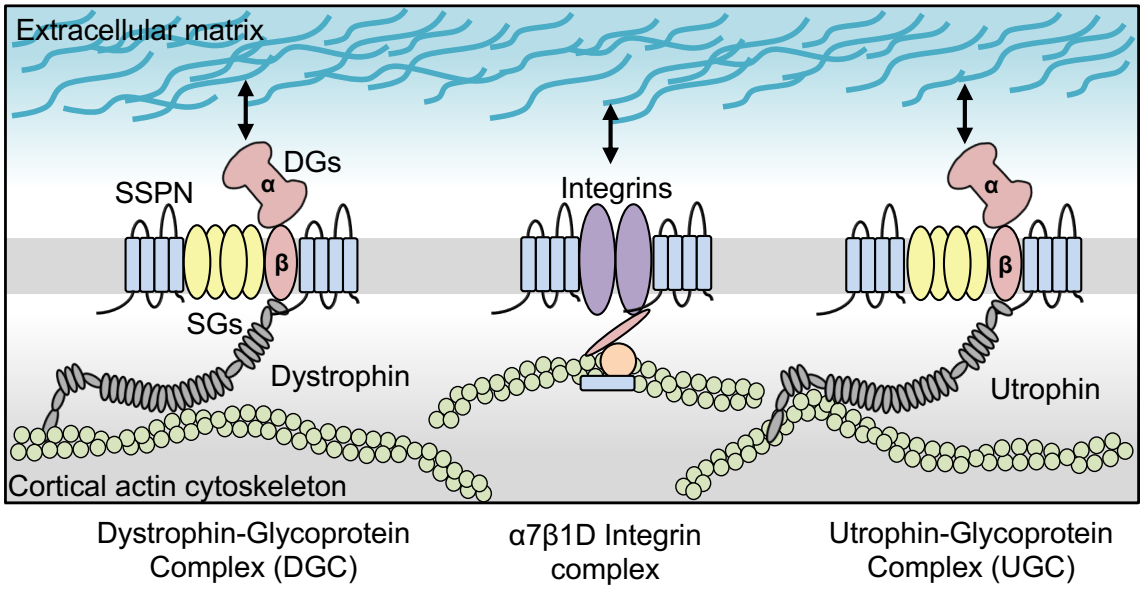

Figure 1-3. The three major adhesion complexes in skeletal muscle. Adhesion complexes create a physical axis of connection between the actin cytoskeleton, sarcolemma, and extracellular matrix to stabilize the muscle during contractions. Skeletal muscle contains three major adhesion complexes: the dystrophin-glycoprotein complex (DGC), the α7β1D-integrin complex and the utrophin-glycoprotein complex (UGC).[5,21,16] Mutations in adhesion protein genes lead to over 30 forms of muscular dystrophy including DMD.

revealed a potential therapeutic approach for DMD and set the path for following transgenic rescue studies.

The α7β1D-integrin complex is a laminin receptor that mediates cell signaling pathways for cell adhesion, proliferation, and migration. Similar to the UGC, the α7β1D-integrin complex is increased in muscle of DMD patients.[40] Transgenic overexpression of the α7β1D-integrin complex in the *mdx* mouse model restores membrane adhesion and prevents muscle pathology.[41]

Transgenic overexpression of sarcospan rescues *mdx* mouse model of DMD

Sarcospan (SSPN) is a 25 kDa integral membrane protein expressed in multiple tissues, including skeletal and cardiac muscle.[21] Through biochemical purification studies, SSPN was determined to be a component of the three major adhesion complexes.[5, 7] Mutagenesis analysis

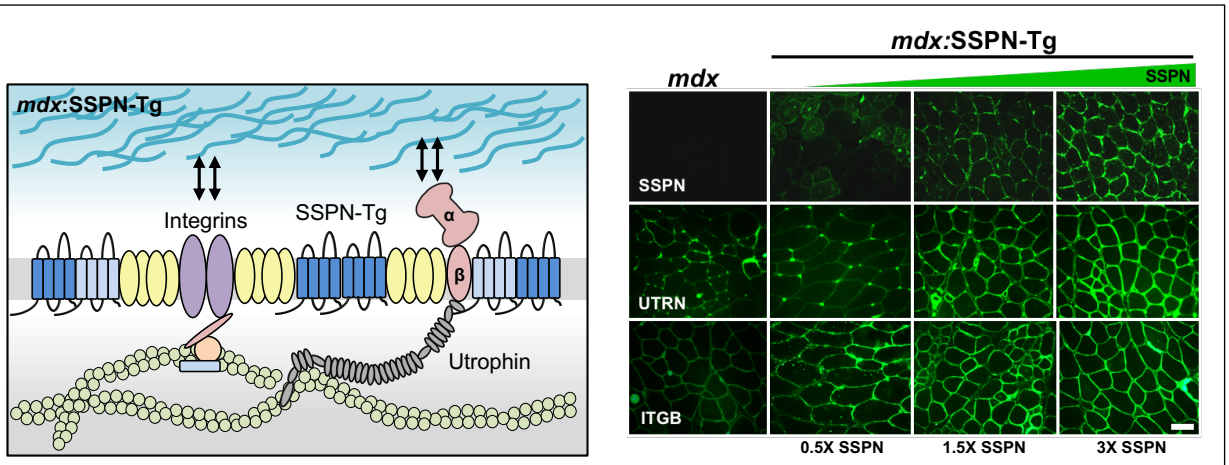

Figure 1-4. Sarcospan overexpression increases membrane localization of compensatory adhesion complexes. Mice that overexpress sarcospan (SSPN) were crossed with *mdx* mice, resulting in the *mdx*:SSPN-Tg line. Overexpression of SSPN increases the sarcolemmal localization of the utrophin-glycoprotein complex and the α7β1D-integrin complex (left). Immunofluorescence staining of skeletal muscle sections from *mdx* and *mdx*:SSPN-Tg mice expressing 0.5, 1.5, and 3X levels of SSPN demonstrate a dose-sensitive increase in compensatory adhesion complexes as SSPN levels increase (right, adapted from[7, 8]). Scale bar = 50 μm.

revealed that SSPN strongly associated with the sarcoglycans and contains multiple oligomer interaction sites, suggesting its role as a scaffold for protein complexes.[42] The early biochemical studies lead our group to hypothesize that increasing levels of SSPN increases adhesion complex formation at the membrane. To test this, our group generated SSPN-Tg mice that overexpress SSPN under control of the α-actin promoter, which is active in striated muscle. The SSPN-Tg line was crossed with the commonly used *mdx* line, which contains a frameshift mutation in exon 23 of the *DMD* gene. The resulting *mdx*:SSPN-Tg lines expressing various levels of SSPN have since been thoroughly characterized on the biochemical, cellular, tissue, and organism level. [4-7, 43, 44]

Overexpression of SSPN increases the extra-synaptic, sarcolemmal localization of the UGC and the α7β1D-integrin complex in a dose-dependent manner (Fig. 1-4). Characterization of the 0.5, 1.5, and 3-fold overexpressing lines revealed that the 3-fold overexpression line was rescued from muscle pathology.[7, 8] This suggests that amount of SSPN overexpression needed for

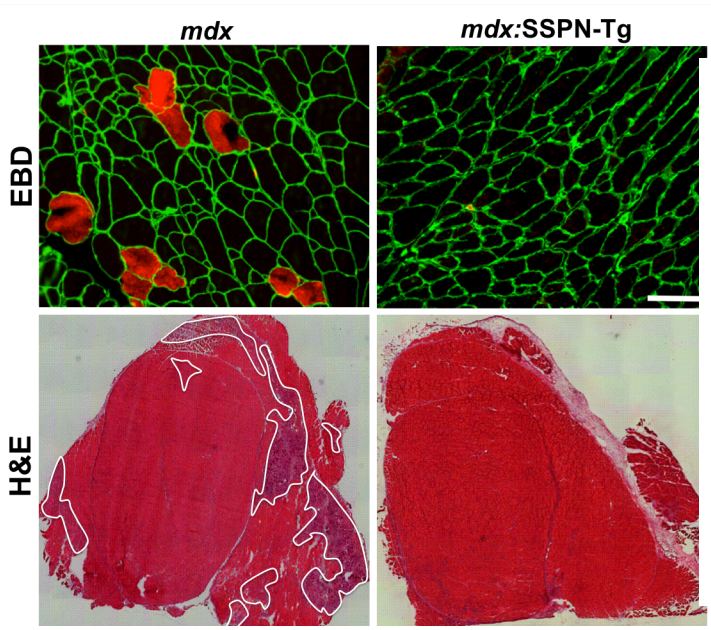

Figure 1-5. Sarcospan overexpression reduces muscle cell membrane damage and muscle degeneration. Cross sections of quadriceps from mice injected with Evan's blue dye (EBD, red), which only stains damaged myofibers, reveals a reduction in damage with SSPN overexpression (laminin, green) (top). Cross sections of quadriceps from *mdx* mice stained with hematoxylin and eosin (H&E) reveal areas of necrosis, outlined in white (bottom left). Quadriceps from *mdx*:SSPN-Tg display WT-like muscle histology (bottom right). Figures adapted from[4, 5]. Scale bar = 100 μm.

a therapeutic benefit is above 1.5-fold. In subsequent studies, mouse lines overexpressing 30-fold levels of SSPN were created and found to rescue *mdx* mice without negative side effects, indicating high levels of SSPN are safe in mice.[4] Analysis of muscle from *mdx* and *mdx*:SSPN-Tg mice revealed that SSPN overexpression protects the sarcolemma from damage, as determined by a tracer uptake assay (Fig. 1-5, top).[4] The membrane stabilization reduces muscle degeneration and necrosis throughout the muscle (Fig. 1-5, bottom)[5]. The benefits on the tissue level result in a significant reduction in serum creatine kinase levels, indicating an improvement in muscle integrity throughout the body (Fig. 1-6A). Importantly, SSPN overexpression improves respiratory and cardiac function, the two main causes of death in patients with DMD (Fig. 1-6B-C). SSPN overexpression protects the hearts of *mdx*:SSPN-Tg mice subjected to cardiac stress using isoproterenol-mediated activation of β-adrenergic receptors.[6] The muscle and system-specific improvements lead to a restoration of post-exercise activity levels, demonstrating the body-wide benefits of SSPN therapy (Fig. 1-6D).

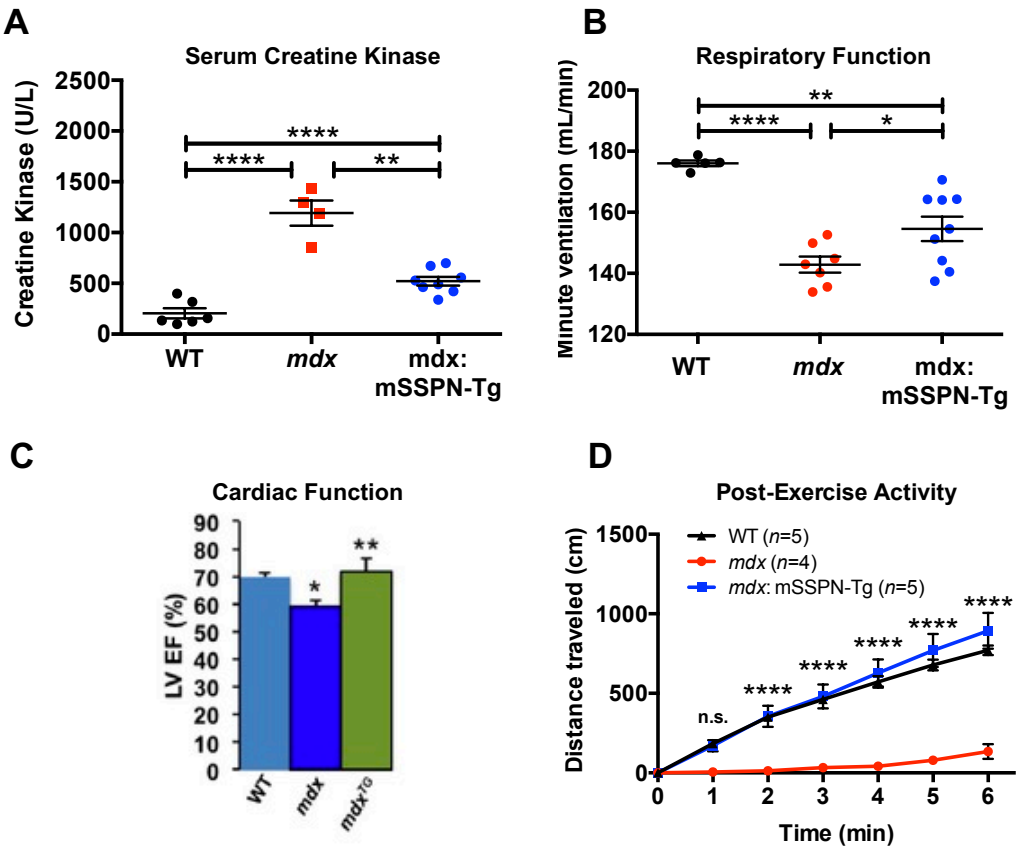

Figure 1-6. Sarcospan overexpression reduces serum creatine kinase and improves respiratory, cardiac, and activity parameters in *mdx* mice. (A) SSPN reduces serum creatine kinase, a clinical biomarker of muscle damage. (B) SSPN improves respiratory function as measured by minute ventilation, the volume of air inhaled and exhaled per minute. (C) SSPN improves cardiac function as measured by left ventricular ejection fraction (LV EF). (D) SSPN restores post-exercise activity levels of *mdx* mice, indicating a whole body rescue. Figures adapted from[4, 6].

Approved therapies for DMD

As of 2020, there are three FDA approved treatments for DMD (Table 1-1). In 2016, Eteplirsen became the first drug approved to treat DMD. Eteplirsen is an antisense oligonucleotide developed by Sarepta Therapeutics for use in patients amenable to exon 51 skipping (14% of DMD patients). In clinical trials, Eteplirsen increased dystrophin protein to approximately 1% of normal levels, preserved muscle strength, and delayed respiratory decline.[14, 45] The following year, Deflazacort, an immunomodulatory corticosteroid developed by PTC Therapeutics, received FDA

Drug	Date Approved	Mechanism of Action	Clinical Outcomes
Eteplirsen	2016	Morpholino targeting exon 51 of *DMD* to restore reading frame	Increased dystrophin to ~1% of normal levels Preserved muscle strength[13] Delayed respiratory decline[14]
Deflazacort	2017	Immunomodulating corticosteroid	Improved motor function Preserved muscle strength Delayed disease progression by ≥1 year[15, 16]
Golodirsen	2019	Morpholino targeting exon 53 of *DMD* to restore reading frame	Increased dystrophin to ~1% of normal levels[17]

Table 1-1. FDA approved therapies for DMD as of 2020.

approval based on clinical trials showing improved motor function, preserved muscle strength, and delayed disease progression.[15] In 2019, the FDA approved Golodirsen, an antisense oligonucleotide also developed by Sarepta Therapeutics for use in patients amenable to exon 53 skipping (7.7% of DMD patients). The approval was based solely on clinical trial data showing an increase in dystrophin to 1% of normal levels, with the anticipation that Golodirsen will provide the same clinical benefits as Eteplirsen.[17]

The FDA approval of these treatments was a significant milestone in the development of therapies of DMD. However, there remains an urgent need for more effective therapies that can further delay the disease and improve the quality of life of individuals with DMD. Various modalities are currently being explored including use of antibodies, gene therapy, small molecules, biologics, and copolymers. A summary of select treatments currently in late pre-clinical or clinical development is presented in Table 1-2 and demonstrates the broad range of approaches being investigated. Antibody-based modalities to inhibit myostatin, an inhibitor of muscle growth, have been tested in clinical trials with negative results. Currently, FibroGen is developing pamrevlumab, an antibody that inhibits the pro-inflammatory connective tissue growth factor (CTGF). Although gene therapy using CRISPR/Cas9 for gene correction is still in development,

Modality	Drug	Company	Mechanism of Action
Antibody	Pamrevlumab	Fibrogen	Anti-fibrotic; inhibitor of pro-inflammatory CTGF
Gene therapy	CRISPR/Cas9	Exonics	Correction of genetic mutation in *DMD* gene
	GALGT2 AAV	Nationwide Children's Hospital	Delivery of GALGT2 to increase glycosylation of alpha-dystroglycan
	Micro-dystrophin AAV	Sarepta Therapeutics, Solid Biosciences	Delivery of truncated dystrophin gene
Small molecule	Edasalonexent	Catabasis Pharmaceuticals	Immunomodulatory NF-kB inhibitor
	AT-300	Akashi Therapeutics	Calcium channel inhibitor to reduce muscle pathology
	DT-200		Modulator of androgen receptors to induce muscle growth
	HT-100		Anti-fibrotic and anti-inflammatory
Biologic	Stem cells	Stem Cells Arabia	Transplantation of healthy or corrected stem cells
	Biglycan	Tivorsan Pharmaceuticals	Proteoglycan that increases utrophin expression
	Laminin 111	StrykaGen	Promotes muscle regeneration and stem cell support
Copolymer	Poloxamer 188 NF	Phrixus Pharmaceuticals	Stabilizes muscle membrane

Table 1-2. Select DMD treatments in late pre-clinical and clinical development.

gene replacement strategies in clinical trials show significant promise. In a small clinical trial testing micro-dystrophin delivery by AAV, Sarepta Therapeutics reported an 81% increase in micro-dystrophin protein levels and a steady reduction in serum creatine kinase, a clinical biomarker of muscle damage, after 270 days of treatment.[46] One of the main uncertainties of viral delivery methods is the ability of patients to tolerate redosing as the current AAVs do not target satellite cells efficiently, leading to loss of the micro-dystrophin gene with myofiber turnover. Catabasis Pharmaceuticals and Akashi Therapeutics are leading the way in small molecule-based therapies, including Edasolonexent, an NF-kB inhibitor, and AT-300, DT-200, and HT-100, which target calcium channels, androgen receptors, and inflammation, respectively. In the biologics field, development of stem cell-based therapies faces many challenges including reliable

reprogramming of induced pluripotent stem cells and low survival rates of transplanted cells (for review see[47]).

High-throughput screening to discover small molecule DMD therapies

Small molecule modalities comprise over 80% of all approved drugs in part due to their ability to bypass the limitations of delivery, immune responses, repeat dosages that exist with viral or cell-based therapies.[48] In both academia and the private sector, small molecules are commonly discovered through high-throughput screening (HTS), a drug discovery process that allows for the automated testing of large numbers of compounds. Generally, HTS begins with creation of a biochemical or phenotypic cell-based assay. Biochemical assays, such as enzymatic or ligand interaction assays, permit the study of specific interactions. However, biochemical assays typically use purified recombinant proteins, which limits interpretation of the results. More recently, cell-based assays have been used to study the effect of small molecules on phenotypes, such as proliferation, cell death, and target expression. Compared to biochemical assays, cell-based assays offer the benefit of live, cellular responses rather than a biochemical reaction. This provides valuable information on how specific cell types respond to treatment. However, a caveat is that the target of the compound cannot be directly assumed using a cell-based assay and must be investigated in additional studies. Another benefit of cell-based assays is the ability to quantify gene and protein expression using either a reporter system or immunofluorescence staining and high content imaging. As with all drug discovery methods, HTS requires careful validation of results and optimization of the lead candidate.

Several groups have used HTS approaches to identify modulators of DMD. Table 1-3 summarizes the targets, screening platforms, hits, and cell or animal models used for validation.

Target	Assay	Result
Exon skipping enhancers	Splicing reporter in C2C12	Identified dantrolene; increased exon skipping in *mdx* mice[1]
Glycosylation of α-dystroglycan	Lectin-based in C2C12	Identified lobeline; increased laminin binding in cells[2]
Human induced pluripotent stem cell fusion	Imaging, fusion index	Identified ginsenoside Rd and fenofibrate; reduced muscle pathology in *mdx* mice[3]
Integrin	Promoter reporter in isolated mouse myoblasts	Identified SU9516; increased α7 integrin in *mdx* mice[9]
Read-through	Read-through reporter in HEK293	Identified PTC124; promoted read-through of premature termination codons in *mdx* mice. Approved for patient use in EU[12]
Rescue of DMD zebrafish	Phenotypic screen	Identified aminophylline; reduced dystrophic pathology in DMD zebrafish[18]
Sarcospan	Promoter reporter in C2C12	Identified drugs that increased sarcospan in *mdx* cells[19]
Utrophin	Promoter reporter in HEK293	Identified SMT C1100; increased utrophin in *mdx* mice. Tested in clinical trials[16, 20]
	ELISA on C2C12	Identified drugs that increased utrophin A levels in *mdx* mice[22]
	5' and 3' UTR reporter in C2C12	Identified drugs that increased post-transcriptional upregulators of utrophin in *mdx* mice[23]

Table 1-3. Summary of high-throughput screening platforms and results for DMD therapies.

The first candidate drug for DMD discovered using HTS is Translarna (PTC124), identified and developed by PTC Therapeutics.[12] PTC Therapeutics created a phenotypic assay using HEK293 cells stably transfected with a luciferase reporter for premature termination codon (PTC) readthrough. Using the assay, they screened 800,000 small molecules with the goal of identifying compounds that promote readthrough of PTC and restore protein production. It was later discovered that their lead candidate PTC124, while effective at read through, also stabilized luciferase, revealing the need for counterscreening systems built into HTS.[49] In 2014, Translarna was approved in the European Union for use in DMD patients with non-sense mutations (10-15% of patients).

A number of groups have conducted HTS for small molecules that upregulate compensatory adhesion complexes. Using a utrophin promoter-reporter luciferase assay, Kay Davies and her group identified Ezutromid (SMT C1100) identified as a modulator of utrophin expression that reduces muscle disease in *mdx* mice. Ezutromid progressed to an open-label phase II clinical trial before it was discontinued after failing to meet the 48 week endpoints, improvements in leg muscles by MRI and utrophin upregulation in DMD patients. A chemical proteomics approach for target identification later revealed that Ezutromid bound strongly to and antagonized the aryl hydrocarbon receptor, introducing the potential for a more targeted approach.[50] In addition, second generation Ezutromid analogues with improved pharmacokinetic profiles have not yet been tested in clinical trials.[51] HTS using a α7 integrin promoter-reporter LacZ assay identified SU9516, a CDK2 inhibitor, as modulator of α7 integrin expression that reduces dystrophic pathology in *mdx* mice.[9] Our group developed a SSPN promoter-reporter assay and identified several compounds that increased SSPN, including L-type calcium channel blockers.[19] In summary, HTS has led to the identification of promising DMD therapies that are either approved for use in patients or being developed for clinical testing.

Pharmacological upregulation of SSPN

The Crosbie group established SSPN as a therapeutic target to treat the muscle pathology, cardiomyopathy, and respiratory dysfunction in *mdx* mice. Based on preclinical evidence, we propose that pharmacological upregulation of SSPN offers benefits over other therapies. Unlike exon skipping modalities, SSPN is expected to benefit all patients regardless of mutation. Small molecule modalities have the advantage of low risk of immune response and potential to redose compared to viral-mediated therapies. Based on our findings that SSPN acts as a scaffold for

protein complexes, we anticipate that SSPN-based therapies can be used in combination with therapies in development to increase localization of adhesion complexes at the sarcolemma.

Based on the extensive validation of SSPN as a therapeutic target for DMD, the objective of this body of work was to develop small molecule modulators of SSPN. The thesis is divided into three sections, each with separate, but related objectives. Figure 1-7 summarizes each phase of the project beginning with phase one, which entailed creation and validation of a SSPN promoter-reporter cell-based assay. In phase two, the assay was used to screen over 200,000 small molecules. The hits were validated on a secondary reporter assay before undergoing hit-to-lead selection to assess activity on endogenous SSPN gene and protein expression levels. In lead characterization, a lead compound was selected for further validation and found to increase compensatory adhesion complex localization at the membrane and improve membrane stability *in vitro*. An *in vivo* study demonstrated the lead compound increased SSPN gene expression in *mdx* mice, validating that the screen is capable of identifying compounds that are active *in vivo*. Finally, in phase three, the lead

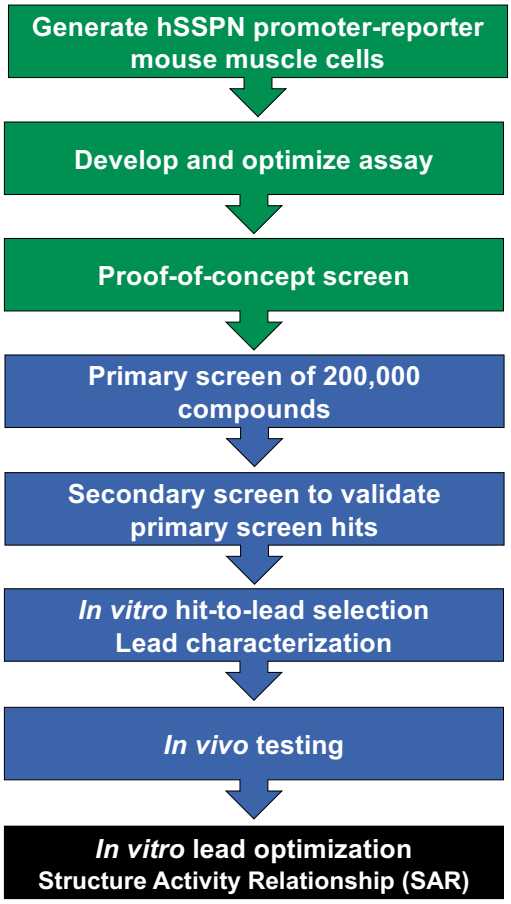

Figure 1-7. Summary of pipeline to develop new chemical entity modulators of sarcospan for the treatment of DMD. The thesis work is divided into three phases. In the first phase (green), we established a screening platform for sarcospan modulators. In the second phase (blue), we screened large chemical libraries and selected lead compounds for *in vitro* and *in vivo* testing. In the third and final phase (black), we optimized the lead compounds using structure activity relationship

compounds were optimized using structure activity relationship analysis resulting in the development of analogues with greater activity and solubility. The work presented in this thesis paves the way for the development of SSPN-mediated small molecule therapies for DMD.

Chapter 2

Development of a high-throughput screen to identify small molecule enhancers of sarcospan for the treatment of Duchenne muscular dystrophy

Cynthia Shu[1-3], Ariana N. Kaxon-Rupp[2], Judd R. Collado[2], Robert Damoiseaux[4, 5], and Rachelle H. Crosbie[1-3, 6]

[1]Molecular Biology Institute, University of California Los Angeles, [2]Department of Integrative Biology and Physiology, University of California Los Angeles, [3]Center for Duchenne Muscular Dystrophy, University of California Los Angeles, [4]Department of Molecular and Medicinal Pharmacology, University of California Los Angeles, [5]California NanoSystems Institute, University of California Los Angeles,[6] Department of Neurology David Geffen School of Medicine, University of California Los Angeles

Abstract

Background: Duchenne muscular dystrophy (DMD) is caused by loss of sarcolemma connection to the extracellular matrix. Transgenic overexpression of the transmembrane protein sarcospan (SSPN) in the DMD *mdx* mouse model significantly reduces disease pathology by restoring membrane adhesion. Identifying SSPN-based therapies has the potential to benefit patients with DMD and other forms of muscular dystrophies caused by deficits in muscle cell adhesion.

Methods: Standard cloning methods were used to generate C2C12 myoblasts stably transfected with a fluorescence reporter for human SSPN promoter activity. Assay development and screening were performed in a core facility using liquid handlers and imaging systems specialized for use with a 384-well microplate format. Drug-treated cells were analyzed for target gene expression using quantitative PCR and target protein expression using immunoblotting.

Results: We investigated the gene expression profiles of SSPN and its associated proteins during myoblast differentiation into myotubes, revealing an increase in expression after 3 days of differentiation. We created C2C12 muscle cells expressing an EGFP reporter for SSPN promoter activity and observed a comparable increase in reporter levels during differentiation. Assay conditions for high-throughput screening were optimized for a 384-well microplate format and a high content imager for visualization of reporter levels. We conducted a screen of 3,200 compounds and identified 7 hits, which include an overrepresentation of L-type calcium channel antagonists, suggesting that SSPN gene activity is sensitive to calcium. Further validation of a select hit, revealed that the calcium channel inhibitor felodipine increased SSPN transcript and protein levels in both wild-type and dystrophin-deficient myotubes, without increasing differentiation.

Conclusions: We developed a stable muscle cell line containing the promoter region of the human SSPN protein fused to a fluorescent reporter. Using the reporter cells, we created and validated a scalable, cell-based assay that is able to identify compounds that increase SSPN promoter reporter, transcript, and protein levels in wild-type and dystrophin-deficient muscle cells.

Introduction

Duchenne muscular dystrophy (DMD) is a progressive muscle wasting disorder that affects approximately 1 in every 5,700 males, making it the most common lethal genetic disorder in children.[24] Individuals with DMD lack dystrophin protein, which normally stabilizes myofibers by connecting the actin cytoskeleton, through the sarcolemma, to the extracellular matrix (ECM).[26, 29] Loss of this essential connection leads to contraction-induced damage of the cell membrane and myofiber.[31] Dystrophin-deficient muscles undergo asynchronous cycles of degeneration and satellite cell-mediated regeneration (for review[27]). As the population of satellite cells is diminished, the regenerative capacity is reduced and muscle undergoes end stage pathology, characterized by replacement of myofibers with fibrotic and adipose tissue[27]. Patients lose the ability to walk at approximately 10 years of age, but with corticosteroid treatment, the initial age of wheel chair reliance is extended to 13 years of age.[52] Approximately 90% of patients over 18 years of age develop dilated cardiomyopathy and respiratory dysfunction, leading to premature death in the third decade of life.[24, 25]

Mutations in the dystrophin gene lead to loss of dystrophin protein from the sarcolemma resulting in DMD[26]. Dystrophin localizes to the cytoplasmic side of the sarcolemma in myofibers and cardiomyocytes, where it binds to the actin cytoskeleton and β-dystroglycan.[32] Dystrophin interacts with transmembrane and peripheral membrane proteins (dystroglycan, sarcoglycans, and sarcospan) to form the dystrophin-glycoprotein complex (DGC), which serves as a receptor for laminin the ECM.[21, 30, 53-55] The physical axis of connection from actin to the ECM is crucial for maintaining membrane integrity. Loss of dystrophin leads to an absence of the entire DGC at the sarcolemma, leaving the myofiber vulnerable to contraction-induced damage.[56]

In addition to the DGC, skeletal muscle contains two other major adhesion complexes, the utrophin-glycoprotein complex (UGC) and the α7β1D-integrin complex, that also interact with actin inside the myofiber and bind to laminin and other ligands in the ECM.[57, 58] The composition of the UGC is highly similar to that of the DGC with the main exception that utrophin, a 395 kDa autosomal paralogue of dystrophin, mediates the interaction between β-dystroglycan and the actin cytoskeleton.[59] The UGC localizes to the neuromuscular and myotendinous junctions in healthy skeletal muscle and throughout the sarcolemma in fetal and regenerating muscle.[38, 39, 59] Utrophin overexpression studies in the genetic mouse model of DMD (*mdx)* demonstrated that a 3 to 4-fold increase of the UGC at the sarcolemma compensated for dystrophin deficiency.[37, 60] The α7β1D-integrin complex connects the sarcolemma to laminin and was also able to significantly rescue disease pathology when overexpressed in *mdx* mice.[41, 61]

Sarcospan (SSPN) is a 25 kDa transmembrane protein expressed in skeletal and cardiac muscle and interacts with all three adhesion complexes.[16, 21, 33] SSPN tightly associates with the sarcoglycan subcomplex that is associated with dystrophin and utrophin.[5, 33, 42] Transgenic overexpression of SSPN in dystrophin-deficient *mdx* mice *(mdx:*SSPN-Tg) stabilized the sarcolemma by increasing the abundance of the UGC and α7β1D-integrin complex at the membrane, effectively restoring laminin-binding.[5, 7, 16, 43] SSPN overexpression in *mdx* mice improved membrane integrity, revealed by reduced membrane-impermeable dye uptake and decreased serum levels of muscle creatine kinase.[4] SSPN-mediated strengthening of the sarcolemma improved resistance to degeneration, indicated by a decrease in central nucleation, a marker of myofiber turnover.[4] These improvements at the cellular level translated to functional improvements in post-exercise activity levels and eccentric contraction-induced force drop assays.[4] SSPN overexpression also addressed cardiac and pulmonary complications, which are

the leading causes of death in DMD patients. *mdx*:SSPN-Tg mice exhibited an improvement in cardiomyocyte membrane integrity, enhanced cardiac function, and increased adhesion complex localization at the cardiomyocyte membrane.[6] The transgenic mice showed improved minute ventilation and peak expiratory flow, indicators of pulmonary fitness.[4] Expression of SSPN-Tg in skeletal muscles of utrophin-null and α7-integrin-null mice on a *mdx* background confirmed that the rescue effect of SSPN is dependent on the presence of both the UGC and the α7β1D-integrin complex.[7, 43]

Knockout studies provide further insight into the mechanism of SSPN as a therapy and in the context of disease. While SSPN-null mice lack an obvious muscle phenotype at baseline, they exhibited reduced membrane levels of the DGC and UGC, and increased levels of the α7β1D-integrin complex.[16, 62] SSPN-deficient skeletal muscle showed reduced laminin-binding and increased susceptibility to eccentric contraction-induced damage at older ages. Cardiotoxin injury of the SSPN-null muscle revealed a diminished regenerative capacity, reduced activation of the pro-regenerative Akt/p70s6K signaling pathway, and reduced regeneration-induced utrophin upregulation response.[7] This diminished regenerative response places SSPN as an upstream regulator of the Akt pathway, a regulator of myofiber repair. In the heart, loss of SSPN exacerbated cardiac hypertrophy and fibrosis after isoproterenol-induced β-adrenergic challenge, revealing the protective role of SSPN in the context of cardiac stress and disease.[6] Overall, these studies concluded that SSPN is a regulator of adhesion complex localization and provides stability to the sarcolemma in both skeletal and cardiac muscle (for review[63, 64]).

The development of therapies for DMD is gaining momentum with the accelerated approval of eteplirsen in 2016 and the increased private sector funding of rare disease programs. However, the existing FDA approved drugs for DMD are not sufficient to substantially slow

disease progression. While corticosteroids dampen inflammation and extend ambulation by several years, they do not address adhesion complex and membrane stability deficiencies. In clinical trials, the antisense oligonucleotide exon skipping therapy eteplirsen increased truncated dystrophin protein production, but at a controversially low rate.[65] Our preclinical studies in *mdx* mice support SSPN as a stand-alone or combinatorial therapeutic target for DMD and Becker muscular dystrophy because of its ability to facilitate localization and stability of compensatory adhesion complexes. Importantly, SSPN overexpression to 30-fold levels does not lead to detrimental side effects in mice, making it a favorable candidate to pursue as a therapy.[4] Small molecule therapies, which comprise over 80% of all approved drugs, are especially appealing due to their ability to bypass the limitations of delivery, repeat dosages, and immune responses seen with virus-mediated gene delivery and stem cell-based approaches.[48] In the case of rare diseases such as DMD, the ability to bring patient-specific gene correction therapies to clinic is not yet feasible. SSPN is expected to benefit all cases of DMD regardless of genetic mutation. In this study, we report the development of a cell-based high-throughput assay to identify small molecule enhancers of SSPN gene expression for the treatment of DMD.

Results

Using transgenic overexpression of SSPN in *mdx* mice, we have previously established that as little as three-fold induction of SSPN expression ameliorates the cardiac, respiratory, and skeletal muscle symptoms in murine models of DMD.[63] To identify a translational SSPN-based therapy, we evaluated *in vitro* model systems, reporters, and assay conditions to develop a high throughput assay for SSPN enhancers that can be used in 384-well format to efficiently survey large chemical libraries.

Defining model systems for screening by evaluating target gene expression during myotube differentiation

As a first step to identifying enhancers of expression, we sought to determine an appropriate cell-based model system. Although SSPN is expressed in a wide range of tissues, we wanted to focus the assay on screening in the context of skeletal muscle and, for this reason, selected immortalized C2C12 myoblasts for the screen due to their ease of culture and ability to grow in large quantities. However, it was unclear to us whether to conduct the assay using immature myoblasts or mature, differentiated myotubes. In order to understand SSPN gene activity in myoblasts and myotubes, we directly interrogated SSPN gene expression in C2C12 cells at each day during differentiation for a total of seven days. Cells undergo fusion starting at day 3 and appear to be fully differentiated at day 6, as previously reported.[66] We found that SSPN mRNA abundance is relatively unchanged during the first three days following incubation of C2C12 cells in differentiation media (Fig. 2-1a). However, SSPN levels begin to increase exponentially at day 3, reaching ten-fold levels by day 5. The increased SSPN gene expression occurs just after the first evidence of visible myotube fusion at day 3 (Supplementary Fig. 2-2). We also evaluated the expression of SSPN associated proteins including dystrophin (DMD), utrophin (UTRN), dystroglycan (DAG), α7 integrin (ITGA7), β1D integrin (ITGB1), α-sarcoglycan (SGCA), and β-sarcoglycan (SGCB). We found that gene activity increased immediately after myoblasts were switched from proliferation to differentiation media (Fig. 2-1b-i and Supplementary Fig. 2-3). While DMD transcripts were not detectable in myoblasts, mRNA levels increased exponentially during differentiation. UTRN, ITGA7, and ITGB1

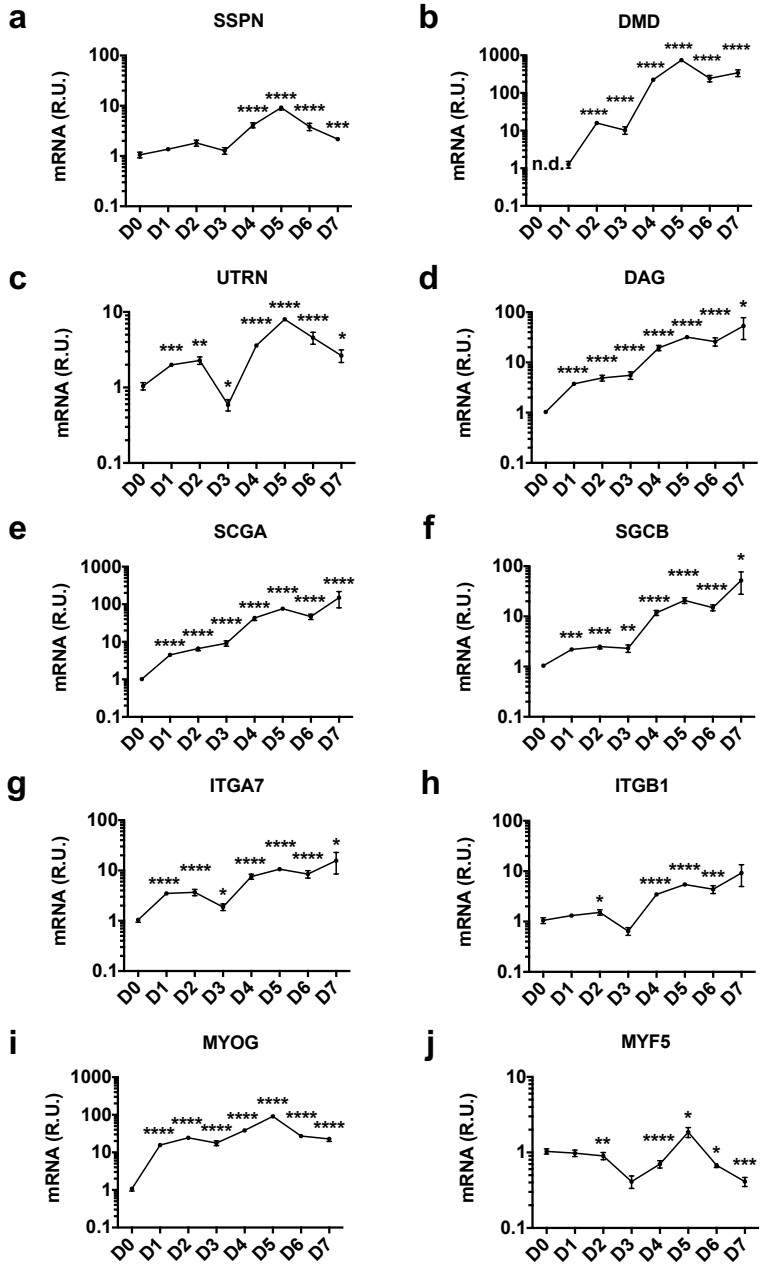

Figure 2-1. Individual components of muscle adhesion complexes increase during C2C12 differentiation. Confluent C2C12 myoblasts (day 0, D0) were switched from proliferation to differentiation media and harvested daily for seven days (D1 to D7). Individual genes encoding protein components of the three major adhesion complexes (DGC, UGC, and α7β1D-integrin complex) were investigated, including: (a) SSPN, sarcospan; (b) DMD, dystrophin; (c) UTRN, utrophin; (d) DAG, dystroglycan, (e) SCGA, α-sarcoglycan; (f) SCGB, β-sarcoglycan; (g) ITGA7, α7 integrin; and (h) ITGB1, β1D integrin. Analysis of myogenin (MYOG, i) and myogenic factor 5 (MYF5, j) are provided as markers for muscle cell differentiation. For DMD D0, n.d. (no data) indicates no detectable expression. Gene expression was calculated using the ddCt method and normalized to β-actin with day 0 (myoblast) values serving as the calibrator sample (n=3). R.U.: relative units. Results are plotted on a log scale. * $p<0.05$, ** $p<0.01$, *** $p<0.001$, **** $p<0.0001$.

expression increased by ten-fold, while the SCGA, SCGB, and DAG increased nearly one hundred-fold during the same time period (Fig. 2-1). As myogenic controls, we evaluated muscle-specific transcription factors, myogenin (MYOG) and myogenic factor 5 (MYF5), that are known regulators of myoblast differentiation.[67] As expected, MYOG gene activity increased immediately upon exposure to differentiation conditions (Fig. 2-1i), while MYF5 gradually decreased (Fig. 2-1j). Based on these results, we chose to treat cells at day 2 of differentiation and assay at day 4 of differentiation as this would allow for increased in gene expression while minimizing possible saturation of gene activation.

Generation and validation of biologically relevant reporters of SSPN gene activity

To identify the human SSPN (hSSPN) promoter region, we used publicly available data from UCSC Genome Browser. By assessing H2K4me3 marks, DNase hypersensitivity regions, and ChIP-seq data showing transcription factor binding sites, the promoter was predicted to be directly upstream of exon 1, including portions of exon 1 (Supplementary Fig. 2-1). Our goal was to develop a low-cost assay that could be ported to large chemical libraries (>100,000 compounds) that can be screened to identify and generate new chemical entities. For this reason, we selected a fluorescence-based reporter for the primary screening assay as gene activity can be rapidly imaged without the need for costly reagents. We used the immortalized C2C12 mouse myoblast cell line to generate stably transfected reporter cells containing an enhanced green fluorescent protein (EGFP) reporter driven by the hSSPN promoter (Fig. 2-2a). The hSSPN-EGFP myoblasts express reporter protein at increasing levels throughout differentiation revealing that the reporters are reflective of endogenous SSPN gene activity (Fig. 2-2b and c). Insulin transferrin selenium (ITS) was selected as the positive control for the screening assay as it broadly increases protein synthesis,

resulting in an increase in SSPN. Treatment with 1% ITS induced a 1.4-fold increase in hSSPN-EGFP reporter, mRNA, and protein levels after 48 hrs of treatment, showing that the reporter cells reflect the endogenous SSPN response to chemical stimulus (Supplementary Fig. 2-4). Cells transfected with reporter plasmids lacking the SSPN promoter did not exhibit fluorescence reporter activity (data not shown). Transfection of the reporter construct into RAW264.7 macrophages (ATCC), a non-SSPN expressing cell line, indicated the cell-type specificity of the reporter (Supplementary Fig. 2-5).

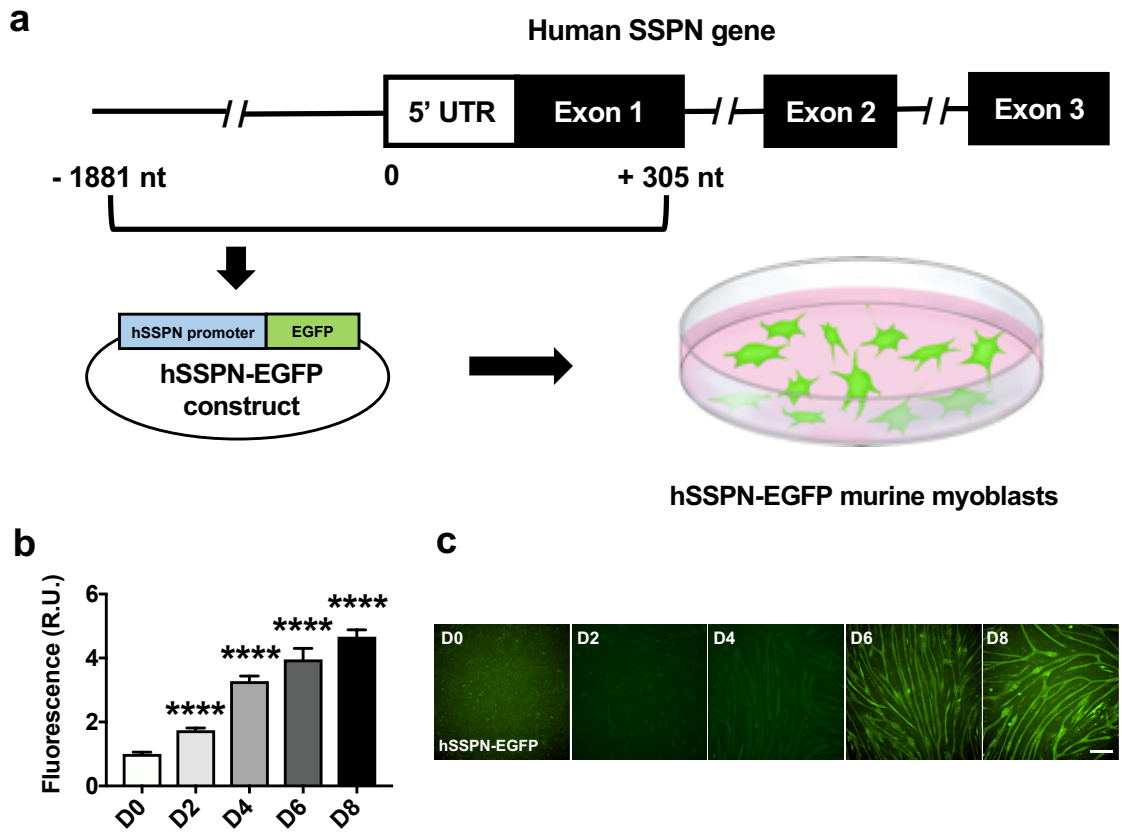

Figure 2-2. Generation and validation of biologically relevant myoblast line show effective reporting of sarcospan gene activity. The promoter region of the muscle-specific human sarcospan (hSSPN) gene was predicted using UCSC genome browser gene regulatory data. Using traditional cloning techniques, (a) a 2 kb region of the predicted hSSPN promoter was amplified and inserted into a promoterless EGFP plasmid. The construct was used to transfect C2C12 murine myoblasts reporter cell lines, which were then selected for stable transfection using antibiotic selection. Confluent myoblasts (day 0, D0) were switched from proliferation to differentiation media and assayed every other day for eight days (D2 to D8). (b-c) High-content imaging of differentiating hSSPN-EGFP cells showed a transition to mature myotube morphology that correlates with an increase in reporter signal (n=88 per time point). Fluorescence values are reported as relative fold change over myoblast values (R.U., relative units). Scale bar, 100 µm. **** $p<0.0001$.

Determining optimal assay conditions for high-throughput screening

Assay development is a challenging and laborious process that requires iterations of optimization. The obstacles that arise during assay development are confounded by the need to miniaturize assays and minimize the number of steps required, which both decrease handling time and directly increase throughput. To effectively screen large compound libraries, we miniaturized our assay to a 384-well microplate format, allowing for reduced reagent consumption and rapid data collection. To optimize assay conditions for high-throughput screening in a 384-well microplate format, we evaluated numerous parameters as listed in Supplementary Table 2-3. One limiting factor in high-throughput screens is the preparation of large quantities of cells. We therefore assessed multiple seeding densities ranging from 500 to 4000 cells per well and determined that seeding 500 cells per well followed by 3 days of incubation was sufficient for myoblasts to reach confluency before differentiation. This also reduced the amount of pre-screen culture required, making it an optimal condition for scaling up to meet high-throughput requirements. We tested the ability of the ITS positive control to increase reporter activity after 24 and 48 hrs and observed a detectable and significant change in reporter activity after 48 hrs of treatment (Supplementary Fig. 2-4). Screening core facilities typically store small molecules in 100% DMSO, which can lead to cell toxicity from the DMSO vehicle alone. To assess DMSO toxicity in our cells, we dosed cells with 0.1-10% DMSO and observed a decrease in cell viability at 2% DMSO and higher after 48 hrs of treatment (data not shown). To ensure proper DMSO mixing to prevent regionally high concentrations of DMSO that can negatively impact cell viability, we tested several mixing methods and conditions. From these tests, we determined that addition of 0.5 µl of 100% DMSO to an initial volume of 40 µl of media in each well, followed by 50 µl of additional media was sufficient to create a homogenous solution of DMSO, as detected

by DMSO spiked with crystal violet dye (data not shown). Image analysis using a custom analysis module in MetaXpress software identifies myotubes based on specified dimensions and quantifies fluorescence pixel intensity of identified cells (Supplementary Fig. 2-6). Imaging two regions of each well at 10X magnification in low fluorescence media was sufficient for the custom analysis module to reliably detect a significant difference between vehicle and positive control treated cells.

High-throughput screening on hSSPN-EGFP myotubes

To gain insight into the pathways involved in SSPN upregulation, we screened libraries of well-characterized FDA approved compounds. Using the hSSPN-EGFP cells, we screened the Library of Pharmacologically Active Compounds (LOPAC), Prestwick Chemical (NPW), and NIHII small molecule libraries totaling 3,200 small molecules (Fig. 2-3). All images were analyzed for cellular fluorescence intensity and compared with values from vehicle-treated cells. Robust strictly standardized mean difference (SSMD*) was used to classify the quality of each plate and the strength of each hit. All plates resulted in an SSMD* $\geq$ 1, indicating a good quality

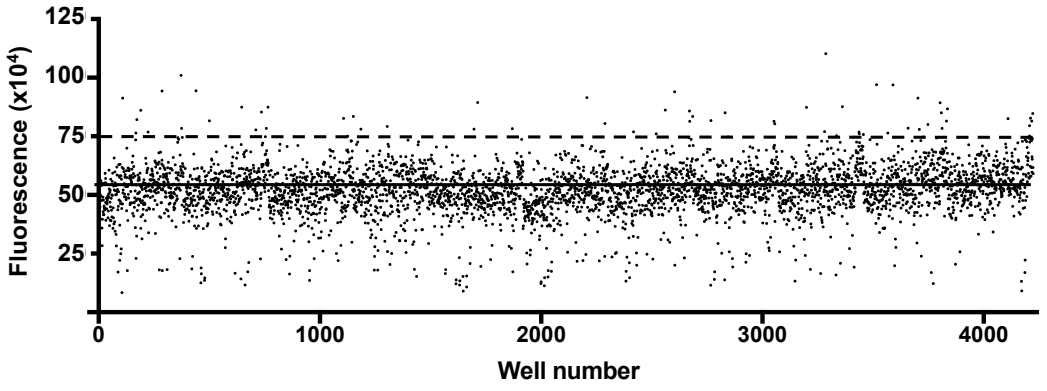

Figure 2-3. High-throughput screening of LOPAC, NIH, and Prestwick libraries on hSSPN-EGFP myotubes. hSSPN-EGFP cells differentiated for two days were used to screen 3,200 molecules in the Library of Pharmacologically Active Compounds, NIHII, and Prestwick libraries (n=1). The reporter cells were treated with 5.5 μM of compound and imaged 48 hours later at day 4 of differentiation into myotubes. Two images per well were captured and analyzed using a MetaXpress custom analysis module to quantify fluorescence intensity. The solid line marking the average fluorescence of all data points and the dashed line marking the initial cut-off for hits (1.4-fold over vehicle).

difference between vehicle and positive control-treated cells (Table 2-1). Generally, SSMD* > 0.25 is the minimum to be considered a hit.[68] Based on the fold change detectable in cells treated with positive control, we set an initial hit cutoff of 1.4-fold fluorescence intensity over vehicle and eliminated images with debris or small molecules that auto-fluoresce, leading to a preliminary hit rate of 0.5% or 13 small molecules (Supplementary Table 2-4). Among hits, four were L-type calcium channel antagonists (felodipine, isradipine, lacidipine, nilvadipine) with felodipine appearing twice from the LOPAC and NPW libraries, indicating the robustness of the assay in reproducibly identifying hits. To confirm the hits, all 13 compounds were rescreened at 5.5 μM in 2 separate plates with n = 24 each plate (Supplementary Table 2-5). Of the 13 compounds, felodipine, GW5074, isoproterenol, isradipine, lacidipine, nandrolone, and nilvadipine resulted in an SSMD* > 0.25 (Table 2-2). In addition, GW5074, isoproterenol, and nandrolone are known to also affect intracellular calcium levels. These data strongly support that endogenous SSPN expression is regulated in a calcium-sensitive manner.

Plate	Library	SSMD*
1	LOPAC1	1.2
2	LOPAC2	1.7
3	LOPAC3	1.3
4	LOPAC4	1.0
5	NPW1	1.7
6	NPW2	1.7
7	NPW3	1.0
8	NPW4	1.5
9	NIHII1	1.8
10	NIHII2	1.1
11	NIHII3	1.1

Table 2-1. Plate quality control using robust strictly standardized mean difference. Robust strictly standardized mean difference (SSMD*) was used a measurement of quality control. Each of the 11 plates resulted in an SSMD* ≥ 1, indicating a good quality effect size between vehicle and positive control-treated cells.

Compound	Description
Felodipine	L-type Ca^{2+} channel blocker
GW5074	cRaf1 kinase inhibitor
Isoproterenol	Sympathomimetic amine acting on β-adrenoceptors
Isradipine	L-type Ca^{2+} channel blocker
Lacidipine	L-type Ca^{2+} channel blocker
Nandrolone	anabolic-androgenic steroid
Nilvadipine	L-type Ca^{2+} channel blocker

Table 2-2. Validated hits from hSSPN-EGFP screen reveal an enrichment of calcium channel blockers. The screen resulted in 13 initial hits, which were further validated with the hSSPN-EGFP reporter with an n=24. The 7 validated hits included an overrepresented number of L-type calcium channel blockers.

In vitro validation in wild-type and dystrophin-deficient muscle cells

To determine whether this increase in human SSPN promoter reporter activity translated to an increase in mouse SSPN transcript levels, we conducted follow-up assays using felodipine because of its effective dose response profile in the hSSPN-EGFP cells and minimal effect on cell viability (Supplementary Fig. 2-7; Supplementary Fig. 2-8). We treated C2C12 myotubes with 1-10 μM of felodipine and observed that after 48 hrs of treatment, SSPN expression increased 1.5-fold over vehicle at the 10 μM dose (Fig. 2-4a). To assess the effect of felodipine in a dystrophin-deficient cell model, we used immortalized *mdx* myoblasts containing a nonsense mutation in exon 23 of the dystrophin gene. We treated *mdx* myotubes with 1-10 μM of felodipine and also observed a 1.5-fold increase in SSPN gene expression with the 10 μM treatment (Fig. 2-4b). Because increases in transcript levels do not necessarily correlate with changes in protein levels, we also assessed SSPN protein levels. Immunoblot analysis on wild-type C2C12 cells treated with 1-10μM of felodipine revealed an increase in SSPN protein levels with the 5 μM and 10 μM treatments (Fig. 2-4c, e). In *mdx* cells, treatment with 1 μM felodipine increased SSPN protein levels (Fig. 2-4d, f).

To determine if felodipine was specifically increasing SSPN, we quantified gene expression of utrophin (UTRN), which increases with differentiation, and the myogenic markers myogenin (MYOG) and myogenic factor 5 (MYF5). In wild-type myotubes, felodipine increased SSPN, UTRN, and MYOG in a dose-dependent manner, indicating the treatment may accelerate differentiation (Fig. 2-5a). However, in *mdx* myotubes, only SSPN increased in a dose-dependent manner, suggesting that felodipine increases SSPN through pathways that are independent from differentiation (Fig. 2-5b). In both cell lines, MYF5 remained relatively stable as expected.

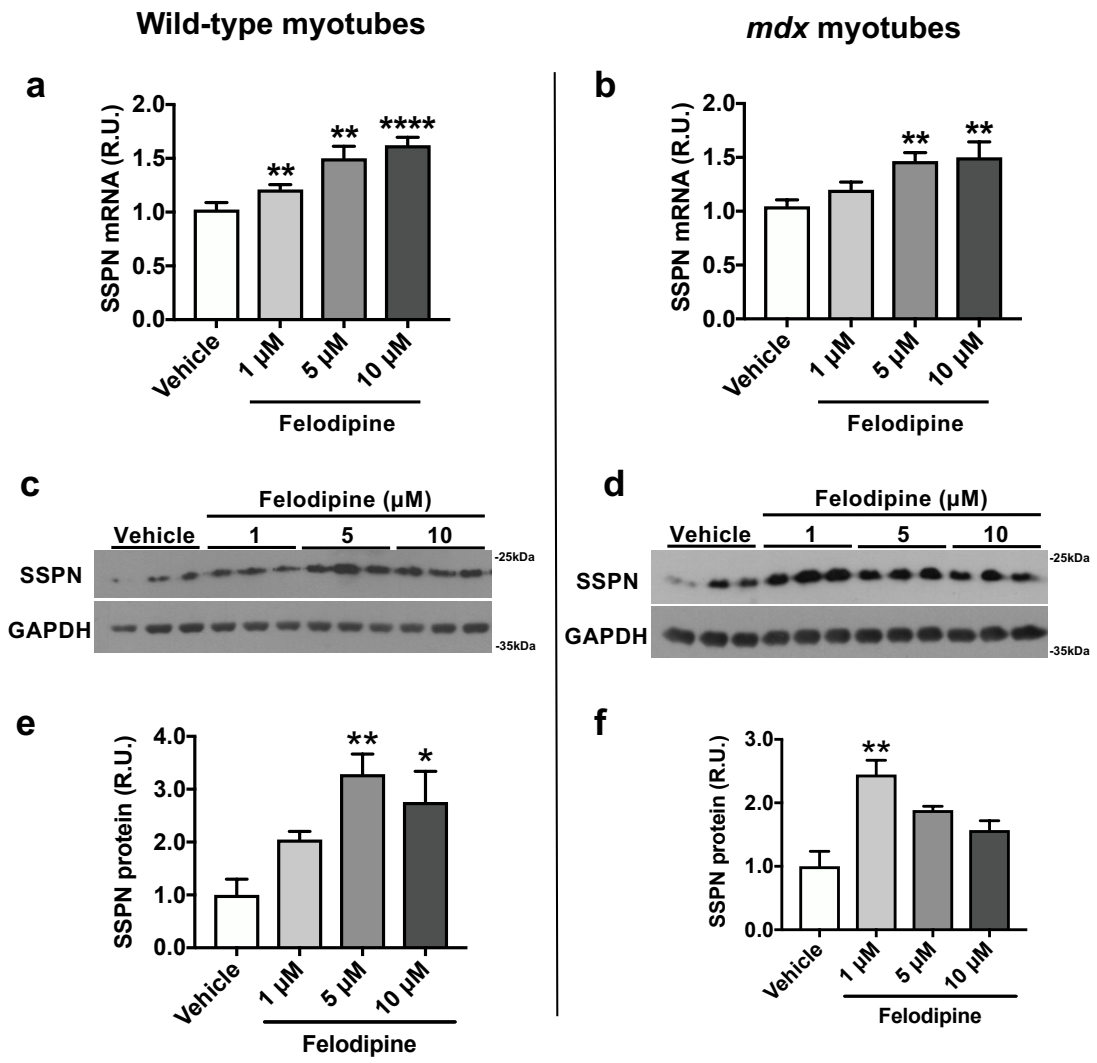

Figure 2-4. Compound identified in high-throughput screen increases sarcospan transcript and protein levels in both wild-type and dystrophin-deficient *mdx* myotubes. Felodipine increases sarcospan gene expression in (a) C2C12 wild-type and (b) *mdx* myotubes (n=3-8) after 48 hours of treatment. Gene expression was calculated using the ddCt method and normalized to β-actin with vehicle-treated cells serving as the calibrator sample. Using immunoblot analysis, total cell lysate from cells treated with felodipine was probed with anti-SSPN antibodies. GAPDH is shown as a loading control. Felodipine increases sarcospan protein levels in both (c) C2C12 wild-type and (d) and *mdx* myotubes (n=3). (e-f) Quantification of SSPN protein levels are normalized to GAPDH. R.U., relative units. All data was obtained from murine myotubes treated for 48 hours and assayed or harvested at day 4 of differentiation. * $p<0.05$, ** $p<0.01$, **** $p<0.0001$.

To determine if felodipine increases the rate myoblast differentiation, we performed a fusion index assay on wild-type and *mdx* myotubes. Felodipine did not increase the number of

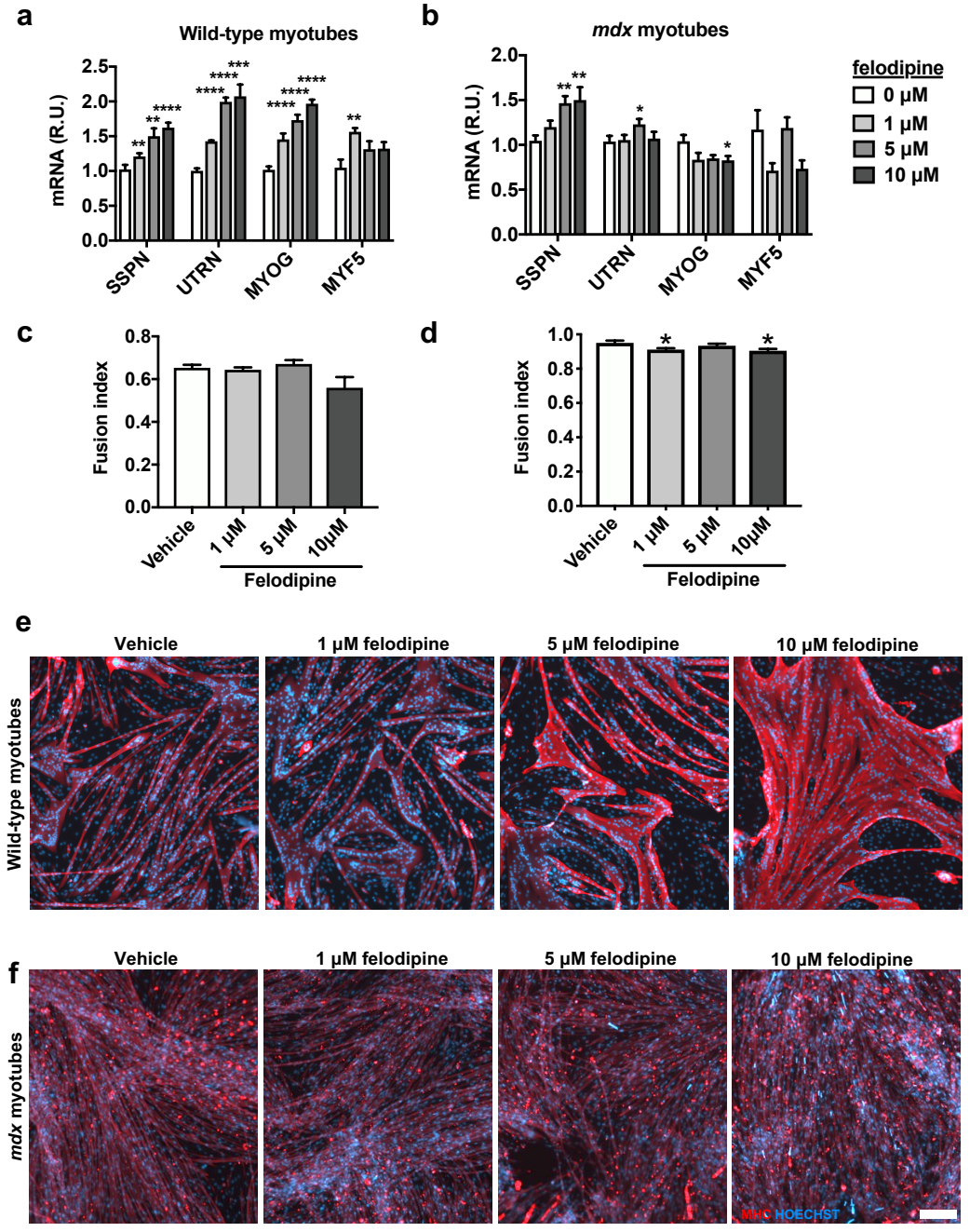

Figure 2-5. Felodipine enhances differentiation in wild-type, but not dystrophin-deficient myotubes. Felodipine increases utrophin and myogenin gene expression in (a) C2C12 wild-type myotubes, but not (b) *mdx* myotubes (n=3-8) after 48 hours of treatment (sarcospan gene expression data from previous figure). (c-d) Felodipine does not increase fusion index (nuclei in myosin heavy chain positive area/total nuclei in field) in wild-type or *mdx* myotubes, (e-f) but does induce the formation of hypertrophic wild-type myotubes. Gene expression was calculated using the ddCt method and normalized to β-actin with vehicle-treated cells serving as the calibrator sample. UTRN, utrophin ; MYOG, myogenin ; MYF5, myogenic factor 5 ; MHC, myosin heavy chain. Scale bar, 200 µm. * $p<0.05$, ** $p<0.01$, *** $p<0.001$, **** $p<0.0001$.

cells fusing into myotubes in either cell line, but did result in the formation of hypertrophic wild-type myotubes (Fig. 2-4c-f).

Discussion

The heterogeneity of mutations and difficulty of delivery to muscle are major challenges in the development of urgently needed therapies to treat DMD. SSPN is able to reduce the pathology of muscular dystrophy in the DMD murine model by increasing membrane localization of the UGC and α7β1D-integrin adhesion complexes, effectively increasing laminin binding to compensate for the loss of dystrophin.[4-7, 16, 43] Development of small molecule therapies that increase SSPN expression may lead to stand-alone or combinatorial therapies to treat DMD and other forms of muscular dystrophy caused by deficits in membrane proteins. Small molecule therapies are ideal due to their ability to bypass the limitations of delivery and immune responses seen with viral and cell-based methods.

In this study, we demonstrate the application a cell-based reporter assay followed by *in vitro* hit-to-lead validation experiments that can be used to identify small molecule modulators of SSPN gene and protein expression. From our screen of 3,200 small molecules using hSSPN-EGFP myotubes, we identified 7 hits that increase reporter levels. We further validated the hit felodipine in wild-type and *mdx* myotubes and found that it increased endogenous SSPN mRNA and protein, showing that candidate drugs derived from the screen have the potential to activate both human and mouse SSPN. In wild-type myotubes, the increase in SSPN coincided with an increase in UTRN and MYOG, indicating that felodipine may be affecting differentiation and fusion of the myotubes. However, this effect was not observed in *mdx* myotubes. These differences in wild-type and *mdx* cell responses to treatment may be explained by findings that *mdx* mice show defective

excitation-contraction coupling, altered calcium homeostasis, and altered expression of calcium handling proteins.[69, 70]

We identified a class of dihydropyridine-derived calcium channel antagonists that increase SSPN reporter activity. Treatment of skeletal muscle cells with L-type calcium channel antagonists increases SSPN gene and protein expression, suggesting that endogenous SSPN gene activity is calcium-sensitive. In cardiac and smooth muscle, L-type calcium channel antagonists interact directly with dihydropyridine receptors (DHPR) to reduce calcium movement through the channel and are used clinically to treat hypertension, regulate heart rate, and address chest pain. In skeletal muscle, DHPR are concentrated in the transverse (T)-tubules and are key regulators of excitation-contraction coupling. Upon depolarization along the T-tubules, DHPR activates the ryanodine receptor to release calcium from the sarcoplasmic reticulum to the cytosol, which facilitates the interaction between actin and myosin required for muscle contraction. DHPR forms a complex with an ATP release channel (pannexin 1), an ATP receptor (P2 purinoreceptor 2), caveolin-3, and dystrophin that is proposed to be involved in excitation-transcription coupling, a calcium and ATP-sensitive regulation of gene expression.[71] In preclinical studies of dystrophic rodents, treatment with L-type calcium channel blocker nifedipine led to an increase in fiber diameter and muscle function and a decrease in serum creatine kinase levels.[72, 73] Multiple studies in human subjects show no improvement in disease outcome with long term calcium channel antagonist treatment (for review[74, 75]). However, calcium dysregulation is a hallmark feature in DMD and recent evidence points to a functional interplay between ion channels and adhesion complexes, indicating that calcium regulation is an important therapeutic target (for review[74, 75]).

In conclusion, we developed and validated a cell-based reporter assay that effectively identifies compounds that enhance SSPN gene and protein expression in wild-type and dystrophin-

deficient myotubes. Future studies will be focused on porting our validated assay system to a larger chemical space to identify and develop new chemical entities for the treatment of DMD.

Conclusions

- Gene expression analysis of individual components of the DGC and UGC revealed an exponential increase in mRNA levels beginning at day 3 of differentiation. During differentiation, SSPN, UTRN, ITGA7, and ITGB1 increase to similar levels (ten-fold over myoblast levels). DAG, SCGA, and SCGB increase fifty to one hundred-fold, while DMD increases up to a thousand-fold over myoblast levels.
- Screening of FDA approved drug libraries on hSSPN-EGFP murine myotubes revealed an enrichment in L-type calcium channel antagonists, indicating a new potential role in calcium regulation of SSPN expression.
- Compounds identified in the screen increase hSSPN-EGFP activity as well as SSPN mRNA and protein levels in wild-type and dystrophin-deficient *mdx myotubes*, demonstrating the ability of the assay to identify relevant compounds that are active in both human, mouse, wild-type, and *mdx* muscle cells.
- In summary, we developed a high-throughput assay using C2C12 myotubes stably transfected with a hSSPN-EGFP reporter that is fully optimized for a 384-well microplate format with minimal reagents and handling and can thus be used for large-scale screens.

Methods and Materials

Gene expression analysis

RNA from myotubes treated for 48 hrs was extracted from cells using Trizol-based (Thermo Fisher Scientific) phase separation, as previously described.[76] RNA concentrations were determined

using a NanoDrop 1000 (Thermo Fisher Scientific) and 750 ng of RNA in a 20 µl reaction was reverse transcribed using iScript cDNA synthesis (Bio-Rad) with the following cycling conditions: 25°C for 5 mins, 42°C for 30 mins, 85°C for 5 mins. For quantitative PCR, SsoFast EvaGreen Supermix (Bio-Rad), 400 nM of each optimized forward and reverse primer (for primer descriptions see Supplementary Table 2-1), and cDNA corresponding to 37.5 ng RNA were used to amplify cDNA measured by Applied Biosystems 7300 (Thermo Fisher Scientific) with the following reaction conditions: 55°C for 2 mins, 95°C for 2 mins, 40 cycles of 95°C for 10 seconds and 62°C for 30 seconds, and dissociation stage. Each sample was run in triplicate. Data was analyzed using the ddCT method and normalized to reference gene, GAPDH or β-actin, with vehicle-treated samples serving as the calibrator (relative expression of vehicle control = 1).

Molecular cloning of SSPN reporter plasmids

The SSPN promoter region was predicted using publicly available data on UCSC Genome Browser (http://genome.ucsc.edu/). Using the GRCh37/hg19 assembly, gene regulatory elements of the cardiac and skeletal muscle-specific SSPN transcript variant 1 (NM_005086.4) of the human SSPN gene (NG_012011.2) were identified. H2K4me3 marks, DNase hypersensitivity regions, and ChIP-seq data showing transcription factor binding locations from human skeletal muscle cultures indicated the promoter region to be upstream of exon 1 and within exon 1 (Supplementary Fig. 2-1). A 2 kb region encompassing the human SSPN promoter was amplified from human genomic DNA (Bioline) using Phusion High Fidelity DNA Polymerase (New England Biolabs) with the primers indicated in Supplementary Table 2-2. The primers contained leader sequences and restriction sites for BglII (AGATCT) or HindIII (TTCGAA). The PCR products were purified using PureLink HiPure Plasmid DNA Purification kit (Life Technologies) and digested with BglII

and HindIII in NEBuffer 3.1 (New England Biolabs). The 2 kb digested PCR products were electrophoresed on agarose gels, excised, and purified using the Zymoclean Gel DNA Recovery Kit (Zymo Research). pmEGFP-1 (Addgene, plasmid #36409) was digested with BglII and HindIII and ligated to PCR products using T4 DNA ligase (Invitrogen). The plasmid constructs were linearized with BglII, which digested the region upstream of the SSPN promoter. The linearized plasmids were purified and used to transform One Shot TOP10 chemically competent *E. coli* (Thermo Fisher) grown on agar containing the appropriate antibiotic. Individual colonies were confirmed by colony PCR to contain the SSPN promoter construct and inoculated in liquid culture overnight. The plasmids were purified using PureLink Quick Plasmid Miniprep (Life Technologies) and subjected to DNA sequencing (Laragen Inc.) using the primers in Supplementary Table 2-2 to confirm presence and accuracy of the SSPN promoter region. Select bacterial cultures were grown in large cultures and collected for plasmid purification using the Plasmid Maxi Kit (Qiagen).

Generation of stable reporter cell lines

C2C12 immortalized murine myoblasts cultured in growth media consisting of DMEM (Gibco) with 20% Fetal Bovine Serum (Sigma-Aldrich) at 37°C with 5% CO_2 were transfected with the hSSPN-EGFP linearized plasmid using Lipofectamine 3000 Transfection Reagent (Thermo Fisher Scientific). Transfected cells were selected using 800 μg/ml of G418 (Sigma-Aldrich) for 4 weeks to generate stable cell lines expressing reporter protein under control of the human SSPN promoter.

High-throughput screening

hSSPN-EGFP myoblasts were seeded at 500 cells per well in 50 µl of growth media in 384-well black, clear bottom microplates (Greiner) using a Multidrop 384 (Thermo Fisher Scientific) and incubated for 3 days. Upon reaching confluency, the growth media was replaced with 50 µl of differentiation media consisting of DMEM with 2% horse serum (Sigma-Aldrich) using an EL406 combination washer dispenser (Biotek). At day 2 of differentiation, the media on the cells was aspirated, left with a residual volume of 10 µl, and replaced with 30 µl of fresh differentiation media. 0.5 µl of small molecule in DMSO or DMSO alone (for vehicle and positive control wells) was added to each well using a Biomek Fx (Beckman). To ensure proper mixing of the DMSO, 50 µl of additional differentiation media was added to all wells except the positive control treated wells, which instead received 50 µl of media containing insulin transferrin selenium (ITS) (Gibco) to reach a final concentration of 1% ITS. The final concentration of drug in each treated well was 5.5 µM in 0.55% DMSO and 0.55% DMSO only for vehicle and positive control treated wells. After 48 hrs of incubation, the media was replaced with Fluorobrite DMEM (Gibco) and each plate was imaged using ImageXpress Micro Confocal High Content Imaging System (Molecular Devices). The fluorescence intensity of imaged cells was determined using a custom module analysis in MetaXpress Analysis software (Molecular Devices). Analysis setting were as follows: top hat (size: 12, filter shape: circle), adaptive threshold (source: top hat, minimum width: 10, maximum width: 800, intensity above local background: 500), filter mask (filter type: minimum area filter, minimum value: 500).

Cell culture

C2C12 cells (American Type Culture Collection) were grown at 37°C with 5% CO_2 in growth media containing DMEM (Gibco) with 20% FBS (Sigma-Aldrich). Upon reaching 90-100%

confluency, the media was replaced with differentiation media containing DMEM with 2% horse serum (Sigma-Aldrich). Conditionally immortalized H2K *mdx* myoblasts [77] with a nonsense mutation in exon 23 of dystrophin were a gift from Terrance Partridge, Ph.D. (Children's National Medical Center, Washington, D.C.) [77]. Cells were allowed to proliferate on 0.01% gelatin (Sigma-Aldrich) coated plates at 33°C with 5% CO_2 with growth media containing DMEM, 20% HI-FBS (Invitrogen), 2% L-glutamine (Sigma-Aldrich), 2% chicken embryo extract (Accurate Chemical), 1% penicillin-streptomycin (Sigma-Aldrich), and 20 U/ml of fresh interferon gamma (Gibco). For differentiation, H2K *mdx* myoblasts were seeded on plates coated with 0.1 mg/ml matrigel (Corning) diluted in DMEM and grown in proliferation conditions. Upon reaching 90-100% confluency, cells were grown at 37°C with 5% CO_2 in differentiation media containing DMEM with 5% horse serum (Sigma-Aldrich), 2% L-glutamine, and 1% penicillin-streptomycin using established protocols [77]. RAW264.7 macrophages (ATCC), a gift from Amy Rowat, Ph.D. (University of California, Los Angeles), were cultured in DMEM containing 20% FBS at 37°C with 5% CO_2.

In vitro treatments

Cells were treated for 48 hrs beginning at day 2 of differentiation with DMSO (vehicle control, ATCC), aceclidine (Sigma-Aldrich), acyclovir (Sigma-Aldrich), alloxazine (Sigma-Aldrich), carbadox (Sigma-Aldrich), felodipine (Sigma-Aldrich), GW5074 (Sigma-Aldrich), isoproterenol (Sigma-Aldrich), isradipine (Sigma-Aldrich), lacidipine (Sigma-Aldrich), nafadotride (Tocris Bioscience), nandrolone (Sigma-Aldrich), nifedipine (Sigma-Aldrich), nilvadipine (Sigma-Aldrich), alloxazine (Sigma-Aldrich) diluted in cell-type specific differentiation media at doses listed in figures.

Immunoblotting

C2C12 murine myotubes treated for 48 hrs were lysed using RIPA buffer (Thermo Fisher Scientific) containing a protease inhibitor cocktail (0.6 μg/ml pepstatin A, 0.5 μg/ml aprotinin, 0.5 μg/ml leupeptin, 0.1 mM PMSF, 0.75 mM benzamidine, 5 μM calpain I inhibitor, 5 μM calpeptin). Cell lysates in RIPA buffer were rocked for 1 hr at 4°C and centrifuged at 1000 RPM for 30 mins at 4°C. The supernatant was collected, quantified for protein concentration using the DC protein assay (Bio-Rad), and normalized to 2 mg/ml in water and Laemmli sample buffer with a final concentration of 10% glycerol (Sigma-Aldrich), 5% beta-mercaptoethanol (Sigma-Aldrich), 3% sodium dodecyl sulfate (Sigma-Aldrich), and 0.05% bromophenol blue (Sigma-Aldrich). For SDS-PAGE, samples were heated to 95°C for 2 mins before loading 40 μg to a 4-12% tris-glycine gel (Novex), run for 2 hrs at 100 volts at RT, and transferred to a nitrocellulose membrane for 2 hrs at 100 volts at 4°C. Ponceau S staining was performed to visualize protein loading. Membranes were blocked with 5% blotto (5% non-fat dried milk) in tris-buffered saline with 0.1% tween-20 (TBST, Sigma-Aldrich) for 1 hr at RT and incubated on a rocker overnight at 4°C with the following primary antibodies and dilutions in 5% blotto: SSPN (sc-393187, 1:200, Santa Cruz Biotechnology), GAPDH (Mab374, 1:10,000, Millipore). Following three 10-minute TBST washes, the membranes were incubated in goat anti-mouse IgG HRP (Ab6789, 1:5000 for SSPN, 1:10,000 for GAPDH, Abcam) diluted in 5% milk for 2 hrs at RT. The membranes were then washed three times for 10 mins each with TBST, incubated in SuperSignal West Pico Chemiluminescent Substrate (Thermo Fisher Scientific) for 5 mins at RT on an orbital shaker, and exposed to autoradiography films (Agfa). Autoradiography films were developed using a SRX-101A tabletop processor (Konica Minolta), scanned to a digital file, and analyzed by densitometry

of bands using ImageJ version 1.51s [78]. Target protein bands were normalized to loading control GAPDH with vehicle-treated cells serving as the calibrator sample (relative protein levels of vehicle control = 1).

Fusion index

Cells in a 96-well plate were treated for 72 hrs beginning at day 2 of differentiation were fixed with 4% PFA for 20 minutes, permeabilized with 0.2% Triton X-100 (Sigma) for 10 minutes, and blocked with 1% BSA for 30 minutes. Myosin heavy chain (MHC) was detected using 10 μg/ml MF-20 (Developmental Hybridoma Studies Bank) in 1% BSA overnight and 10 μg/ml goat anti-mouse Alexa Fluor Plus 594 (Thermo Fisher Scientific) in 1% BSA for 1 hr. PBS washes were performed between each step above. Nuclei were stained with 5 μg/ml Hoechst (Thermo Fisher Scientific) for 20 minutes before imaging. Each treatment was performed in three wells and three fields per well were captured. ImageJ was used to count the number of total nuclei and nuclei within a MHC positive cell. Fusion index was calculated as nuclei in a MHC positive cell/total nuclei.

Cell viability assay

Cells in a 384-well plate were treated for 48 hrs beginning at day 2 of differentiation. CellTiter-Glo Luminescent Cell Viability Assay was used to assess cell viability by adding the assay reagent and media on cells at a ratio of 1:1. Luminescence was measured using a standard plate reader.

Statistics

Robust strictly standardized mean difference (SSMD*) was used to assess plate quality and for hit

selection. SSMD* = $X_P - X_N/1.4826\sqrt{s_P^2 + s_N^2}$, where X_P, X_N, S_P, and S_N are the medians and median absolute deviations of the positive and negative controls, respectively[68]. For plate quality, SSMD* ≥ 1 indicates a good quality moderate positive control. For initial hit selection, a 1.4-fold increase over vehicle and SSMD* > 0.25 was considered a hit. Statistical analysis was performed using Prism version 7.0 (GraphPad Software) for Mac OS X using the two-tailed, non-parametric Kolmogorov-Smirnov test. Data are reported as mean ± SEM. A p-value of <0.05 was considered statistically significant. * p<0.05, ** p<0.01, *** p<0.001, **** p<0.0001.

Abbreviations

DAG: dystroglycan; DMD: Duchenne muscular dystrophy/dystrophin; DGC: dystrophin-glycoprotein complex; DMSO: dimethyl sulfoxide; ECM: extracellular matrix; EGFP: enhanced green fluorescent protein; hSSPN: human sarcospan; HTS: High-throughput screening; ITGA7: α7 integrin; ITGB1: β1D integrin; ITS: insulin transferrin selenium; MTA: methylthioadenosine; MYF5: myogenic factor 5; MYOG: myogenin; SGCA: α-sarcoglycan; SCGB: β-sarcoglycan; SSPN: sarcospan; UTRN: utrophin; UGC: utrophin-glycoprotein complex.

Ethics approval and consent to participate

All protocols and procedures were performed in accordance with guidelines set by Environmental Health, and Safety at the University of California Los Angeles. No animals were used in the study.

Funding

Support for this work was provided by the Virology and Gene Therapy Training Grant (NIH T32 AI060567), Muscle Cell Biology, Pathogenesis, and Therapeutics Training Grant (NIH T32

AR065972), Pilot and Feasibility Seed Grant program (NIH/NIAMS P30 AR057230), UCLA Department of Integrative Biology & Physiology Eureka Scholarship, Muscular Dystrophy Association (MDA 274143), NIH/NIAMS (R01 AR048179), and NIH NHLBI (R01 HL126204).

Authors' Contributions

C.S. designed the screening assays, including creation of stable cell lines. C.S. performed all experiments including high-throughput screening and *in vitro* studies with assistance from A.N.R. during cell culture and imaging. C.S. conducted all data analysis, prepared all figures and wrote the manuscript. A.N.R. and J.R.C. performed immunofluorescence, imaging, and image analysis for fusion index. R.D. designed assays, screening cascade, and provided core services for screening. R.H.C. conceived of the project and consulted on all experiments, data analysis, figures, and manuscript drafting.

Acknowledgements

We thank Molecular Screening Shared Resource (University of California Los Angeles) for providing screening services, Terrance Partridge, Ph.D. (Children's National Medical Center, Washington, DC) for providing the H2K *mdx* myoblasts, Amy Rowat, Ph.D. (University of California Los Angeles) for providing the RAW264.7 macrophages, Benjamin Glick, Ph.D. (University of Chicago, Chicago, IL) for providing the pmEGFP-1 plasmid (Addgene plasmid #36409), Ronny C. Choe (University of California Los Angeles) for statistical analysis consultation, and Katie G. Hammond (University of California Los Angeles) for figure illustration.

Supplemental Figures and Tables

PRIMER	SEQUENCE (5' → 3')	LOCATION	AMPLICON LENGTH	AE
UTRN F	GTATGGGGACCTTGAAGCCAG	exons 1-2	125BP	118%
UTRN R	ATCGAGCGTTTATCCATTTGGT			
DMD F	GGAAAGCAACACATAGACAACCT	exons 3-4	65BP	111%
DMD R	GGGCATGAACTCTTGTAGATCC			
ITGA7 F	GATCGTCCGAGCCAACATCACA	exons 23-24	165BP	115%
ITGA7 R	CTAACAGCCCAGCCAGCACT			
ITGB1 F	ATGCCAAATCTTGCGGAGAAT	exons 3-4	209BP	105%
ITGB1 R	TTTGCTGCGATTGGTGACATT			
DAG1 F	CAGACGGTACGGCTGTTGTC	exons 3-4	126BP	112%
DAG1 R	AGTGTAGCCAAGACGGTAAGG			
SGCA F	GCAGCAGTAACTTGGATACCTC	exons 2-3	113BP	117%
SGCA R	AAAGGATGCACAAACACACGA			
SGCB F	AGCACAACAGCAATTTCAAAGC	exon 2	112BP	100%
SGCB R	AGGAGGACGATCACGCAGAT			
SSPN F	TGCTAGTCAGAGATACTCCGTTC	exons 1-2	103BP	94%
SSPN R	GTCCTCTCGTCAACTTGGTATG			
MYOG F	GAGATCCTGCGCAGCGCCAT	exon 1	97BP	107%
MYOG R	CCCCGCCTCTGTAGCGGAGA			
MYF5 F	AAGGCTCCTGTATCCCCTCAC	exon 1	249BP	117%
MYF5 R	TGACCTTCTTCAGGCGTCTAC			
ACTB F	TCCTGACCCTGAAGTACCCCAT	exons 1-2	131BP	104%
ACTB R	CTCGGTGAGCAGCACAGGGT			
GAPDH F	CAACTTTGGCATTGTGGAAGG	exons 4-5	135BP	92%
GAPDH R	GTGGATGCAGGGATGATGTT			

Supplementary Table 2-1. Primers used for gene expression analysis. Primers optimized by standard curve method using cDNA corresponding to 75ng RNA, diluted 2-fold. AE: amplification efficiency, calculated using the equation AE = (10(-1/slope))/-1. SSPN, sarcospan; DMD, dystrophin; UTRN, utrophin; DAG, dystroglycan, SCGA, α-sarcoglycan; SCGB, β-sarcoglycan; ITGA7, α7 integrin; ITGB1, β1D integrin; MYOG, myogenin; MYF5, myogenic factor 5; ACTB, β-actin; GADPH, glyceraldehyde 3-phosphate dehydrogenase.

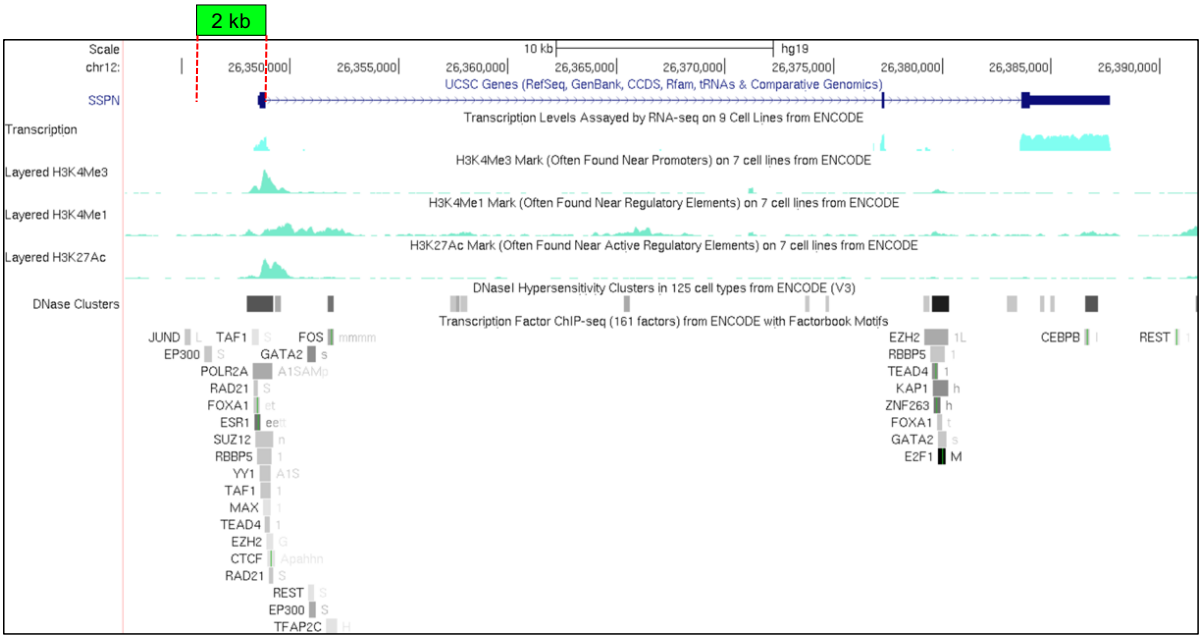

Supplementary Figure 2-1. Predicted human SSPN promoter region determined using UCSC genome browser. H2K4me3 marks, DNase hypersensitivity regions, and ChIP-seq data reveal predicted transcription factor binding sites in human skeletal muscle cultures. These analyses indicate that the SSPN promoter includes region upstream of exon 1 and within exon 1. Shown is skeletal muscle and cardiac-specific transcript variant 1 (NM_005086.4) of the human SSPN gene (NG_012011.2) in UCSC Genome browser human Feb. 2009 (GRCh37/hg19) assembly. Location shown: chr12:26,342,405-26,392,014.

PRIMER	SEQUENCE (5' → 3')	LOCATION
EGFP construct forward primer	GTGTAGATCTCAGGTGGGTGTCCTGGTATAA	2kb upstream of hSSPN TSS
EGFP construct reverse primer	GTGTAAGCTTCTCCTCCCCGCACTCCTT	Exon 1 of hSSPN
EGFP sequencing forward primer 1	ATAACCGTATTACCGCCATGCATTA	25bp upstream of hSSPN promoter
EGFP sequencing forward primer 2	CTCTAAGTGCTACTGAGTAGAGGTA	600bp within hSSPN promoter
EGFP sequencing forward primer 3	CAGCCACTTGGAGACTGAGGAGAGA	1200bp within hSSPN promoter

Supplementary Table 2-2. Primers used for reporter construct cloning and sequencing. Cloning optimized for human sarcospan (SSPN) gene region and pmEGFP-1 plasmid (EGFP).

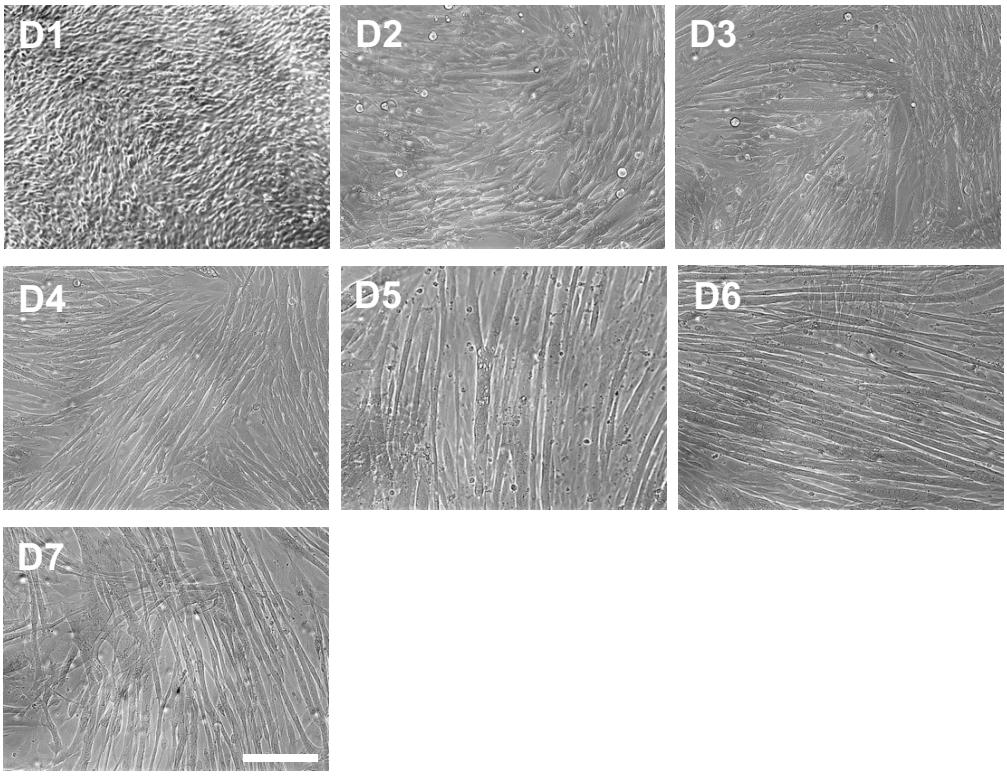

Supplementary Figure 2-2. C2C12 myoblasts undergoing differentiation and fusion into myotubes. Confluent C2C12 myoblasts (day 0, D0) were switched from proliferation to differentiation media and imaged daily using phase contrast microscopy for seven days (D1 to D7). Scale bar = 200 μm.

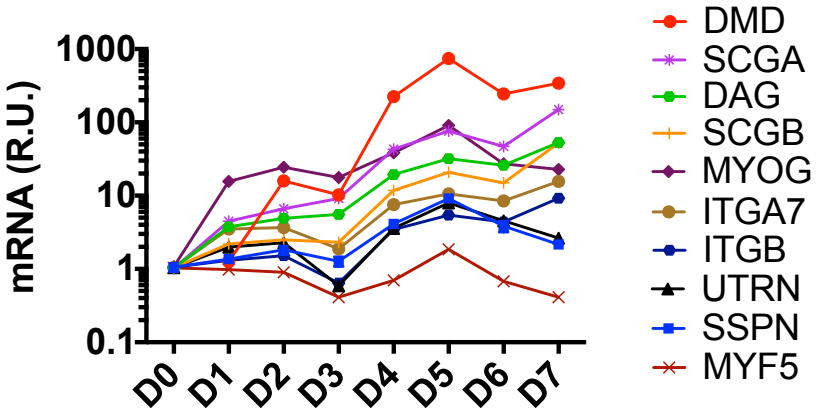

Supplementary Figure 2-3. Summary of gene expression of myofiber membrane adhesion complex members during C2C12 differentiation. Expression of individual genes encoding protein components of the three major adhesion complexes (DGC, UGC, and α7β1D-integrin complex) were investigated, including: (a) SSPN, sarcospan; (b) DMD, dystrophin; (c) UTRN, utrophin; (d) DAG, dystroglycan, (e) SCGA, α-sarcoglycan; (f) SCGB, β-sarcoglycan; (g) ITGA7, α7 integrin; and (h) ITGB1, β1D integrin. Gene expression was calculated using the ddCt method and normalized to β-actin with day 0 (myoblast) values serving as the calibrator sample (n=3). R.U., relative units.

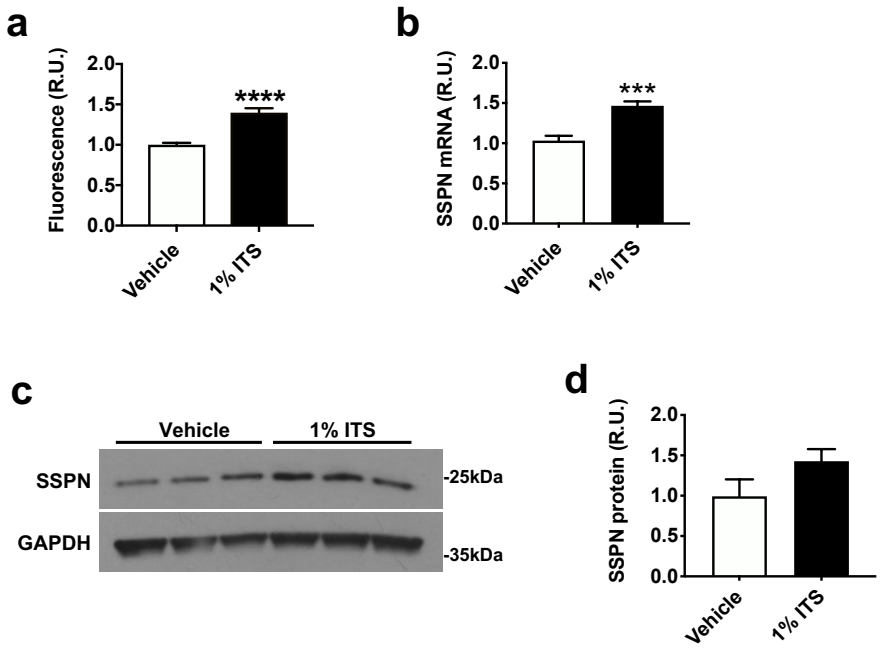

Supplementary Figure 4-4. Sarcospan reporter, gene, and protein levels increase similarly after treatment with positive control. Treatment with positive control, 1% insulin transferrin selenium (ITS), increased (a) reporter levels of hSSPN-EGFP reporter cells (n=10-21), (b) SSPN mRNA in wild-type C2C12 cells, and (c-d) SSPN protein in wild-type C2C12 cells. Images of the hSSPN-EGFP cells were analyzed using a MetaXpress custom analysis module. Gene expression was calculated using the ddCt method and normalized to β-actin with vehicle control values serving as the calibrator sample. For immunoblot analysis, total cell lysate was probed with anti-SSPN antibody. GAPDH is shown as a loading control. Quantification for immunoblot shown in panel (d). All cells were treated at day 2 of differentiation and assayed at day 4 of differentiation. Data reported as fold-change over vehicle-treated cells. *** $p<0.001$, **** $p<0.0001$.

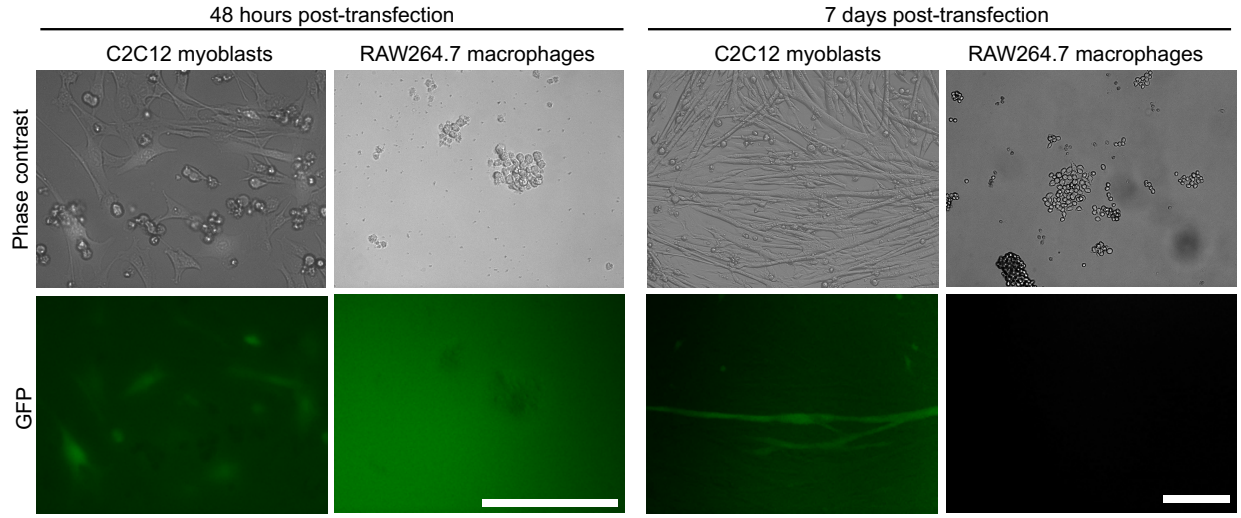

Supplementary Figure 2-5. hSSPN-EGFP construct is expressed in a cell-type specific manner. The hSSPN-EGFP plasmid was transfected into C2C12 murine myoblasts or RAW264.7 murine macrophages. At 48 hours and 7 days post-transfection EGFP was detected in the myoblasts, but not the macrophages. Scale bar = 100 μm.

Assay component	Optimized condition
Plate format	384-well black clear-bottom microplates
Seeding density	500 cells/well
Differentiation protocol	Serum deprivation at ~90% cell confluency (3 days post-seeding)
Treatment period	48 hours beginning at day 2 of differentiation
Vehicle/DMSO toxicity	Viability unaffected at <2% DMSO
Mixing	Mix DMSO by media addition to treated wells
Positive control	1% insulin transferrin selenium for 48 hours
Treatment dose	5.5 μM compound
Final DMSO conc.	0.55% DMSO
Imaging conditions	Fluorobrite low fluorescence media, 10X, 2 tile capture (40% well coverage)
Analysis	Custom analysis module to detect fluorescence intensity

Supplementary Table 2-3. Assay parameters optimized for high-throughput screening of hSSPN-EGFP myotubes. High-throughput assay conditions were optimized for a 384-well microplate format screen on hSSPN-EGFP reporter myotubes treated with a concentrated stock solution of 1 mM small molecule in 100% DMSO. Assay parameters optimized for C2C12 myotube screening were developed in the Molecular Screening Shared Resource facility using specialized, automated equipment (see Methods).

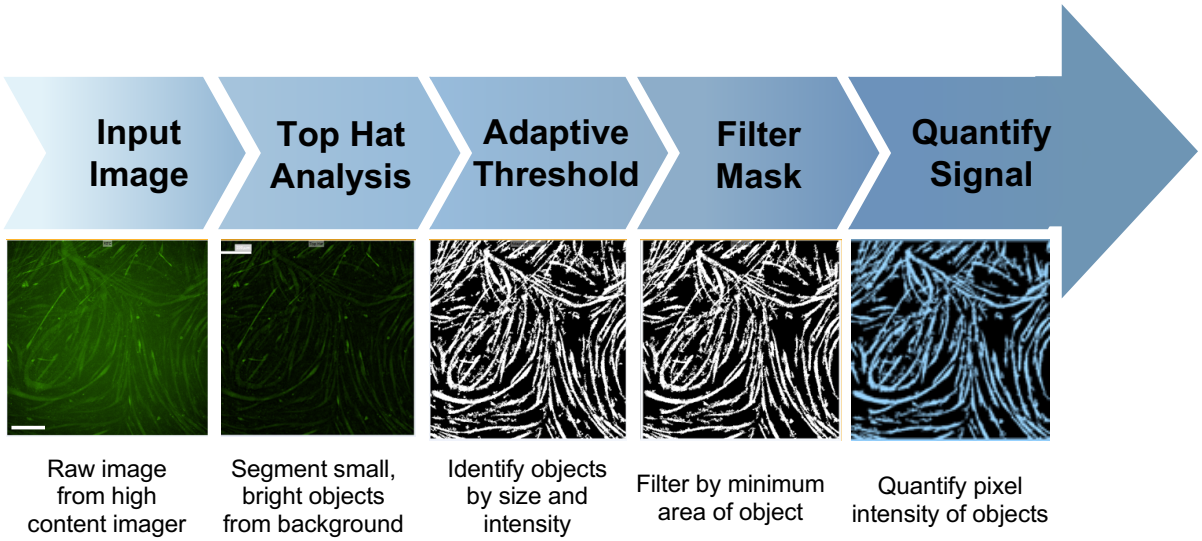

Supplementary Figure 2-6. High-content image analysis workflow. The MetaXpress custom analysis module processed images from high-content imaging by transforming the input image to remove background (Top Hat Analysis), identifying cells by size and intensity above local background (Adaptive Threshold), excluding debris by minimum area (Filter Mask), and quantifying fluorescence intensity of each resulting image. Scale bar, 220 μm.

Compound	Fluorescence (R.U.)	SSMD*	Description
Aceclidine	1.4	3.4	agonist of muscarinic receptors
Acyclovir	2.0	3.4	Herpesvirus DNA polymerase inhibitor
Alloxazine	1.9	3.2	Selective A2b adenosine receptor antagonist
Carbadox	1.4	3.6	antibacterial
Felodipine	1.8	3.2	L-type Ca^{2+} channel blocker
Felodipine	1.9	5.8	L-type Ca^{2+} channel blocker
GW5074	1.6	2.6	cRaf1 kinase inhibitor
Isradipine	1.6	2.3	L-type Ca^{2+} channel blocker
Lacidipine	1.4	3.8	L-type Ca^{2+} channel blocker
Nafadotride	1.5	2	dopamine antagonist
Nandrolone	2.7	5.2	anabolic-androgenic steroid
Nifedipine	1.4	1.9	L-type Ca^{2+} channel blocker
Nilvadipine	1.8	2.3	L-type Ca^{2+} channel blocker
Isoproterenol	1.7	3.1	Sympathomimetic amine acting on β-adrenoceptors

Supplementary Table 2-4. Initial hits from high-throughput screening of hSSPN-EGFP myotubes. The screen of 3,200 compounds resulted in 13 initial hits, which included an overrepresented number of L-type calcium channel blockers (felodipine, isradipine, lacidipine, nifedipine, and nilvadipine) and one hit (felodipine) which appeared as a hit twice from two independent libraries. Robust strictly standardized mean difference (SSMD*) was used to classify the strength of each hit. SSMD* > 0.25 and 1.4-fold change over vehicle was the minimum to be considered an initial hit. R.U., relative units normalized to vehicle control.

	hSSPN-EGFP			
	Plate 1		Plate 2	
Compound	R.U.	SSMD*	R.U.	SSMD*
Aceclidine	1.1	-0.07	1.1	0.25
Acyclovir	0.9	-0.37	1.0	0.19
Alloxazine	1.0	-0.03	1.1	0.21
Carbadox	1.1	0.21	1.1	0.43
Felodipine	1.4	1.75	1.4	1.56
GW5074	1.2	0.67	1.2	0.78
Isoproterenol	1.1	0.26	1.1	0.26
Isradipine	1.5	1.79	1.4	1.50
Lacidipine	1.3	0.69	1.2	1.02
Nafadotride	1.1	-0.09	1.0	-0.01
Nandrolone	1.2	0.44	1.1	0.41
Nifedipine	1.3	0.41	1.0	0.22
Nilvadipine	1.6	1.08	1.5	0.97

Supplementary Table 2-5. Validation of hits from screen on hSSPN-EGFP myotubes. Initial hits from the screen were retested on hSSPN-EGFP myotubes at 5.5 μM in 2 plates (n=24 per plate). R.U., relative units normalized to vehicle control. *SSMD, robust strictly standardized mean difference.

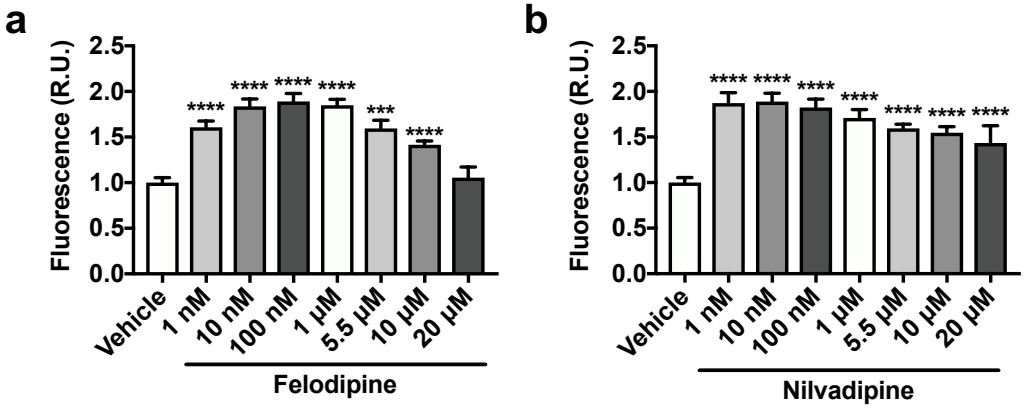

Supplementary Figure 2-7. Titration of screen hits on hSSPN-EGFP myotubes. hSSPN-EGFP myotubes were treated with 1 nM-20 μM of (a) felodipine of (b) nilvadipine for 48 hours and imaged at day 4 of differentiation using a high-content imager (n=12). Images were analyzed using a MetaXpress custom module to calculate fluorescence over vehicle (R.U., relative units).

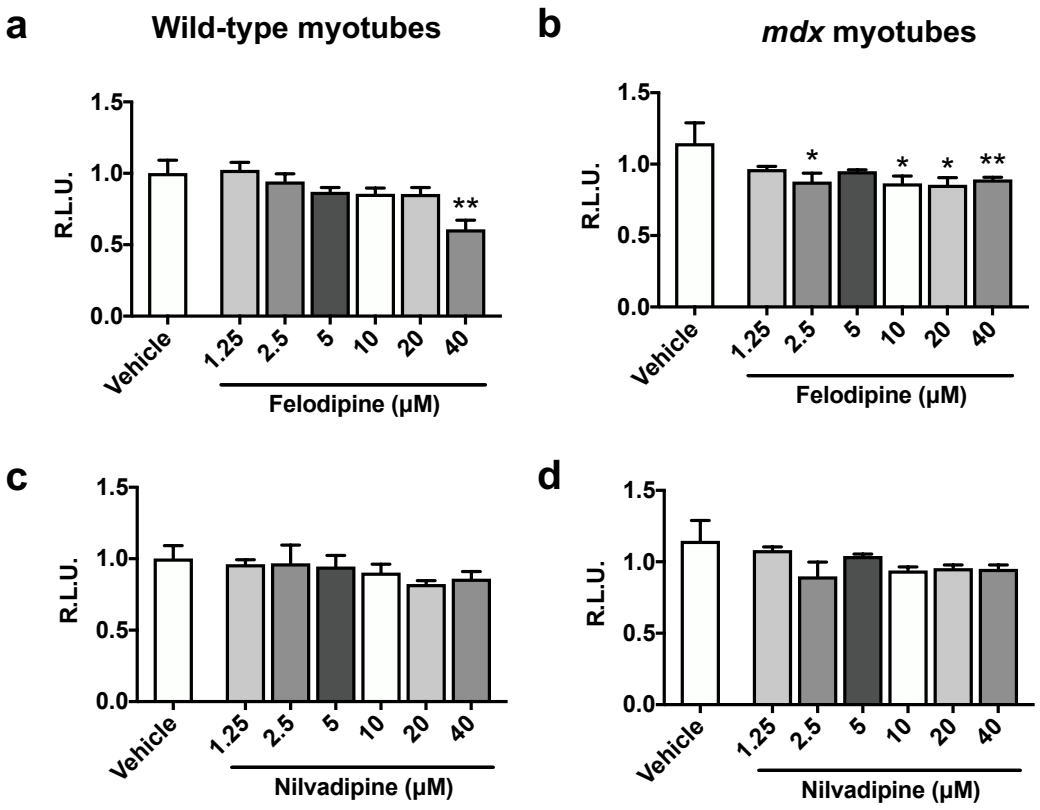

Supplementary Figure 2-8. Effect of felodipine and nilvadipine on cell viability of C2C12 wild-type and H2K *mdx* myotubes. C2C12 wild-type and H2K *mdx* myotubes were treated with 1.25-40 μM of felodipine for 48 hours and assayed at day 4 of differentiation using an ATP-based cell viability assay.

Chapter 3

High-throughput screening identifies modulators of sarcospan that stabilize the muscle cell membrane and exhibit *in vivo* activity in mouse model of Duchenne muscular dystrophy

Cynthia Shu[1-3], Liubov Parfenova[2], Ekaterina Mokhonova[2,3], Judd R. Collado[2], Robert Damoiseaux[4,5], Jesus Campagna[6,7], Varghese John[6,7], and Rachelle H. Crosbie[1-3,6]

[1]Molecular Biology Institute, University of California Los Angeles, [2]Department of Integrative Biology and Physiology, University of California Los Angeles, [3]Center for Duchenne Muscular Dystrophy, University of California Los Angeles, [4]Department of Molecular and Medicinal Pharmacology, University of California Los Angeles, [5]California NanoSystems Institute, University of California Los Angeles [6]Department of Neurology, David Geffen School of Medicine, University of California Los Angeles, [7]Drug Discovery Lab, University of California Los Angeles

Abstract

Duchenne muscular dystrophy (DMD) is a degenerative muscle disease caused by mutations in the dystrophin gene. Loss of dystrophin prevents the formation of a critical connection between the muscle cell membrane and the extracellular matrix. Overexpression of sarcospan (SSPN) in the mouse model of DMD restores the membrane connection and reduces disease severity, making SSPN a promising therapeutic target. Using cell-based reporter assays of SSPN gene expression, we conducted high-throughput screening to identify small molecule

enhancers of SSPN. We identified and validated lead compounds that increased SSPN gene and protein expression in dystrophin-deficient mouse and DMD human muscle cells. The lead compound OT-9 increased cell membrane localization of laminin-binding adhesion complexes and improved membrane stability in DMD myotubes as determined by an osmotic shock assay. We demonstrated that the membrane stabilizing benefit is dependent on SSPN. Intramuscular injection of OT-9 in the mouse model of DMD increased SSPN gene expression. This study identifies a novel method to treat DMD through pharmacological upregulation of SSPN.

Introduction

Duchenne muscular dystrophy (DMD) is a degenerative muscle disease that affects 1 in every 5,700 males.[24] DMD is caused by mutations in the gene encoding for the dystrophin protein. Currently, the only Food and Drug Administration approved treatments for DMD are corticosteroids and exon skipping therapies. In clinical trials, corticosteroids and morpholinos extend age of loss of ambulation by several years, but are not considered a cure.[15, 65] Although significant progress has been made in the development DMD therapies, there remains a need for treatments that can improve the quality of life and life expectancy of individuals affected by DMD. Small molecules are the most common modality used to treat diseases due to ease of delivery and reduced risk for immune responses relative to viral or cell-based modalities. In this study, we report on the identification and characterization of a small molecules that are predicted to benefit all DMD patients regardless of mutation. Lastly, we demonstrate the *in vivo* efficacy of a lead hit compound using the dystrophin-deficient *mdx* murine model for DMD.

In healthy muscle, dystrophin localizes to the intracellular surface of myofibers where it connects the actin cytoskeleton, cell membrane (sarcolemma), and extracellular matrix (ECM) to

stabilize the muscle cell during contractions.[26, 29] Dystrophin associates with sarcospan (SSPN), the sarcoglycans, the dystroglycans, and numerous other proteins to form the dystrophin-glycoprotein complex (DGC).[21, 53-55] Within the DGC, dystrophin interacts directly with F-actin and β-dystroglycan, which associates with the laminin-binding protein, α-dystroglycan (α-DG).[32] The DGC is one of three major adhesion complexes in muscle that serve to connect the myofiber to the ECM and its presence is critical for proper muscle maintenance. In individuals with DMD, loss of dystrophin and the DGC leads to contraction-induced damage and muscle degeneration.[56] By the second to third decade of life, individuals with DMD experience severe muscle wasting that also affects the heart and respiratory system.[24]

Along with the DGC, the utrophin-glycoprotein complex (UGC) and the α7β1D-integrin complex serve as adhesion complexes between the cell membrane and the ECM.[57, 58] The UGC localizes to neuromuscular junctions and has a similar composition to the DGC, with utrophin taking the place of dystrophin.[38, 39, 59] Extra-synaptic redistribution of the UGC is well documented in dystrophin-deficient muscle, suggesting the existence of a compensatory mechanism involving upregulation of endogenous adhesion complexes.[79] Decades of research have since established that transgenic upregulation of the UGC and α7β1D-integrin complex prevents muscle pathology in the *mdx* mouse model of DMD by compensating for the loss of the DGC.[41, 60]

SSPN is a 25 kDa transmembrane protein that is expressed in striated muscle and associates with all three adhesion complexes.[5, 33, 42] Mutagenesis studies demonstrated that SSPN protein contains multiple oligomer interaction sites and that it forms a tight association with the sarcoglycans, suggesting that SSPN acts as a protein scaffold.[42] Transgenic overexpression of SSPN in *mdx* mice increased the membrane localization of the UGC and the α7β1D-integrin

complex, leading to improved membrane stability, reduced muscle pathology, and improved muscle function.[4, 5, 43] In addition to the improvements in skeletal muscle, SSPN upregulation improved cardiac and respiratory function, the major cause of mortality among DMD patients.[4, 6] Importantly, 30-fold increased levels of SSPN did not induce detrimental side effects, demonstrating that SSPN therapies are both safe and effective in pre-clinical studies.[4] In the current study, we identified and characterized small molecule modalities to increase SSPN. Our results demonstrate that pharmacological targeting of SSPN produces therapeutic levels of SSPN protein in dystrophin-deficient myotubes.

Results

We previously created and validated a muscle cell-based high-throughput assay to identify small molecule enhancers of human SSPN gene expression.[19] Using the assay, we screened libraries of clinical compounds and demonstrated that the assay is capable of identifying small molecules that increase SSPN gene and protein expression in both wild-type and dystrophin deficient myotubes.[19] In this current study, we screened large chemical libraries with the goal of identifying compounds that can be developed into new chemical entity enhancers of SSPN. The curated libraries were developed to maximize drug-likeness based on Lipinski's rule of 5, which defines parameters that can be used to predict optimal oral bioavailability in humans.[80]

High-throughput screening of 200,000 small molecules

High-throughput screening of over 200,000 small molecules from curated libraries was conducted using a cell-based assay for human SSPN gene expression. The reporter cells used in the assay were C2C12 murine myoblasts stably transfected with a construct containing the human SSPN promoter region followed by the coding sequence for enhanced green fluorescent protein

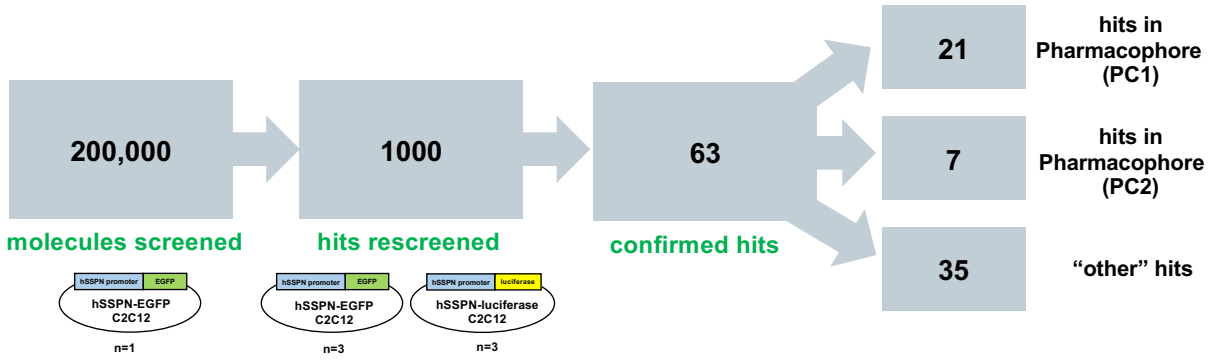

Figure 3-1. Pipeline for high-throughput screening and hit confirmation. Large chemical libraries were screened using the hSSPN-EGFP C2C12 reporter cell line (n=1). The top 1000 hits were rescreened in both hSSPN-EGFP and hSSPN-luciferase C2C12 reporter cell lines (n=3 each). 63 of the 1000 compounds increased reporter expression in both cell lines and were therefore considered confirmed hits. The confirmed hits were sorted into 3 groups based on common structural features: pharmacophore 1 (PC1), pharmacophore 2 (PC2), and other, which had no unifying structural theme.

(hSSPN-EGFP). Using the hSSPN-EGFP assay, we screened compounds at a dose of 5.5 μM (n=1) (Fig. 3-1). Plate quality was calculated using robust strictly standardized mean difference (SSMD*) (Supplementary Table 3-1). To rule out assay-specific false positives, we counterscreened using a stably transfected reporter cell line containing a luciferase reporter for human SSPN promoter activity (hSSPN-luc). The top 1000 hits were rescreened in both hSSPN-EGFP (n=3) and hSSPN-luciferase promoter reporter myotubes (n=3). Of the 1000 hits, 63 compounds increased reporter expression in both reporter cell lines and were therefore considered confirmed hits. The confirmed hits were sorted into three groups based on common structural features: pharmacophore 1, pharmacophore 2, and the other category, which had no unifying structural features. Pharmacophore 2 compounds consisted of flat, multi-ring structures known to intercalate into DNA, which was considered a liability. We therefore focused on the pharmacophore 1 and other class of compounds.

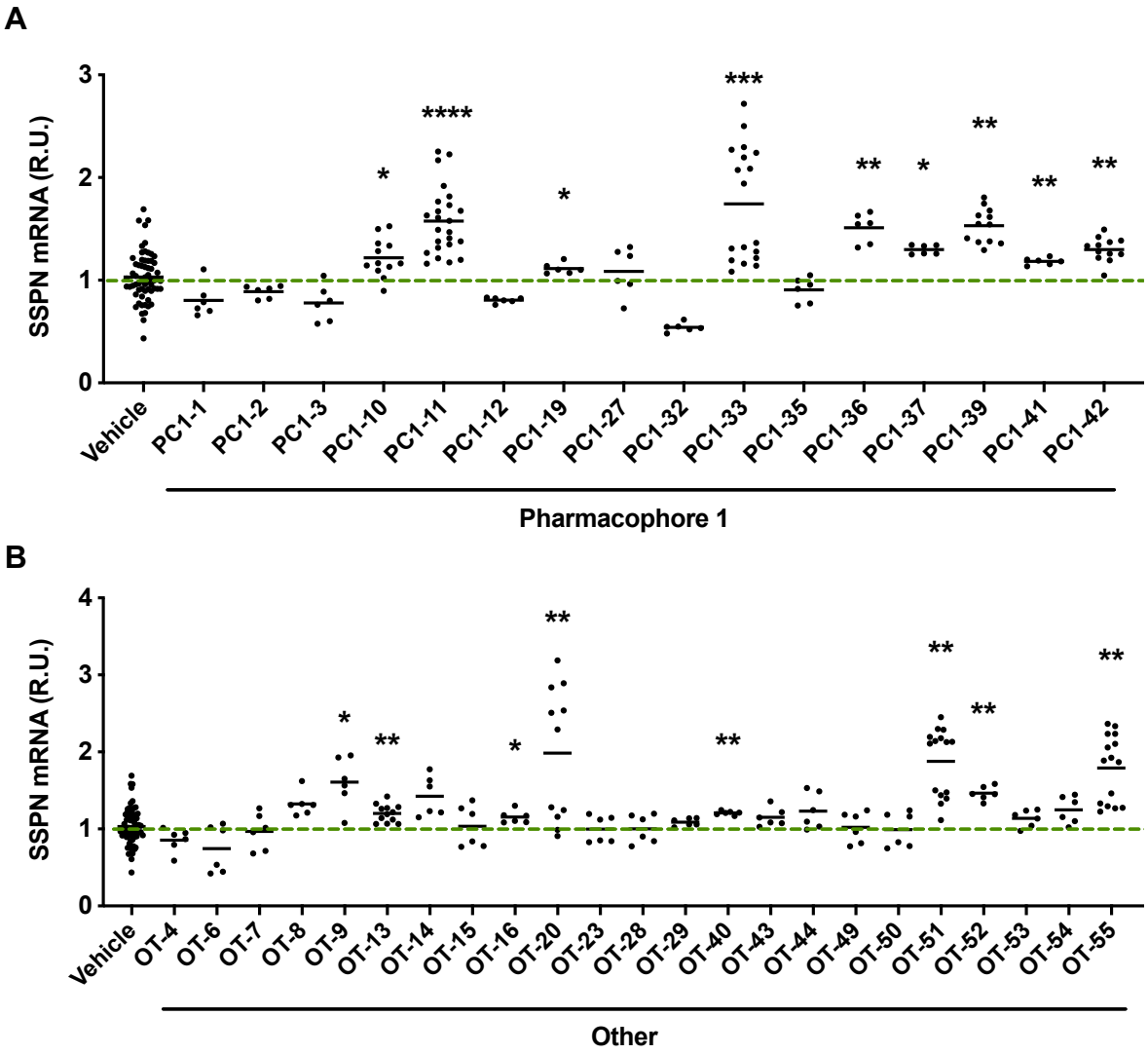

Figure 3-2. Hit-to-lead selection: Single dose treatment and quantification of SSPN gene expression in H2K mdx myotubes. Dystrophin-deficient H2K mdx cells were treated with 5.5 μM of (A) pharmacophore 1 (PC1) or (B) other compounds for 48 hours. All cells were treated at day 2 of differentiation and harvested 48 hours post-treatment. Gene expression was normalized to housekeeping gene β-actin and vehicle-treated cells (0.5% DMSO). Data represents individual replicates and mean value. n=3-8. *p<0.05, **p<0.01, ***p<0.001, ****p<0.0001.

Hit-to-lead selection using dystrophin deficient murine and human muscle cells

For the initial hit-to-lead selection, all commercially available confirmed hits were tested at a dose of 5.5 μM in dystrophin-deficient murine *mdx* myotubes to determine if the compounds were active in a relevant disease model. Within the pharmacophore 1 group, nine of the sixteen hits increased SSPN gene expression between 1.1 to 1.8-fold relative to the vehicle control (Fig.

3-2A). With the other group, eight of the twenty three other hits increased SSPN gene expression between 1.2 to 2.0-fold (Fig. 3-2B). The initial hit-to-lead selection demonstrated that sequential screening with two separate reporter cell lines enables identification of compounds that increase SSPN mRNA levels in both wild-type and dystrophin-deficient murine muscle cells.

After excluding compounds that were unstable in solution or that produced highly variable results, nine compounds remained. These nine compounds were tested at six different doses ranging from 0.5 to 50 μM in *mdx* myotubes to determine the activity of the compounds across a broad range of concentrations. All the compounds except PC1-41 demonstrated activity with at least one dose (Fig. 3-3A). PC1-36, PC1-42, and OT-9 induced a dose-dependent response that peaked at the 5.5 μM dose. To determine if the increase in SSPN mRNA was also evident at the protein level, we treated *mdx* myotubes with 2.5 to 10 μM of OT-9, PC1-36, and PC1-42 and analyzed total protein lysates by immunoblotting with SSPN antibodies. We found that PC1-42 did not induce an increase in SSPN protein (data not shown). Compounds OT-9 and PC1-36 increased SSPN protein levels in the *mdx* myotubes by 1.5-fold, demonstrating that these compounds increased both SSPN gene and protein abundance in dystrophin-deficient muscle cells (Fig. 3-3B-C).

Previously, we profiled SSPN gene expression in differentiating myotubes and found that SSPN mRNA begins to increase on day three and reaches 10-fold increased levels on day five of differentiation, indicating that SSPN levels increase as cells differentiate.[19] To determine if the drug-induced increase in SSPN expression was due to enhanced differentiation, we treated *mdx* myotubes with OT-9 and assessed fusion index and expression of the myogenic transcription factor MYOG, markers of differentiation. OT-9 induced a slight increase in fusion index and MYOG gene expression in *mdx* myotubes, suggesting OT-9 may, in part, work through differentiation

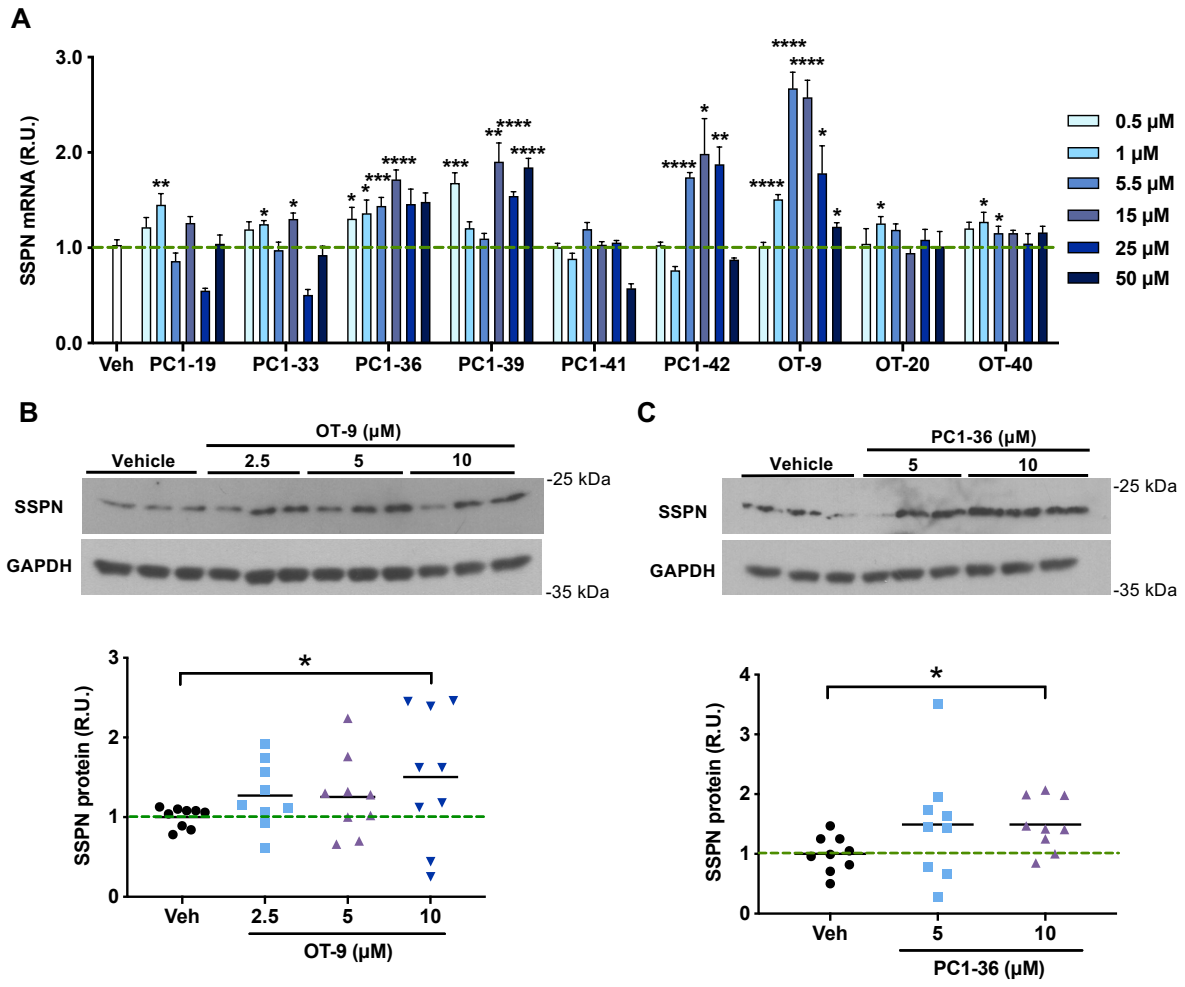

Figure 3-3. Confirmed hits increase SSPN gene and protein expression in H2K mdx myotubes. (A) Relative SSPN gene expression in dystrophin-deficient H2K mdx cells treated with 0.5-50 µM of pharmacophore 1 or other compounds for 48 hours. Data are represented as mean + SEM. n=3-6. (B) SSPN immunoblot of dystrophin-deficient H2K mdx cells treated with 2.5 to 10 µM of compounds for 48 hours. All cells were treated at day 2 of differentiation and harvested 48 hours post-treatment. Gene expression was normalized to housekeeping gene β-Actin and vehicle-treated cells (0.29% DMSO). SSPN protein levels were quantified in ImageJ and normalized to GAPDH and vehicle-treated cells (0.2% DMSO). Cell lysates were probed between 2-4 times in independent western blots. Representative blots shown. Quantification includes all experiments. Data represents individual replicates and mean value. n=3 per dose. *p<0.05, **p<0.01, ***p<0.001, ****p<0.0001.

pathways or that the increase in SSPN may increase the rate of differentiation (Supplementary Fig. 3-1).

To validate that the confirmed hits were not acting in a cell line-specific manner, we tested OT-9 and PC1-36 in wild-type C2C12 myotubes and immortalized myotubes from a healthy

human patient. We found that the compounds increased SSPN mRNA levels in both cell lines, demonstrating that the hits worked across a range of cell lines (Supplementary Fig. 3-2). Treatment of C2C12 murine, human, H2K WT murine, and H2K *mdx* murine myoblasts revealed that OT-9, but not PC1-36, increased SSPN transcript levels in all myoblast lines, suggesting that OT-9 and PC1-36 have different biological targets (Supplementary Fig. 3-3). To determine if increased myoblast proliferation accounted for the elevation in SSPN gene expression upon drug treatment, we quantified healthy human myoblasts after 24 hours of treatment with 5 μM of OT-9 (Supplementary Fig. 3-4). We found that OT-9 did not increase the number of cells per well and therefore concluded that the increase in SSPN gene expression was not due to increased proliferation.

To determine if the confirmed hits increase SSPN protein levels in human muscle cells, we first created an enzyme-linked immunosorbent assay (ELISA) capable of detecting changes in human SSPN levels across samples. Using recombinant human SSPN as a standard, we tested three pairs of commercially available antibodies that recognize different epitopes of the human SSPN polypeptide (Supplementary Fig. 3-5A-B). The antibodies were either conjugated to the plate to capture SSPN protein (capture) or used to detect captured SSPN protein (detecting). The E2 capture + LS-N detecting (E2 cap + LS-N det) antibody combination produced the highest signal (Supplementary Fig. 3-5C). We determined that using this antibody pair, the ELISA was capable of detecting as little as 1-2 pg of SSPN (Supplementary Fig. 3-5D-E). Using the ELISA, we found that DMD human myotubes treated for 48 hours with 5 μM of OT-9 and PC1-36 exhibited an increase in SSPN protein of 1.5 and 1.25-fold, respectively (Fig. 3-4A). Confirmation by immunoblot analysis using SSPN antibodies revealed a 1.3-fold increase in SSPN protein abundance after 48 hours of OT-9 treatment (Fig. 3-4B-C). We selected the more effective

compound, OT-9, for further assessment using functional assays.

OT-9 compound increases laminin-binding adhesion complexes at the cell surface

In striated muscle, SSPN is a scaffold for the three major laminin-binding adhesion complexes that connect the cell membrane (sarcolemma) to the extracellular matrix: the DGC, UGC, and α7β1D-integrin. Overexpression of SSPN in *mdx* muscle increases the localization of the UGC and α7β1D-integrin complex.[4, 5, 43] To determine if the OT-9-affects SSPN localization at the cell membrane in myotubes, we labeled cell surface proteins with an amine-reactive biotin. C2C12 myotubes treated with OT-9 were incubated in cell impermeable biotin, lysed to solubilize proteins, affinity purified with avidin, and eluted with LSB to obtain cell surface proteins. Using antibodies that recognize the laminin-binding glycoepitope of α-DG (IIH6) and the

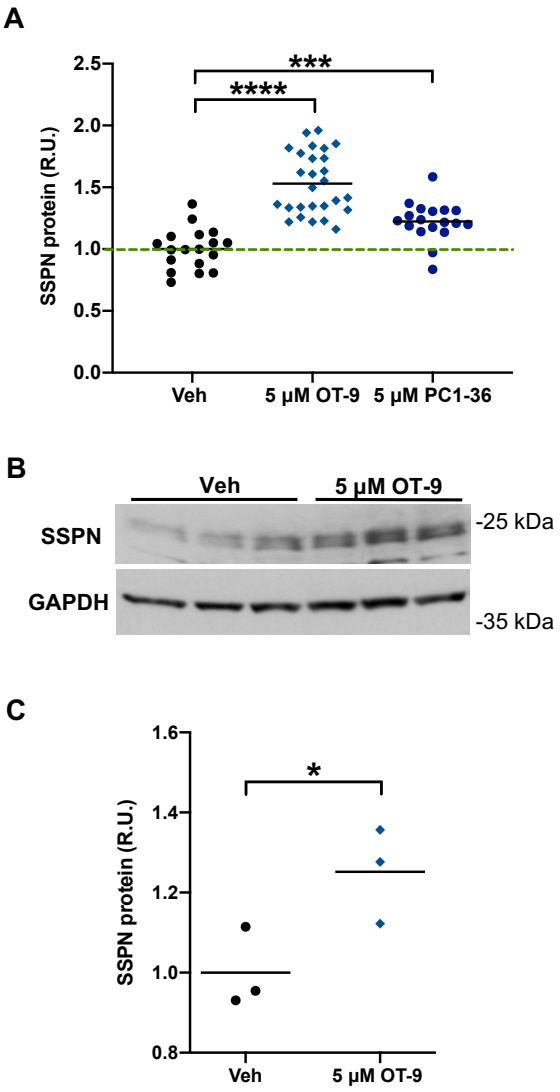

Figure 3-4. OT-9 increases sarcospan protein levels in human DMD myotubes. DMD myotubes treated with OT-9 exhibit an increase in SSPN protein levels as quantified by (A) an indirect sandwich ELISA and (B) immunoblot analysis. (C) Quantification of immunoblot results. Cells were treated on day 2 of differentiation and harvested after 48 hours. R.U. = relative units normalized to protein concentration for the ELISA and GAPDH for the immunoblot analysis. Data represents individual replicates and mean value. n=3-27. *p<0.05, ****p<0.0001.

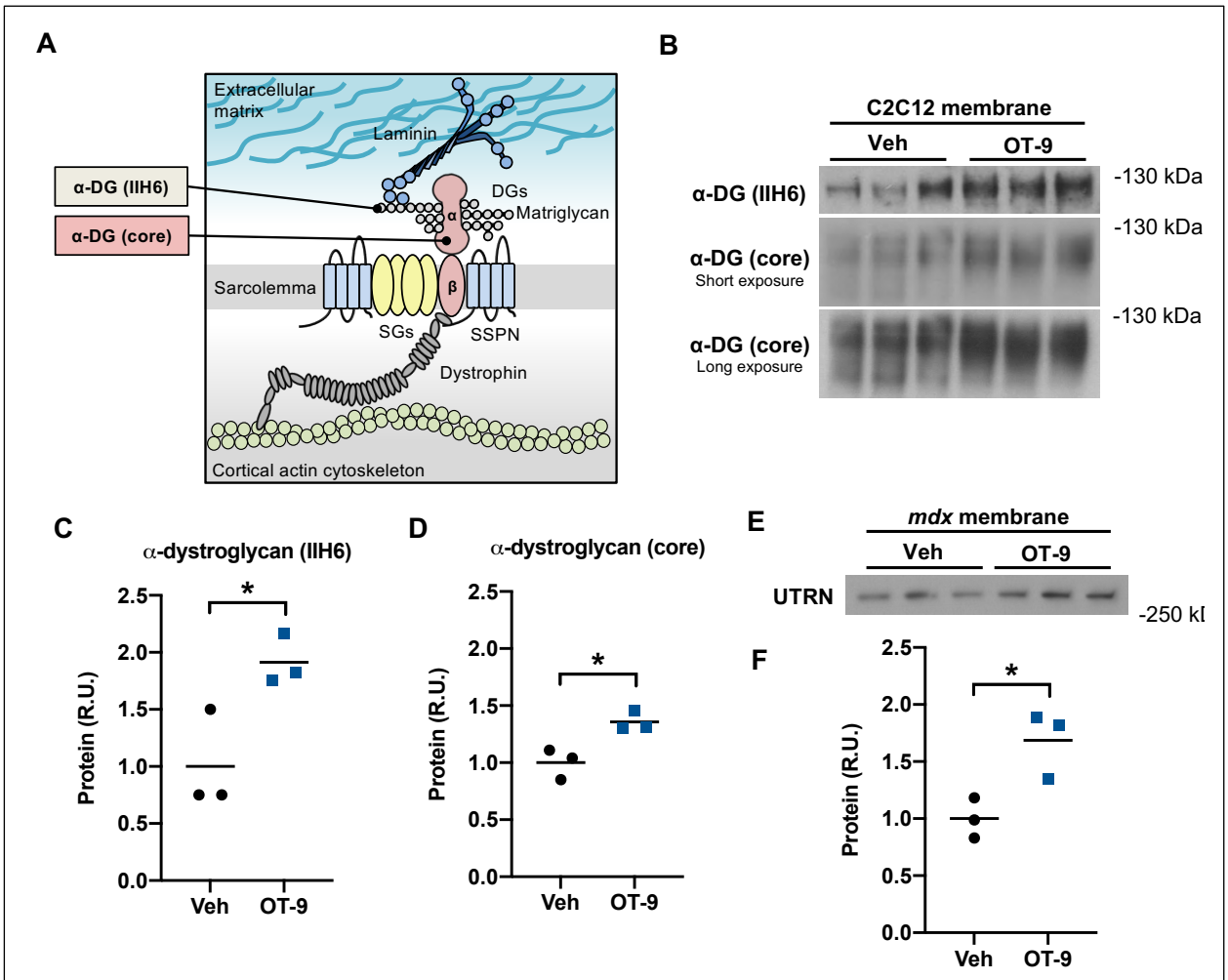

Figure 3-5. OT-9 increases laminin-binding adhesion complexes at cell surface. C2C12 myotubes treated with vehicle or 5 μM of OT-9 for 48 hours were incubated in amine-reactive biotin to label cell surface proteins. Avidin was used to affinity purify the labelled proteins before immunoblot analysis with (A) antibodies recognizing the laminin-binding glycoepitope of α-dystroglycan (α-DG (IIH6)) or core α-dystroglycan (B) In cells treated with OT-9, both glycosylated α-dystroglycan (IIH6) and core α-dystroglycan are increased at the cell surface. (C-D) Quantification of immunoblots. (E) *mdx* myotubes treated with vehicle or 5 μM of OT-9 for 48 hours were incubated in biotin to label cell surface proteins and affinity purified with avidin. Immunoblot analysis demonstrates upregulation of utrophin associated with biotin-labelled cell surface proteins. (F) Quantification of utrophin immunoblot. Data represents individual replicates and mean value. n=3. R.U. = relative units normalized to vehicle control.

core α-DG protein (Fig. 3-5A), we performed immunoblot analysis of the biotinylated cell surface proteins and total lysate. OT-9 increased the mature form of α-DG (IIH6) by 1.8-fold and core α-DG by 1.6-fold at the cell surface (Fig. 3-5B-D). Immunoblot analysis of total protein lysates revealed that OT-9 increased core α-DG by 1.5-fold, but did not increase α-DG IIH6

(Supplementary Fig. 3-6).

In *mdx* mice overexpressing SSPN, the dystrophin paralogue utrophin is upregulated at the sarcolemma and contributes to the increase in membrane to ECM adhesion.[4, 5, 43] Using the same biotinylation experimental approach, we assessed whether OT-9 affected utrophin expression at the cell surface membrane. While utrophin is intracellular and therefore not directly biotinylated, the solubilization buffer contained a gentle detergent that preserved interactions within adhesion complexes, including that of utrophin, β-dystroglycan, and the cell surface α-DG. *mdx* myotubes treated with OT-9 exhibited a 1.6-fold increase in membrane-associated utrophin protein (Fig. 3-5E-F). Taken together, our findings demonstrate that OT-9 increased the sarcolemmal localization of both α-DG and utrophin, suggesting an upregulation of the laminin-binding utrophin glycoprotein complex.

OT-9 improves membrane stability in dystrophin-deficient myotubes through upregulation of sarcospan

To determine if the increase in utrophin and dystroglycan at the cell membrane resulted in a functional improvement in membrane stability, we used a modified protocol for an *in vitro* creatine kinase (CK) release assay.[81] The assay entails subjecting myotubes to osmotic shock, which causes cell swelling and membrane damage, allowing for intracellular CK to be released from the cell into the surrounding media (Fig. 3-6A). To determine the optimal conditions for osmotic shock that result in a detectable change in CK release, we subjected *mdx* and DMD myotubes treated with vehicle or 5 μM of OT-9 for 48 hours prior to osmotic shock using solutions ranging from 28.5 to 223.5 milliosmoles (mosmol), with 223.5 mosmol being closest to physiological osmolarity (280 mosmol). Both *mdx* and DMD myotubes exhibited higher CK

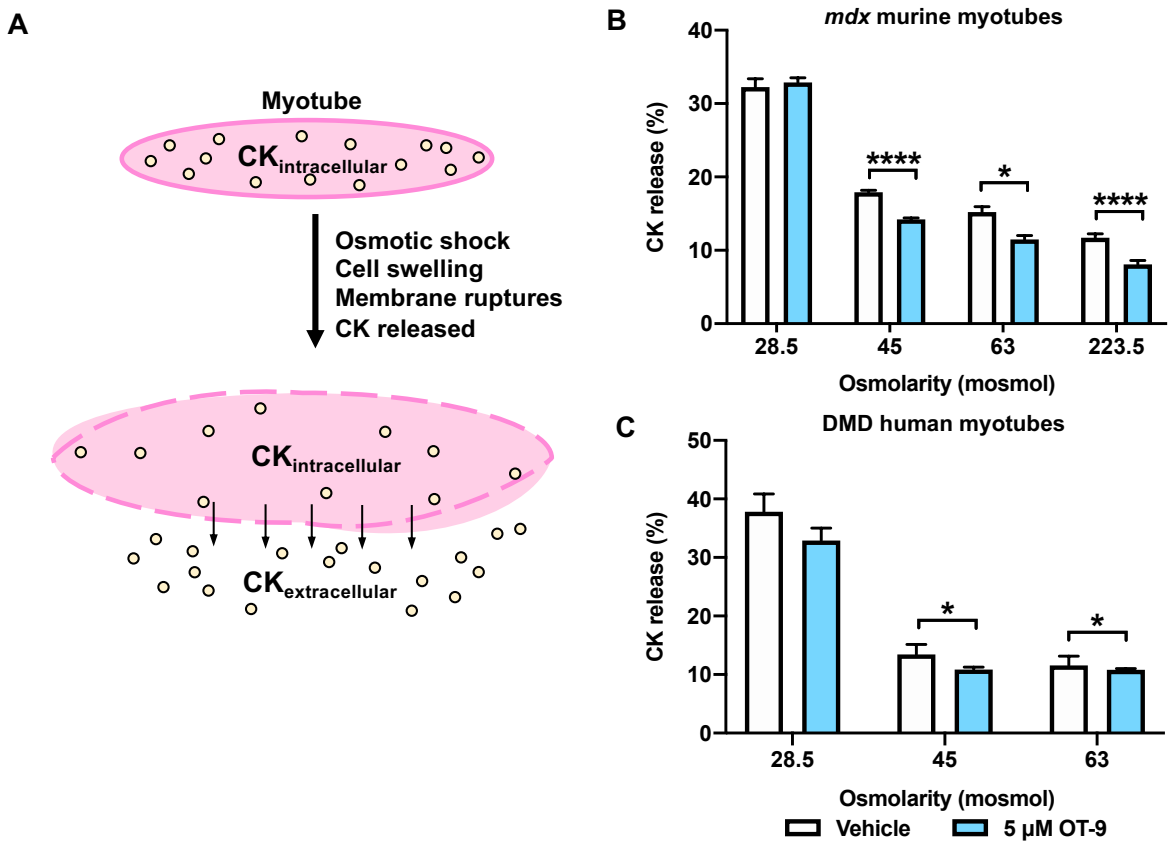

Figure 3-6. Creatine kinase release assay shows that OT-9 improves membrane stability of *mdx* murine and DMD human myotubes. (A) The creatine kinase (CK) release assay entails subjecting myotubes to osmotic shock, which causes cell swelling and membrane damage, allowing for intracellular CK to be released from the cell into the surrounding media. CK release is calculated by taking the ratio of $CK_{supernatant}/(CK_{supernatant} + CK_{intracellular})$. Day 2 **(A)** *mdx* and **(B)** DMD myotubes treated were treated for 48 hours with 5 µM of OT-9 and subjected to osmotic shock with solutions ranging from 28.5 to 224.5 milliosmols (mosmol). Data represents mean + SEM. n=3. *p<0.05, ****p<0.0001.

release with lower, more damaging osmolarity concentrations (Fig. 3-6B-C). Osmotic shock with the 28.5 mosmol solution resulted in a 30-40% CK release in both cell lines, while the 45 and 63 mosmol solution caused a 10-15% CK release, indicating relatively less membrane damage. In cells subjected to osmotic shock with 45, 63, and 223.5 mosmol, OT-9 significantly reduced CK release, revealing that OT-9 stabilized the sarcolemma to protect it from osmotic shock-induced membrane damage. Treatment with OT-9 did not reduce CK release in cells subjected to osmotic shock with 28.5 mosmol solutions, indicating that OT-9 was not able to stabilize the membrane likely due to severe membrane damage caused by the extremely low osmolarity.

To determine if the membrane stabilizing effect induced by OT-9 was dependent on SSPN, we performed siRNA-mediated knockdown of SSPN in parallel with drug treatment. To assess knockdown efficiency, we first treated *mdx* myotubes with 1, 5, or 10 μM of OT-9 and 24 pmol of scramble siRNA or siRNA targeting SSPN transcript (SSPN siRNA). In vehicle-treated cells, SSPN siRNA reduced SSPN transcript levels by 76% relative to the scramble control (Supplementary Fig. 3-7). In cells treated with scramble siRNA and OT-9, SSPN mRNA increased by up to 1.4-fold relative to the vehicle control. In cells treated with SSPN siRNA and OT-9, SSPN levels were reduced relative to their respective scramble siRNA controls. However, even with SSPN siRNA, OT-9 increased SSPN mRNA levels due to the incomplete knockdown, leading us to use a higher siRNA dose in subsequent experiments.

To assess the effect of SSPN knockdown on membrane stability in the absence of any drug treatment, we transfected *mdx* myotubes with 24 and 48 pmol of scramble and SSPN siRNA and subjected the cells to osmotic shock with 45 mosmol solutions. In cells transfected with 24 pmol of siRNA, knockdown of SSPN did not affect CK release (Fig. 3-7A). However, in cells transfected with 48 pmol of siRNA, knockdown of SSPN increased CK release from 9% to 13%, indicating that loss of SSPN itself renders the sarcolemma more susceptible to membrane damage. To prevent confounding the data with changes in baseline CK release induced by SSPN knockdown, we selected the 24 pmol siRNA dose for following studies because it did not affect baseline CK release. We treated *mdx* myotubes with 10 μM of OT-9 in parallel with 24 pmol of scramble or SSPN siRNA for 48 hours prior to osmotic shock and discovered that depletion of SSPN increased the CK release from 6.5% to 8% (Fig. 3-7B). The results revealed that knockdown of SSPN reduced the ability of OT-9 to stabilize the sarcolemma, indicating that SSPN expression

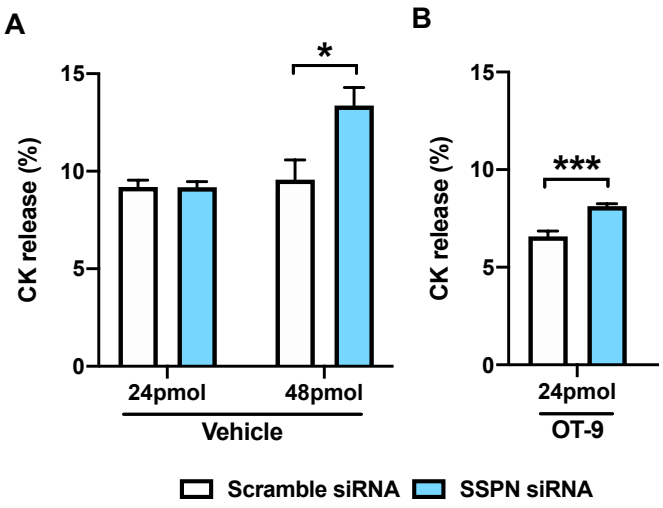

Figure 3-7. Loss of sarcospan exacerbates *in vitro* membrane damage and reduces ability of OT-9 to stabilize membrane. (A) *mdx* myotubes were transfected with 24 or 48 pmol of siRNA targeting sarcospan transcript. After 48 hours, myotubes were subjected to osmotic shock with 45 mosmol solutions. At 24 pmol of SSPN siRNA, there is no change between scramble control. At 48 pmol of SSPN siRNA, the CK release increases relative to the scramble control. (B) *mdx* myotubes treated in parallel with 24 pmol of SSPN siRNA and 10 μM of OT-9 show that depletion of sarcospan reduced the ability of OT-9 to improve membrane stability, indicating sarcospan contributes to membrane stability regardless of drug treatment. Data represents mean + SEM. n=3. *p<0.05, **p<0.01, ***p<0.001, ****p<0.0001.

is required for the full membrane stabilizing effect of OT-9.

Intramuscular injection of OT-9 increases SSPN gene expression in *mdx* mice

After demonstrating the ability of OT-9 to increase SSPN protein and laminin-binding adhesion complexes at the membrane, which in turn led to improved membrane stability in dystrophin-deficient myotubes, we next interrogated the capacity of OT-9 to increase SSPN gene expression *in vivo*. Estimation of OT-9 stability revealed a large difference in half-life of the drug in mouse plasma (7.7 hours) versus PBS (49 mins) (Supplementary Table 3-1 and 3-2). Because cell culture media is distinct from both solutions, we quantified SSPN transcript stability in C2C12 myotubes treated with 5 μM of OT-9 for 4 hours to determine if short-term treatment could induce SSPN expression. After 4 hours of treatment with OT-9, media containing the drug was removed

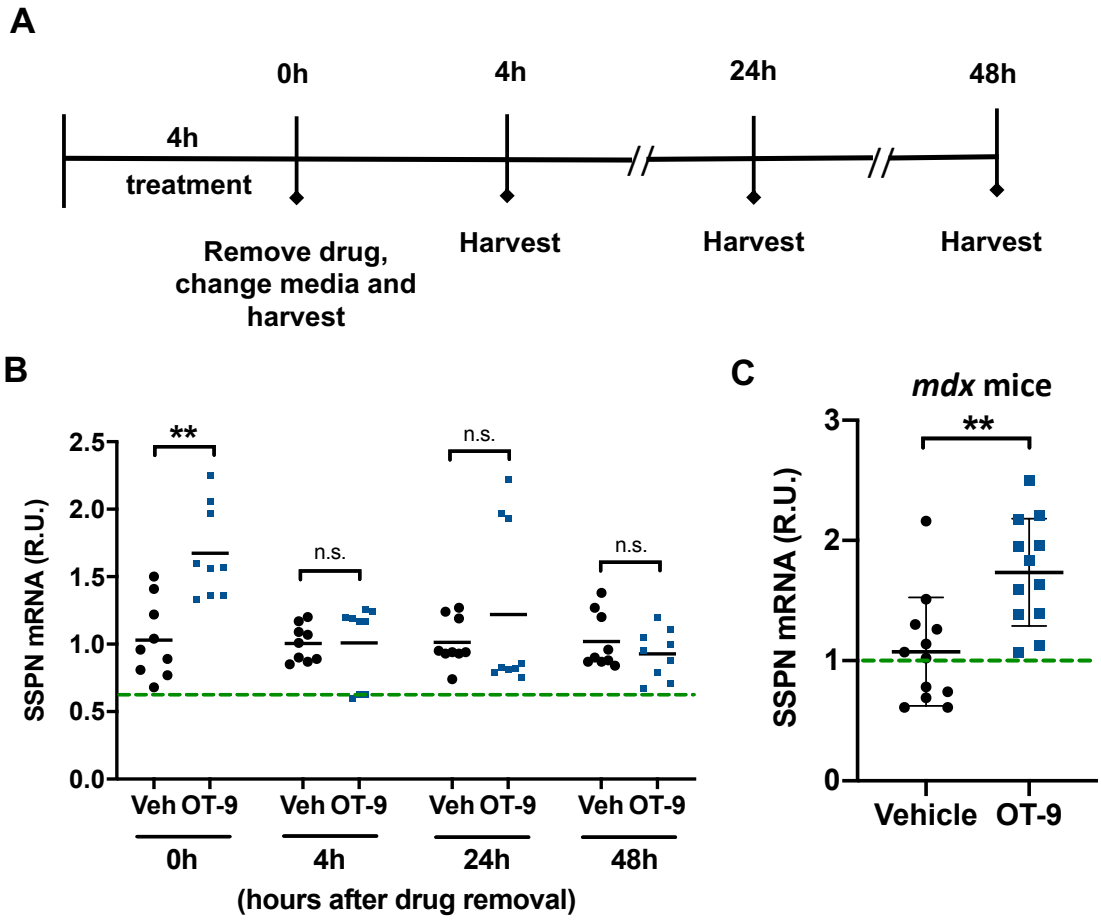

Figure 3-8. Sarcospan transcript is increased after 4 hours of treatment *in vitro* and *in vivo* in *mdx* muscle. (A) Schematic overview of experimental setup to test SSPN transcript stability *in* vitro. C2C12 myotubes were treated on the second day of differentiation with 5 μM of OT-9. After 4 hours, the media containing OT-9 was removed and changed to fresh media without drug. The cells were harvested for gene expression analysis immediately after media change (0h), and 4h, 24h, and 48h after. (B) OT-9 induces SSPN gene expression after 4 hours of treatment (0h). After extended removal of the drug (4 to 48h), SSPN mRNA levels were the same in cells treated with vehicle and OT-9. (C) 20-week old male *mdx* littermates were injected in both tibialis anterior muscles with vehicle (5% DMSO, 95% PBS) or 86 μg of OT-9. After 4 hours, the muscles were harvested and processed for gene expression analysis. R.U. = relative units normalized to housekeeping gene BACT and vehicle control-treated cells. Data represents individual replicates and mean value. n=3 for *in vitro* and n=2 for *in vivo* study. **p<0.01, ****p<0.0001.

and changed to fresh media. The cells were harvested at 0, 4, 24, and 48 hours after drug removal (Fig. 3-8A). Immediately after drug removal (0h), SSPN mRNA levels were elevated by 1.5-fold over the vehicle control, demonstrating that OT-9 induces SSPN gene expression after just 4 hours of treatment (Fig. 3-8B). However, 4, 24, and 48 hours after drug removal, SSPN transcript levels

returned to baseline levels, which suggested that SSPN transcript was present for several hours after induction by OT-9.

To evaluate the *in vivo* safety and activity of OT-9, we performed two pilot studies in wild-type C57/Bl6 and *mdx* mice. For the preliminary safety assessment of OT-9, we performed IP injections in 6 month old C57/Bl6 males. The mice were injected with vehicle, 30 mg/kg of OT-9, or 50 mg/kg of OT-9 (n=1 mouse per treatment). No signs of inflammation, necrosis or drug accumulation were observed at the injection site. The liver, kidneys, pancreas, and intestine appeared to be of normal weight and size. As some insoluble particles were observed in 50 mg/kg solution of OT-9, the 30 mg/kg dose was chosen for assessment of *in vivo* activity.

After the preliminary safety evaluation, we tested the ability of OT-9 to increase SSPN gene expression *in vivo*. We chose to assess activity after 4 hours of treatment based on the finding presented in Figure 3-8B, which demonstrated that 4 hours of treatment with OT-9 was sufficient to significantly increase SSPN transcript levels *in vitro*. Five 20-weeks old male *mdx* littermates were subjected to intramuscular injections in both tibialis anterior (TA) muscles. Two mice were injected in both TAs with vehicle and two mice were injected with 86 μg of OT-9 (3mg/kg; molar equivalent of 9.4 mM used in the safety assessment). After 4 hours of treatment, the TAs were harvested and processed for gene expression analysis. No adverse effects were observed after local OT-9 injections in the mice. OT-9 induced a 1.7-fold increase in SSPN gene expression relative to the vehicle control-treated group, demonstrating that OT-9 is capable of increasing SSPN gene expression in *mdx* mice (Fig. 3-8C).

Discussion

In this study, we performed high-throughput screening for SSPN enhancers and identified three classes of compounds. We then validated OT-9 and PC1-36 as small molecule upregulators of SSPN gene and protein expression in dystrophin-deficient muscle cells. We demonstrated that OT-9 increased sarcolemmal localization of utrophin, α-dystroglycan, and the laminin-binding glycoepitope of α-dystroglycan (α-DG IIH6), revealing that OT-9 increased adhesion complex formation at the membrane. We did not observe an increase in α-DG IIH6 in total lysate, suggesting that OT-9 increases the expression of existing α-DG IIH6 at the cell surface membrane. This finding supports our understanding of SSPN as a scaffold for the three major adhesion complexes in skeletal muscle.[5, 21, 33, 42] We previously showed that overexpression of SSPN in *mdx* mice increased the membrane localization of the utrophin-glycoprotein complex.[4, 5] Further supporting the role of SSPN as a scaffold, mutagenesis studies of SSPN polypeptide revealed that it contained multiple oligomer interaction sites and that it tightly associated with the sarcoglycans.[42]

Combined with our previous findings, this study suggests that OT-9 increased SSPN protein levels, which in turn increased the membrane localization of laminin-binding adhesion complexes. OT-9 protected *mdx* and DMD myotubes from osmotic shock-induced membrane damage. Knockdown of SSPN reduced the ability of OT-9 to protect the cell membrane, indicating that upregulation of SSPN was necessary for the full membrane-stabilizing effect of OT-9. Intramuscular injections in *mdx* mice demonstrated that OT-9 is increased SSPN gene expression in as little as 4 hours, suggesting it quickly targets SSPN gene expression. However, further studies are needed to determine if OT-9 directly or indirectly interacts with SSPN protein or mRNA as part of the mechanism of action.

In conclusion, we discovered a pharmacological upregulator of SSPN expression that possesses *in vivo* efficacy. Future studies will assess drug target, mechanism, and the potential for use as a combinatorial therapy to boost existing therapies and treatments in development.

Methods

Reporter cell lines

The human sarcospan EGFP reporter C2C12 cell line (hSSPN-EGFP) was used as described by Shu and colleagues.[19] Using an identical approach, a human sarcospan luciferase (hSSPN-luc) C2C12 cell line was created and used in secondary screening.

Small molecules

Screening libraries were provided by the Molecular Screen Shared Resource at the University of California Los Angeles.[80] Commercially available compounds used in follow-up studies were purchased from Asinex and Life Chemicals Inc.

High-throughput screening

hSSPN-EGFP myoblasts were seeded at 500 cells per well in 50 µl of growth media in 384-well black, clear bottom microplates (Greiner) using a Multidrop 384 (Thermo Fisher Scientific) and incubated for 3 days. Upon reaching confluency, the growth media was replaced with 50 µl of differentiation media consisting of DMEM with 2% horse serum (Sigma-Aldrich) using an EL406 combination washer dispenser (Biotek). At day 2 of differentiation, the media on the cells was aspirated, left with a residual volume of 10 µl, and replaced with 30 µl of fresh differentiation media. 0.5 µl of small molecule in DMSO or DMSO alone (for vehicle and positive control wells)

was added to each well using a Biomek Fx (Beckman). To ensure proper mixing of the DMSO, 50 µl of additional differentiation media was added to all wells except the positive control treated wells, which instead received 50 µl of media containing insulin transferrin selenium (ITS) (Gibco) to reach a final concentration of 1% ITS. The final concentration of drug in each treated well was 5.5 µM in 0.55% DMSO and 0.55% DMSO only for vehicle and positive control treated wells. After 48 hrs of incubation, the media was replaced with Fluorobrite DMEM (Gibco) and each plate was imaged using ImageXpress Micro Confocal High Content Imaging System (Molecular Devices). The fluorescence intensity of imaged cells was determined using a custom module analysis in MetaXpress Analysis software (Molecular Devices). Analysis setting were as follows: top hat (size: 12, filter shape: circle), adaptive threshold (source: top hat, minimum width: 10, maximum width: 800, intensity above local background: 500), filter mask (filter type: minimum area filter, minimum value: 500).

Luciferase assay

hSSPN-luciferase myoblasts were cultured as described above. After 48 hrs of treatment, plates were allowed to equilibrate to RT before the media was aspirated using an EL406 combination washer dispenser. Bright-Glo luciferase assay system reagent (Promega) and differentiation media were added to cells at a 1:2 dilution using a Multidrop 384. After a 3-minute incubation at RT, luminescence signal was quantified using an Envision plate reader (PerkinElmer). The relative luminescence units were analyzed to determine fold change of treated over vehicle treated cells.

Cell culture

C2C12 cells (American Type Culture Collection) were grown at 37°C with 5% CO_2 in growth media containing DMEM (Gibco) with 20% FBS (Sigma-Aldrich). Upon reaching 90-100% confluency, myoblasts were induced to differentiate by replacing the media with differentiation media consisting of DMEM with 2% horse serum (Sigma-Aldrich). Conditionally immortalized H2K WT and *mdx* myoblasts with a nonsense mutation in exon 23 of dystrophin were a gift from Terrance Partridge, Ph.D. (Children's National Medical Center, Washington, D.C.).[77] Myoblasts were allowed to proliferate on 0.01% gelatin (Sigma-Aldrich) coated plates at 33°C with 5% CO_2 with growth media containing DMEM, 20% HI-FBS (Invitrogen), 2% L-glutamine (Sigma-Aldrich), 2% chicken embryo extract (Accurate Chemical), 1% penicillin-streptomycin (Sigma-Aldrich), and 20 U/ml of fresh interferon gamma (Gibco). For differentiation, H2K myoblasts were seeded on plates coated with 0.1 mg/ml matrigel (Corning) diluted in DMEM and grown in proliferation conditions. Upon reaching 90-100% confluency, cells were grown at 37°C with 5% CO_2 in differentiation media containing DMEM with 5% horse serum (Sigma-Aldrich), 2% L-glutamine, and 1% penicillin-streptomycin using established protocols. The immortalized human DMD myoblast cell line was grown in Skeletal Muscle Basal Medium (Promocell) containing 20% FBS (Fisher Scientific), Skeletal Muscle Growth Supplement Mix (Promocell), and 1% penicillin-streptomycin at 37°C with 5% CO_2.[82] Upon, reaching 100% confluency, the media was replaced with differentiation media containing Skeletal Muscle Basal Medium, Skeletal Muscle Differentiation Supplement Mix (Promocell), and 1% penicillin-streptomycin.

Gene expression analysis

RNA from myotubes treated for 48 hrs was extracted from cells using Trizol-based (Thermo Fisher Scientific) phase separation, as previously described.[76] RNA concentrations were determined

using a NanoDrop 1000 (Thermo Fisher Scientific) and 750 ng of RNA in a 20 µl reaction was reverse transcribed using iScript cDNA synthesis (Bio-Rad) with the following cycling conditions: 25°C for 5 mins, 42°C for 30 mins, 85°C for 5 mins. For mouse qPCR, SsoFast EvaGreen Supermix (Bio-Rad), 400 nM of each optimized forward and reverse primer (SSPN F: 5' TGCTAGTCAGAGATACTCCGTTC 3', SSPN R: 5' GTCCTCTCGTCAACTTGGTATG 3', BACT F: 5' GAGCACCCTGTGCTGCTCACCG 3', BACT R: 5' CAATGCCTGTGGTACGACCA 3'), and cDNA corresponding to 37.5 ng RNA were used to amplify cDNA measured by QuantStudio 5 Real-Time PCR System (Thermo Fisher Scientific) with the following reaction conditions: 55°C for 2 mins, 95°C for 2 mins, 40 cycles of 95°C for 10 seconds and 62°C for 30 seconds, and dissociation stage. For qPCR of human samples, TaqMan assays were used to quantify SSPN (assay ID Hs01025520m_1) and ACTB (assay ID Hs01060665_g1) with the following reaction conditions: 50°C for 2 mins, 95°C for 10 mins, 40 cycles of 95°C for 15 seconds and 62°C for 1 minute. Each sample was run in triplicate. Data was analyzed using the ddCT method and normalized to reference gene ACTB with vehicle-treated samples serving as the calibrator (relative expression of vehicle control = 1).

Immunoblotting

Myotubes treated for 48 hrs were lysed using RIPA buffer (Thermo Fisher Scientific) containing Halt Protease Inhibitor Cocktail (Thermo Fisher Scientific). Cell lysates in RIPA buffer were rocked for 1 hr at 4°C and centrifuged at 1,000 RPM for 30 mins at 4°C. The supernatant was collected, quantified for protein concentration using the DC protein assay (Bio-Rad), and normalized to 2 mg/ml in water and Laemmli sample buffer with a final concentration of 10% glycerol (Sigma-Aldrich), 5% beta-mercaptoethanol (Sigma-Aldrich), 3% sodium dodecyl sulfate

(Sigma-Aldrich), and 0.05% bromophenol blue (Sigma-Aldrich). For SDS-PAGE, samples were heated to 95°C for 2 mins before loading 40 μg onto a 4-12% tris-glycine or Bolt bis-tris polyacrylamide gels (Novex), electrophoresed for 2 hrs at 100 volts at RT, and transferred to a nitrocellulose membrane for 2 hrs at 100 volts at 4°C. Ponceau S staining was performed to visualize protein loading and verify protein transfer. Membranes were blocked with 5% Blotto (5% non-fat dried milk) in tris-buffered saline pH 7.4 with 0.1% tween-20 (TBST, Sigma-Aldrich) for 1 hr at RT and incubated on a rocker overnight at 4°C with the following primary antibodies diluted in 5% Blotto unless otherwise noted: SSPN (sc-393187, Santa Cruz Biotechnology, 1:200), glycosylated alpha-dystroglycan (IIH6 C4, Developmental Studies Hybridoma Bank, 1:100 in 1% Blotto, core alpha-dystroglycan (Beadle Lab, 1:1000 in 1% Blotto), UTRN (MANCHO3, Developmental Studies Hybridoma Bank, 1:100), and GAPDH (Mab374, Millipore, 1:10,000). Following three 10-minute TBST washes, the membranes were incubated in goat anti-mouse IgG HRP (ab6789, Abcam, 1:5000 for all, 1:10,000 for GAPDH in 5% Blotto) or goat anti-rabbit IgG HRP (ab6721, Abcam, 1:10,000 in 1% Blotto) for 1 hr at RT. The membranes were then washed three times for 10 mins each with TBST, incubated in SuperSignal West Pico Chemiluminescent Substrate (Thermo Fisher Scientific) for 5 mins at RT on an orbital shaker, and exposed to autoradiography films (Agfa). Autoradiography films were developed using a SRX-101A tabletop processor (Konica Minolta), scanned to a digital file, and analyzed by densitometry of bands using ImageJ version 1.51s [78]. Target protein bands were normalized to loading control GAPDH with vehicle-treated cells serving as the calibrator sample (relative protein levels of vehicle control = 1).

ELISA to quantify SSPN protein levels

DMD myotubes were lysed in modified RIPA buffer containing 1% Triton X-100, 0.05% DOC, 0.05% SDS, and Halt protease and phosphatase inhibitors and subjected to 3 rounds of sonication. The lysate was centrifuged at 12,000 xg for 10 min and the supernatant transferred to new tubes. Protein concentration was determined using DC assay. A 96-well Nunc MaxiSorp plate (Invitrogen) was coated with 100 µl of 1 µg/ml SSPN antibody (sc-393187, Santa Cruz Biotechnology) per well overnight at 4°C. washed three times with 1X TBS containing 0.05% Tween-20, blocked for 1 hour at RT in 1% bovine serum albumin (BSA), and washed again. Recombinant human SSPN standards (100 µl ; Novus Biologicals) and lysates were added to plate, incubated overnight at 4°C, and washed. SSPN antibody (Life Span Biosciences, LS-C747357, 100 µl of 400 ng/ml) was added to each well and incubated for 2 hrs at RT and washed. Goat anti-rabbit IgG HRP (Abcam, 1:10,000, 100 µl) was added to each well, incubated for 2 hours at RT, and washed. 100 µl of tetramethylbenzidine (TMB) (Fisher Scientific) was added to each well and incubated for 30-40 min RT. After signal development, 100 µl of stop solution was added to each well and the absorbance at 450 nm was measured for each well using a plate reader the SpectraMax M2 microplate reader (Molecular Devices). The concentration of SSPN protein for each sample was calculated using the standard curve and normalized to protein concentration and vehicle-treated controls.

Analysis of cell surface proteins

After 48 hours of treatment, myotubes were washed with ice cold PBS with 0.1g/L of both $CaCl_2$ and $MgCl_2$ (Corning) three times and incubated in 0.5mg/ml of EZ-Link Sulfo-NHS-SS-Biotin (Thermo Fisher Scientific) at 4°C with gentle rotation for 30 mins to label cell surface proteins. All steps were performed at 4°C unless otherwise mentioned. The cells were washed three times

with ice cold 100 mM glycine in PBS for 5 minutes with gentle rotation to remove non-reacted biotin. Following a PBS wash, the cells were lysed in solubilization buffer composed of 50 mM Tris-HCl pH 7.8, 500 mM NaCl, 1% digitonin (Biosynth), and Halt protease and phosphatase inhibitors. The samples were rotated 4°C for 10 minutes and centrifuged at 4°C at 14,000 rpm for 20 minutes to pellet debris. The DC assay (Bio-Rad) was used to determine the protein concentration of the supernatant (total lysate). Pierce High Capacity Neutravidin Agarose (Thermo Fisher Scientific) beads were washed with solubilization buffer before being combined with equal concentrations of total lysate and incubated at 4°C overnight with rotation. The beads were centrifuged at 4°C at 2,500 rpm for 5 mins and washed with solubilization buffer containing 0.1% digitonin. This was repeated for a total of 4 washes. The biotinylated cell surface proteins were cleaved from biotin-avidin using 2 x Laemmli sample buffer (LSB) with 50 mM DTT, rotated at RT for 60 minutes, and heated at 95°C for 5 minutes. The samples were centrifuged at 2,500 rpm at 4°C for 5 minutes and the supernatant (membrane fraction) was collected for immunoblot analysis.

Membrane stability assay

The membrane stability assay was modified from previously described methods.[81] The solutions for osmotic shock were prepared from a base solution containing 5 mM HEPES, 5mM KCl, 1mM $MgCl_2$, 5mM NaCl, 1.2 mM $CaCl_2$, and 1 mM glucose. Sucrose was added to the base solutions to reach osmolarities of 50, 80, 100, 280, and 300 mosmols. The actual osmolarity was determined using a VAPRO vapor pressure osmometer (Wescor Inc.) Myotubes were treated for 48 hours and at day 4 of differentiation were subjected to 20 mins of osmotic shock at 37°C using 28.5 to 223.5 milliosmole (mosmols) solutions. The supernatant was collected and centrifuged to

separate cell debris. Adherent cells were trypsinized and pelleted before lysis with water and 3 freeze-thaw cycles. The Creatine Kinase Assay (Sekisui Diagnostics) was used to measure creatine kinase (CK) levels in both the supernatant and lysate fractions. In a 96-well plate, 4 µl of each sample and 140 µl of reagent was loaded per well in triplicate. The U/L of CK was calculated as follows : (mOD/min)(total volume in mL)(dilution factor)/(6.22M-1cm-1)(light path in cm)(sample volume in mL). The percent CK release was calculated as follows : CK sup/(CKsup + Cklysate) * 100.

siRNA-mediated knockdown

Lipofectamine RNAiMAX Transfection Reagent (Life Technologies) was used to transfect H2K *mdx* myotubes with 24 or 48 pmol of Silencer Select SSPN siRNA (siRNA ID s68932, Life Technologies) or MISSION siRNA Fluorescent Universal Negative Control #1, Cyanine 3 (Sigma Aldrich) diluted in Opti-MEM Reduced Serum Media (Thermo Fisher Scientific).

Myotube fusion index

Myoblasts in a 96-well plate were treated for 72 hrs beginning at day 2 of differentiation were fixed with 4% paraformaldehyde (PFA) for 20 mins, permeabilized with 0.2% Triton X-100 (Sigma) for 10 minutes, and blocked with 1% BSA for 30 minutes. Myosin heavy chain (MHC) was detected using 10 µg/ml MF-20 (Developmental Hybridoma Studies Bank) in 1% BSA overnight and 10 µg/ml goat anti-mouse Alexa Fluor Plus 594 (Thermo Fisher Scientific) in 1% BSA for 1 hr. PBS washes were performed between each step above. Nuclei were stained with 5 µg/ml Hoechst (Thermo Fisher Scientific) for 20 minutes before imaging. Each treatment was performed in three wells and three fields per well were captured. ImageJ was used to count the

number of total nuclei and nuclei within a MHC positive cell. Fusion index was calculated as nuclei in a MHC positive cell/total nuclei.

Half-life analysis

Half-life analysis was performed by Eurofins Panlabs Inc. using 1 μM of compound with a final DMSO concentration of 0.5%. PBS or plasma from CD-1 mice was pre-warmed to 37°C for 5 mins before addition of the test compounds and continued incubation at 37°C. At 0, 30, 60, 120, 240, and 1440 mins an aliquot of solution containing compounds was mixed with acetonitrile/methanol, mixed, and centrifuged. The supernatants were used for HPLC-MS/MS analysis.

Animals

All mouse experiments were performed according to the rules and regulations approved by the Institutional Animal Care and Use Committee at the University of California, Los Angeles (approval # 2000-029-61A).

***In vivo* treatment**

For the preliminary safety assessment of OT-9, we performed IP injections in 6 month old C57/Bl6 males. The mice were injected with 100 μl of vehicle (5% DMSO (Sigma), 95% PBS), 100 μl of 30 mg/kg of OT-9 in vehicle, or 100 μl of 50 mg/kg of OT-9 in vehicle (n=1 mouse per treatment). The mice were observed for 72 hours, then sacrificed for visual evaluation of injection site and internal organs (data not shown). For assessment of activity, 20-week old male *mdx* littermates were injected in both tibialis anterior muscles with vehicle (5% DMSO, 95% PBS) or 86 μg of

OT-9. Two mice were injected in both Tas with vehicle and three mice were injected in both Tas with 20 μl of OT-9 (9.4 mM solution containing 86 μg of OT-9). After 4 hours, the muscles were harvested and processed for gene expression analysis.

Data analysis

Robust strictly standardized mean difference (SSMD*) was used to assess plate quality and for hit selection. SSMD* = $X_P - X_N/1.4826\sqrt{s_P^2 + s_N^2}$, where X_P, X_N, S_P, and S_N are the medians and median absolute deviations of the positive and negative controls, respectively.[68] For plate quality, SSMD* ≥ 1 indicates a good quality moderate positive control. For initial hit selection, a 1.4-fold increase over vehicle and SSMD* > 0.25 was considered a hit. Statistical analysis was performed using Prism version 7.0 (GraphPad Software) for Mac OS X using the two-tailed, non-parametric Kolmogorov-Smirnov test. Data are reported as mean + SEM. A p-value of <0.05 was considered statistically significant. * $p<0.05$, ** $p<0.01$, *** $p<0.001$, **** $p<0.0001$.

Author Contributions

C.S. designed the high-throughput assays, including creation of the stable cell lines, performed high-throughput screening, validation screening, fusion index, proliferation assays, biotinylation assays, creatine kinase release assays, siRNA knockdown experiments, figure and manuscript preparation. R.D. designed assays, screening cascade, and provided core services and libraries for screening. C.S. and L.P. performed cell culture and gene and protein expression analysis for hit confirmation. L.P. and E.M. developed the ELISA and conducted *in vitro* protein assays. L.P., E.M., and C.S. performed pre-*in vivo* transcript stability assays. E.M. and C.S. performed the *in vivo* pilot study and gene expression analysis. J.R.C. performed gene expression analysis and

fusion index. V.J. and J.C. consulted on hit categorization. R.H.C. conceived of the project and consulted on all experiments, data analysis, figures, and manuscript drafting.

Acknowledgments

Support for this work was provided by the Muscle Cell Biology, Pathogenesis, and Therapeutics Training Grant (NIH T32 AR065972), Pilot and Feasibility Seed Grant program (NIH/NIAMS P30 AR057230), UCLA Department of Integrative Biology & Physiology Eureka Scholarship, Muscular Dystrophy Association (MDA 274143; Venture Philanthropy Program), NIH/NIAMS (R01 AR048179), and NIH NHLBI (R01 HL126204). Thank you to Ariana N. Kaxon-Rupp for generating fusion index data and Mohammad Parvez Alam for consultation in hit categorization.

Supplementary Figures

Supplementary Table 3-1. Plate quality. Robust strictly standardized mean difference (SSMD*) was used to assess plate quality and for hit selection.

Plate #	SSMD *	Plate #	SSMD *	Plate #	SSMD *	Plate #	SSMD *	Plate #	SSMD *	Plate #	SSMD *	Plate #	SSMD *
1	1.1	**77**	2.16	**153**	1.12	**229**	1.34	**305**	1.52	**381**	1.71	**457**	2.16
2	1	**78**	1.2	**154**	2.07	**230**	1.31	**306**	1.47	**382**	2.28	**458**	1.6
3	1	**79**	1.01	**155**	1.34	**231**	1	**307**	1.81	**383**	1.79	**459**	1.62
4	1.01	**80**	1.33	**156**	2	**232**	1.09	**308**	2.74	**384**	2.59	**460**	1.98
5	1.85	**81**	1.23	**157**	2.37	**233**	1.7	**309**	1.68	**385**	2.59	**461**	2.5
6	1.04	**82**	1.53	**158**	2.16	**234**	1.37	**310**	1.34	**386**	2.19	**462**	1.75
7	1.68	**83**	1.24	**159**	2.15	**235**	1.97	**311**	1.97	**387**	1.83	**463**	2.37
8	1.21	**84**	1.19	**160**	1.39	**236**	1.24	**312**	1.68	**388**	2.02	**464**	1.98
9	1.54	**85**	1.37	**161**	1.63	**237**	1.35	**313**	1.68	**389**	2.66	**465**	1.93
10	1.28	**86**	1.24	**162**	1.23	**238**	1.07	**314**	1.88	**390**	2.03	**466**	2.69
11	1.11	**87**	1.4	**163**	1.31	**239**	1.8	**315**	2.03	**391**	2.15	**467**	1.67
12	1	**88**	1.1	**164**	1.51	**240**	1.08	**316**	2.24	**392**	2.41	**468**	2.67
13	1.49	**89**	1	**165**	1.18	**241**	1.03	**317**	2.28	**393**	3.07	**469**	2.36
14	1	**90**	1.15	**166**	1.17	**242**	1.04	**318**	1.73	**394**	3.1	**470**	2.36
15	1.17	**91**	1.14	**167**	2.05	**243**	1.1	**319**	1.56	**395**	2.22	**471**	1.66
16	1.66	**92**	1.05	**168**	2.55	**244**	1	**320**	2.68	**396**	2.24	**472**	1.34
17	1.22	**93**	1.33	**169**	1.25	**245**	1.1	**321**	2.41	**397**	3.27	**473**	2.48
18	1	**94**	1.67	**170**	2.21	**246**	1.55	**322**	1.73	**398**	1.96	**474**	2.11
19	1.53	**95**	1.42	**171**	2.79	**247**	1.07	**323**	3.3	**399**	2.63	**475**	2.78
20	1	**96**	1.05	**172**	1.53	**248**	1.03	**324**	2.42	**400**	1.5	**476**	3.62
21	1.14	**97**	1.49	**173**	2.63	**249**	1.8	**325**	2.01	**401**	2.75	**477**	2.41
22	1.32	**98**	1.19	**174**	1.85	**250**	1.08	**326**	1.77	**402**	1.31	**478**	3.22
23	1.22	**99**	1.05	**175**	2.62	**251**	1.59	**327**	2.42	**403**	2.32	**479**	1.05
24	1	**100**	1.25	**176**	1.82	**252**	1.65	**328**	2.28	**404**	2.81	**480**	2.16
25	1.08	**101**	1.53	**177**	2.33	**253**	1.08	**329**	2.05	**405**	2.47	**481**	1
26	1.5	**102**	1.12	**178**	2.16	**254**	2.05	**330**	3.35	**406**	2.24	**482**	1.26
27	1.17	**103**	1.29	**179**	1.68	**255**	1.56	**331**	1.53	**407**	2.83	**483**	1.1
28	1	**104**	1.72	**180**	2.38	**256**	1.18	**332**	1.48	**408**	2.71	**484**	1.25
29	1.36	**105**	1.42	**181**	1.49	**257**	1.54	**333**	1.51	**409**	1.09	**485**	1.67
30	2.23	**106**	1.81	**182**	1.77	**258**	1.51	**334**	1.83	**410**	1.03	**486**	1.4
31	2.79	**107**	1.42	**183**	2.03	**259**	1	**335**	1.07	**411**	1	**487**	1.4
32	1.68	**108**	1.74	**184**	2.56	**260**	1.04	**336**	2.38	**412**	1.01	**488**	1
33	1.01	**109**	1.27	**185**	1.95	**261**	1.04	**337**	1.62	**413**	1.33	**489**	1.36
34	2.37	**110**	1.01	**186**	1.28	**262**	1.14	**338**	1.62	**414**	1.35	**490**	1.27
35	1.65	**111**	1.62	**187**	1.62	**263**	1.26	**339**	2.31	**415**	1.65	**491**	1.07
36	2.03	**112**	1.03	**188**	1.11	**264**	1.44	**340**	1.2	**416**	1.98	**492**	1.46
37	1.85	**113**	1.46	**189**	1.02	**265**	1.53	**341**	1.58	**417**	1.66	**493**	1.1
38	1.32	**114**	1	**190**	1.38	**266**	1.82	**342**	1.77	**418**	1.75	**494**	1.56
39	1.49	**115**	1.4	**191**	1.43	**267**	1.4	**343**	1	**419**	1.62	**495**	1.26
40	1.49	**116**	1.22	**192**	1.61	**268**	1.47	**344**	1.17	**420**	1.7	**496**	1.54

41	2.21	**117**	1.32	**193**	2.07	**269**	1.5	**345**	1.12	**421**	2.1	**497**	1.81
42	2.21	**118**	1.05	**194**	1.05	**270**	1.86	**346**	1.37	**422**	2.09	**498**	1.3
43	1.46	**119**	1.59	**195**	1.31	**271**	1.84	**347**	1.85	**423**	1.77	**499**	1.5
44	1.38	**120**	1.12	**196**	1.03	**272**	1.41	**348**	1.49	**424**	1.6	**500**	1.91
45	1	**121**	1.86	**197**	1.13	**273**	1.65	**349**	1.73	**425**	1.5	**501**	1.44
46	1	**122**	1.68	**198**	1.4	**274**	2.36	**350**	1.58	**426**	1.4	**502**	1.66
47	1.02	**123**	1	**199**	1.21	**275**	2.13	**351**	1.92	**427**	1.45	**503**	2.01
48	1.17	**124**	2.24	**200**	1.42	**276**	2.38	**352**	2.32	**428**	1.89	**504**	1.45
49	1	**125**	1.61	**201**	1	**277**	1.22	**353**	2.11	**429**	1.7	**505**	1.75
50	1.18	**126**	1.27	**202**	1.13	**278**	1.73	**354**	1.77	**430**	1.57	**506**	1.64
51	1	**127**	1.04	**203**	1.19	**279**	2.36	**355**	2.19	**431**	1.56	**507**	2.1
52	1.01	**128**	1.39	**204**	1.44	**280**	2.31	**356**	2.79	**432**	1.88	**508**	1.9
53	1.39	**129**	1.98	**205**	1.43	**281**	2.25	**357**	1.55	**433**	1.88	**509**	2.13
54	1.4	**130**	1	**206**	1.52	**282**	2.59	**358**	1.38	**434**	1.82	**510**	1.72
55	1.01	**131**	1.46	**207**	1.03	**283**	2.48	**359**	1.49	**435**	2.1	**511**	2.68
56	1.08	**132**	1.23	**208**	1.2	**284**	2.23	**360**	1.49	**436**	1.8	**512**	1.37
57	1	**133**	1.2	**209**	1.25	**285**	2.2	**361**	1.59	**437**	1.53	**513**	1.09
58	1.52	**134**	1.68	**210**	1.01	**286**	1.96	**362**	1.69	**438**	2.13	**514**	1.63
59	1	**135**	1.36	**211**	1.06	**287**	2.02	**363**	1.47	**439**	1.48	**515**	1.05
60	1.48	**136**	2.4	**212**	1.17	**288**	2.48	**364**	1.65	**440**	2.11	**516**	1
61	3.02	**137**	1.01	**213**	1.33	**289**	2.8	**365**	2.45	**441**	1.43	**517**	1.23
62	1.29	**138**	1.18	**214**	1.63	**290**	2.5	**366**	1.95	**442**	2.36	**518**	1.22
63	1.24	**139**	1.09	**215**	1.27	**291**	2.94	**367**	1.69	**443**	1.82	**519**	1.02
64	1.02	**140**	1.64	**216**	1	**292**	2.41	**368**	1.8	**444**	3.29	**520**	1
65	1.04	**141**	1.5	**217**	1.81	**293**	2.56	**369**	2.2	**445**	1.23	**521**	1.33
66	1	**142**	1	**218**	1.35	**294**	2.31	**370**	2.07	**446**	1.19	**522**	2.04
67	1.29	**143**	1	**219**	1.45	**295**	1.35	**371**	2.62	**447**	1.59	**523**	1.08
68	1.12	**144**	1.09	**220**	1.72	**296**	1.33	**372**	2.4	**448**	1.73	**524**	2.16
69	1	**145**	1.06	**221**	1.97	**297**	1.02	**373**	2.77	**449**	1.93	**525**	1.76
70	1.38	**146**	1.63	**222**	1.2	**298**	1.78	**374**	1.78	**450**	1.32	**526**	1.04
71	2.08	**147**	1.28	**223**	1.49	**299**	1.19	**375**	1.71	**451**	1.58	**527**	1.88
72	1.87	**148**	1.34	**224**	1.23	**300**	1.77	**376**	2.13	**452**	2.73	**528**	1.64
73	1.3	**149**	1.84	**225**	1.41	**301**	1.92	**377**	1.49	**453**	2.28	**529**	1.74
74	1.11	**150**	1.3	**226**	1.33	**302**	1.73	**378**	1.94	**454**	1.78	**530**	2.42
75	1.32	**151**	1.08	**227**	1.38	**303**	1.93	**379**	2.24	**455**	1.73	**531**	1.41
76	2.14	**152**	1.03	**228**	1.33	**304**	1.71	**380**	1.87	**456**	1.57	**532**	1.29

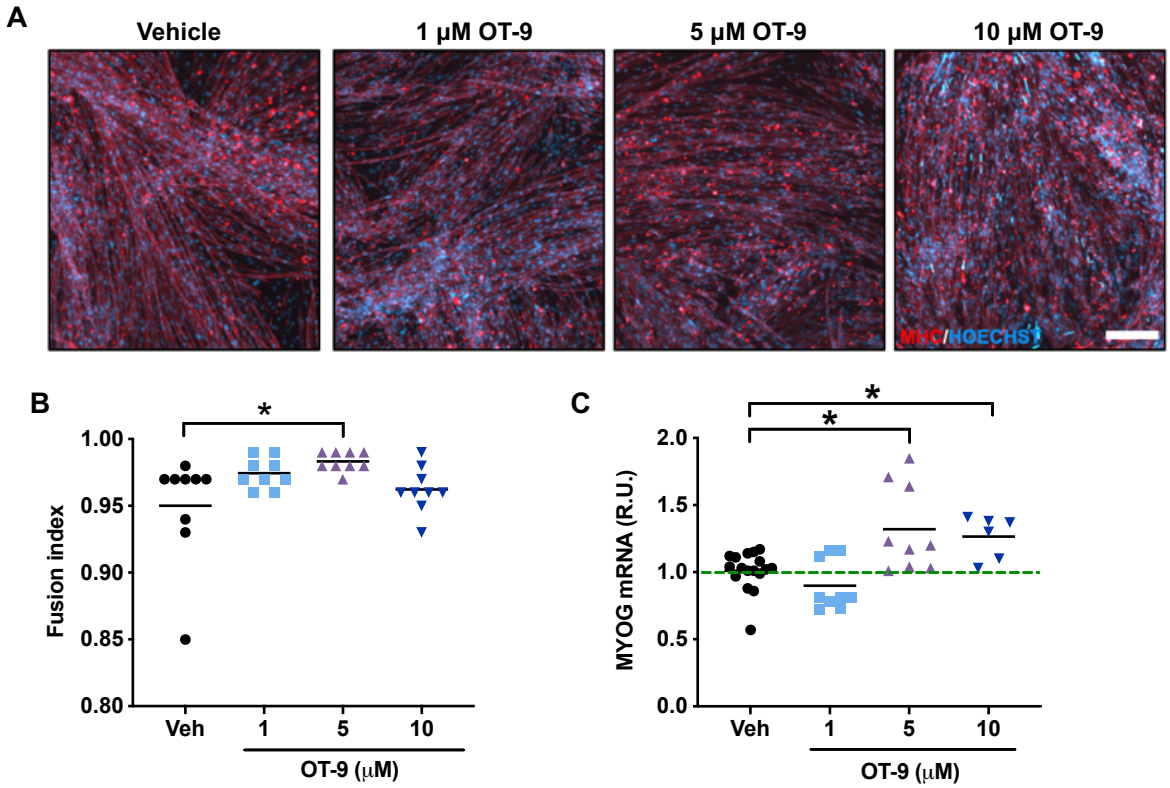

Supplementary Figure 3-1. OT-9 increases differentiation in mdx myotubes. mdx myotubes were treated with 1, 5, and 10 μM of OT-9 on day 2 and assayed on day 4 of differentiation. (A-B) OT-9 induces slight increase in H2K mdx myotube differentiation as measured by fusion index and (C) MYOG gene expression. Data represents individual replicates and mean value. n=3. Scale bar = 200 μm. *p<0.05, **p<0.01.

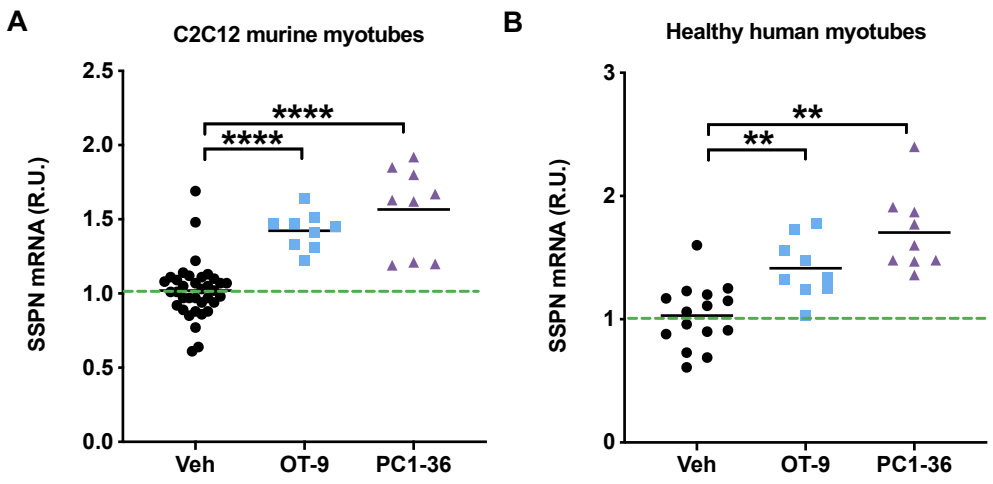

Supplementary Figure 3-2. OT-9 and PC1-36 are effective in multiple myotube lines. Myotubes were treated for 48 hours with 5.5 µM of OT-9 and PC1-36. (A) C2C12 myotubes were treated at day 2 and harvested on day 4 of differentiation. (B) Healthy human myotubes were treated on day 1 and harvested on day 3 of differentiation. Gene expression was normalized to housekeeping gene β-actin and vehicle-treated cells (0.1% DMSO). Data represents individual replicates and mean value. n=3-12. **p<0.01, ****p<0.0001.

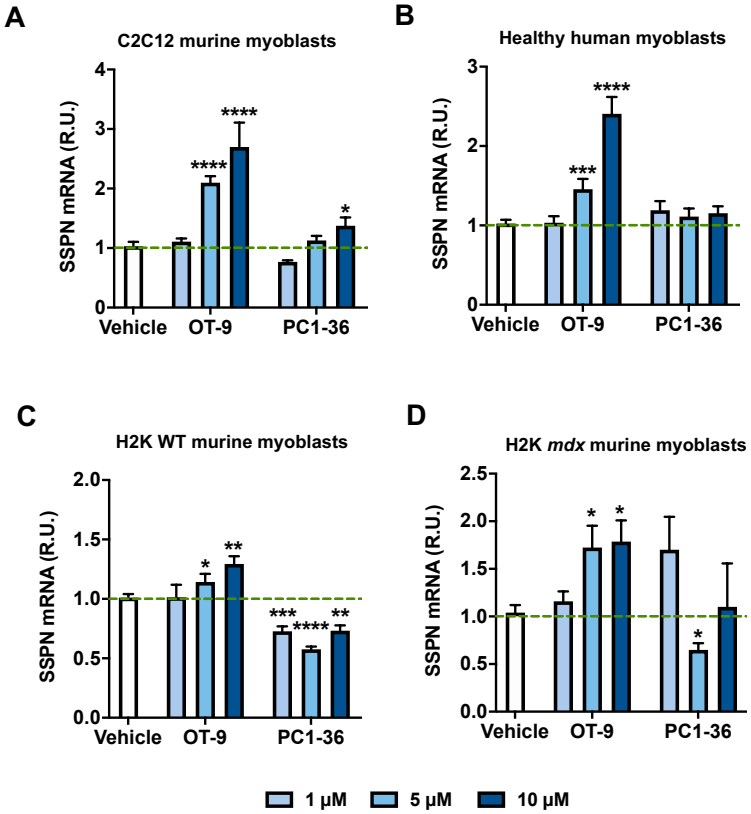

Supplementary Figure 3-3. OT-9 is effective in multiple myoblast lines. C2C12, healthy human, H2K WT, and H2K *mdx* myoblasts are responsive to OT-9, but not PC1-36. Myoblasts were treated for 24 hours with 1, 5, and 10 µM of OT-9 or PC1-36. Gene expression was normalized to housekeeping gene β-actin and vehicle-treated cells (0.1% DMSO). Data represents individual replicates and mean value. n=3-6. *p<0.05, **p<0.01, ***p<0.001, ****p<0.0001.

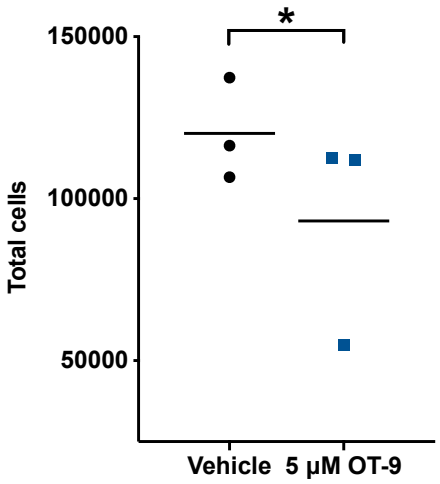

Supplementary Figure 3-4. OT-9 does not increase Mouly CTRL myoblast proliferation after 24 hours of treatment. Data represents individual replicates and mean value. n=3.

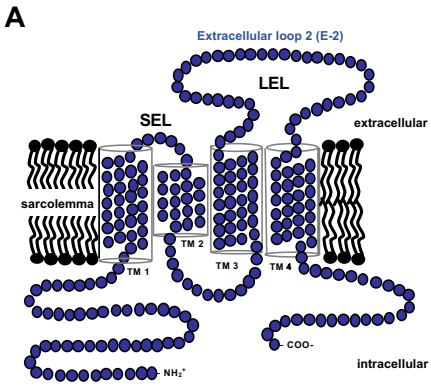

B

Antibody	Company	Clonality	Host	Epitope
LS-N	LifeSpan BioSciences	polyclonal	rabbit	Human AA 1-60 (N-terminus)
E2	Santa Cruz Biotechnology	monoclonal	mouse	Human AA 162-199 extracellular loop 2 (E-2)
NV	Novus Biologicals	polyclonal	mouse	Human AA 1-243 full length

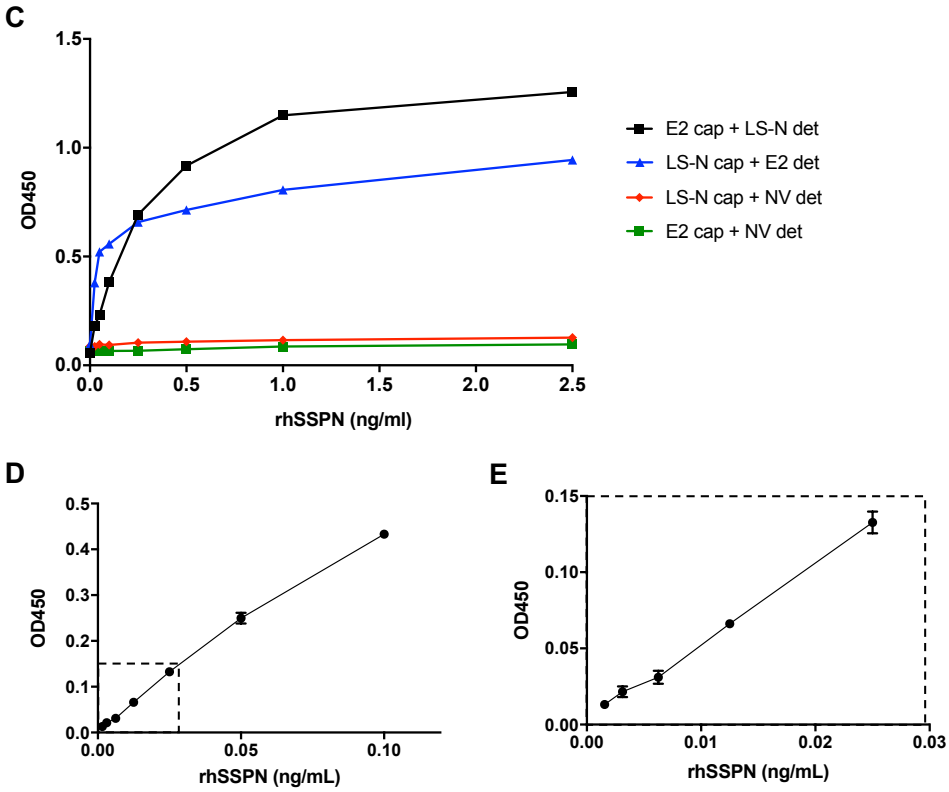

Supplementary Figure 3-5. Development of an indirect sandwich ELISA to quantify human sarcospan protein. (A) Schematic of the topology of sarcospan in the sarcolemma. Sarcospan contains four transmembrane domains (TM1-4) and 2 extracellular loops (SEL: small extracellular loop; LEL: long extracellular loop or extracellular loop 2 (E-2)). (B) The commercially available antibodies against sarcospan used in the development of the ELISA target the N-term, E-2 loop, or full-length protein. (C) The standard curves using serially diluted recombinant human SSPN (rhSSPN) protein demonstrates that the "E2 cap + LS-N det" antibody combination detects rhSSPN with the greatest sensitivity. (D) A standard curve generated using the E2 cap + LS-N det antibody combination and 0.002-0.1 ng/ml of rhSSPN. (E) A zoomed in version of the same standard curve illustrates that the ELISA can detect as little as 1-2 pg of rhSSPN.

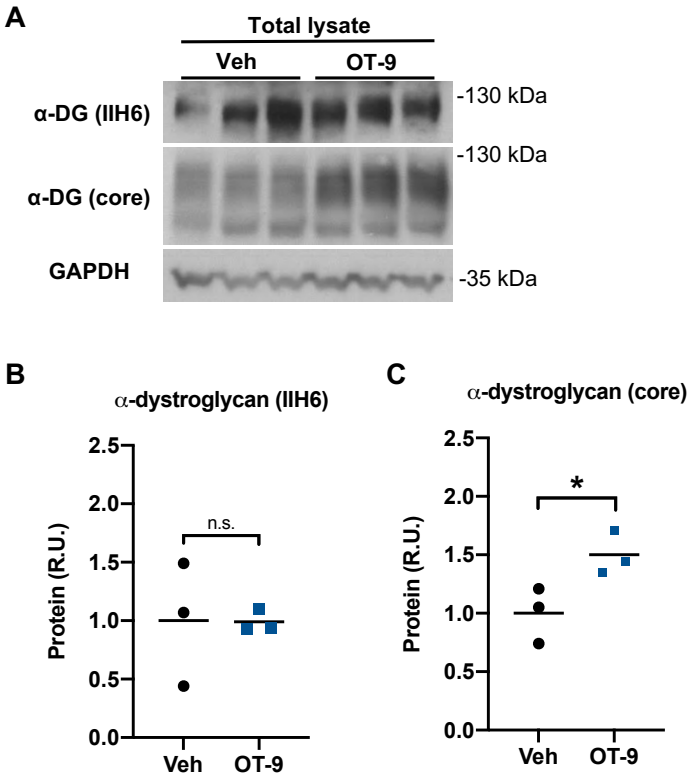

Supplementary Figure 3-6. OT-9 increases laminin-binding adhesion proteins in total lysate. C2C12 myotubes treated with vehicle or 5 μM of OT-9 for 48 hours before immunoblot analysis. (A) Cells treated with OT-9 do not show an increase in the fully glycosylated, laminin binding α-dystroglycan (α-DG (IIH6)), but do show an increase in core α-dystroglycan. GAPDH is shown as a loading control. (B-C) Quantification of immunoblots. Data represents individual replicates and mean value. n=3. R.U. = relative units normalized to GAPDH and vehicle control.

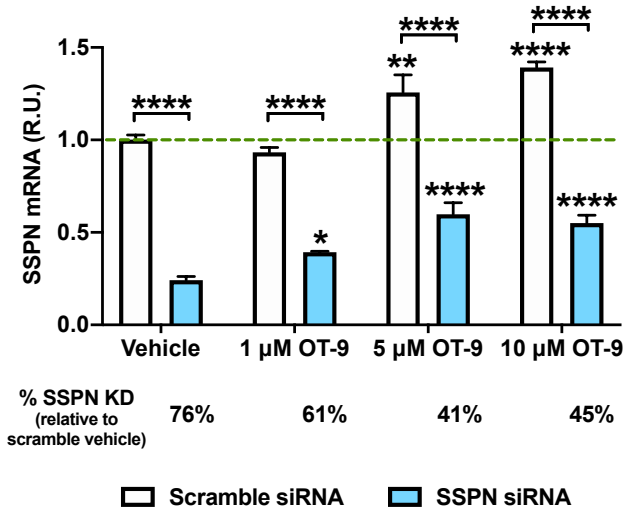

Supplementary Figure 3-7. siRNA-mediated knock down of SSPN results in a 76% knock down efficiency. *mdx* myotubes were treated in parallel with 1, 5, and 10 μM of OT-9 and scramble control siRNA or siRNA targeting SSPN transcript. Gene expression was normalized to housekeeping gene β-actin and vehicle and scramble siRNA treated cells. Data represents mean + SEM. n=3. *p<0.05, **p<0.01, ****p<0.0001.

Supplementary Table 3-2. Half-life of 1 µM of OT-9 and PC1-36 in CD-1 mouse plasma. Data shown represents individual values and mean. n=2.

Compound	Incubation Time (minutes)	% Compound Remaining			Half-Life (minutes)		
		1st	2nd	Mean	1st	2nd	Mean
OT-9	0	100.0	100.0	100	470.7	452.4	462
	30	94.0	89.5	92			
	60	84.7	86.3	86			
	120	78.3	78.1	78			
	1440	11.6	10.5	11			
PC1-36	0	100.0	100.0	100	644.4	643.2	644
	30	94.8	88.2	92			
	60	71.0	69.6	70			
	120	43.7	48.5	46			
	1440	17.3	17.2	17			

Supplementary Table 3-3. Half-life of 1 µM of OT-9 and PC1-36 in PBS pH 7.4. Data shown represents individual values and mean. n=2.

Compound	Incubation Time (minutes)	% Compound Remaining			Half-Life (minutes)		
		1st	2nd	Mean	1st	2nd	Mean
OT-9	0	100.0	100.0	100	50.1	48.1	49
	30	28.3	33.8	31			
	60	9.8	10.1	10			
	120	3.6	2.5	4			
	240	2.7	2.1	2			
	1440	0.6	0.5	1			
PC1-36	0	100.0	100.0	100	131.5	140.4	136
	30	81.5	79.7	81			
	60	66.8	55.9	61			
	120	37.1	46.4	46			
	240	27.5	29.0	28			
	1440	0.8	1.0	1			

Chapter 4

Second generation new chemical entity enhancers of sarcospan with improved solubility and activity

Cynthia Shu[1-3], Liubov Parfenova[2], Ekaterina Mokhonova[2,3], Judd R. Collado[2], Jesus Campagna[4,5], Barbara Jagodzinska[4,5], Varghese John[4,5], and Rachelle H. Crosbie[1-4]

[1]Molecular Biology Institute, University of California Los Angeles, [2]Department of Integrative Biology and Physiology, University of California Los Angeles, [3]Center for Duchenne Muscular Dystrophy, University of California Los Angeles, [4]Department of Neurology, David Geffen School of Medicine, University of California Los Angeles [5]Drug Discovery Lab, University of California Los Angeles

Introduction

Duchenne muscular dystrophy (DMD) is the most common, fatal, inherited disease in children.[24] It is characterized by progressive muscle degeneration, loss of muscle strength, and wheelchair reliance in childhood years. Approximately 90% of individuals with DMD develop dilated cardiomyopathy, respiratory system dysfunction, and succumb to death by the third decade of life.[24, 25] The current standard of care includes corticosteroid treatment, which reduces inflammation and extends the initial age of wheelchair reliance from 10 to 13 years of age.[52] In addition to corticosteroids, the FDA recently approved exon skipping modalities, but no therapies are considered a cure. Thus, there remains an unmet need for the development of more effective treatments for DMD.

DMD is caused by mutations in the gene encoding for the dystrophin protein.[26] In healthy muscle, dystrophin localizes to the intracellular surface of the cell membrane (sarcolemma) where it forms the dystrophin-glycoprotein complex (DGC). Within the DGC, dystrophin associates with the actin cytoskeleton and the integral membrane protein β-dystroglycan, which interacts with the laminin-binding α-dystroglycan (α-DG).[30, 53, 54, 59] Several other proteins, including sarcospan (SSPN) and the sarcoglycans, are established members of the complex.[21] The DGC is expressed uniformly around the sarcolemma and serves to anchor the cell to the extracellular matrix (ECM). This essential connection stabilizes the myofiber during contractions. In patients with DMD, dystrophin is absent from the cell, resulting in loss of cell-to-ECM adhesion. In the absence of the DGC, the myofiber undergoes extensive membrane damage that leads to muscle degeneration and weakness.[56]

Skeletal muscle contains three major adhesion complexes: the DGC, the utrophin-glycoprotein complex (UGC), and α7β1D-integrin complex. Previous studies established that transgenic overexpression of the UGC or α7β1D-integrin complex prevented disease onset in the *mdx* mouse model of DMD.[37, 41] Overexpression of the complexes increased cell-to-ECM binding in the absence of dystrophin, leading to improved membrane integrity and overall muscle health. SSPN is a component of all three adhesion complexes and serves to provide scaffolding for proteins within the complex. Through numerous studies, our group demonstrated that overexpression of SSPN prevented muscle disease in *mdx* mice by increasing the membrane localization of the UGC and the α7β1D-integrin complex.[4, 5, 7, 16] Importantly, SSPN overexpression improved cardiac and respiratory performance, indicating SSPN is capable of addressing the major causes of death in the DMD population.[4, 6]

To identify SSPN-based pharmacological therapies, we previously created a muscle cell-based high-throughput assay capable of identifying small molecule enhancers of SSPN protein levels in dystrophin-deficient models.[19] Using the assay, we screened over 200,000 curated, drug-like small molecules suited for the development of new chemical entities. We identified two lead compounds (OT-9 and PC1-36) that increased SSPN protein levels in dystrophin-deficient muscle cells. Lead characterization revealed that OT-9 increases laminin-binding adhesion complexes in muscle cells and improved membrane stability as determined by an osmotic shock assay. Knockdown of SSPN demonstrated that SSPN is necessary for the full membrane-stabilizing effects of OT-9. In an *in vivo* pilot study, we discovered that OT-9 increased SSPN gene expression by 1.8-fold in *mdx* skeletal muscle after only 4 hours of treatment, indicating that OT-9 has the potential to be developed into a therapy for DMD.

Our group previously found that a 1.5-fold overexpression of SSPN in *mdx* mice was insufficient to prevent muscular dystrophy, but that a 3-fold overexpression of SSPN significantly reduced muscle pathology.[7] Therefore, the 1.8-fold increase in SSPN gene expression induced by OT-9 may be insufficient to prevent muscle pathology. In this study, we conducted lead optimization of the SSPN modulators OT-9 and PC1-36 through three series of SAR analysis with the goal of improving properties such as solubility and activity. Lead optimization is a critical phase of drug development that focuses on improving the drug-likeness of a compound. Understanding structure activity relationship (SAR) allows for the rational design of desirable small molecules. Optimization of these properties are expected to progress the development of SSPN modulating small molecules with sufficient bioavailability and activity.

Results

To identify SSPN-based pharmacological therapies, we previously created a muscle cell-based high-throughput assay capable of identifying small molecule enhancers of SSPN protein levels in dystrophin-deficient models.[19] Using the assay, we screened over 200,000 curated, drug-like small molecules suited for the development of new chemical entities (NCEs) (Chapter 3). We identified two lead compounds (OT-9 and PC1-36) that increase SSPN protein levels in dystrophin-deficient muscle cells. Lead characterization revealed that OT-9 increases laminin-binding adhesion complexes in muscle cells and improved membrane stability as determined by an osmotic shock assay. Knockdown of SSPN demonstrated that SSPN is necessary for the full membrane-stabilizing effects of OT-9. In an *in vivo* pilot study, we discovered that OT-9 increases SSPN gene expression by 1.8-fold in *mdx* skeletal muscle after only 4 hours of treatment, indicating that OT-9 has the potential to be developed into a therapy for DMD.

Our group previously showed that a 1.5-fold overexpression of SSPN in *mdx* mice was insufficient to prevent muscular dystrophy, but that a 3-fold overexpression of SSPN significantly reduced muscle pathology.[5] In the *in vivo* pilot study on *mdx* mice, OT-9 induced a 1.8-fold increase in SSPN gene expression, which may be insufficient to induce a rescue effect. In this current study, we focused on lead optimization of OT-9 and PC1-36 to improve properties such as solubility and activity.

Development and validation of sarcospan protein reporter fusion cell line

To develop a rapid method to test analogues, we created a C2C12 cell line expressing endogenous SSPN protein with an N-term fusion protein called the HiBiT, an 11 amino acid subunit of a luciferase enzyme (Fig. 4-1A, Supplementary Fig. 4-1). The SSPN-HiBiT protein is quantified through addition of substrate and an additional, larger subunit of the luciferase enzyme

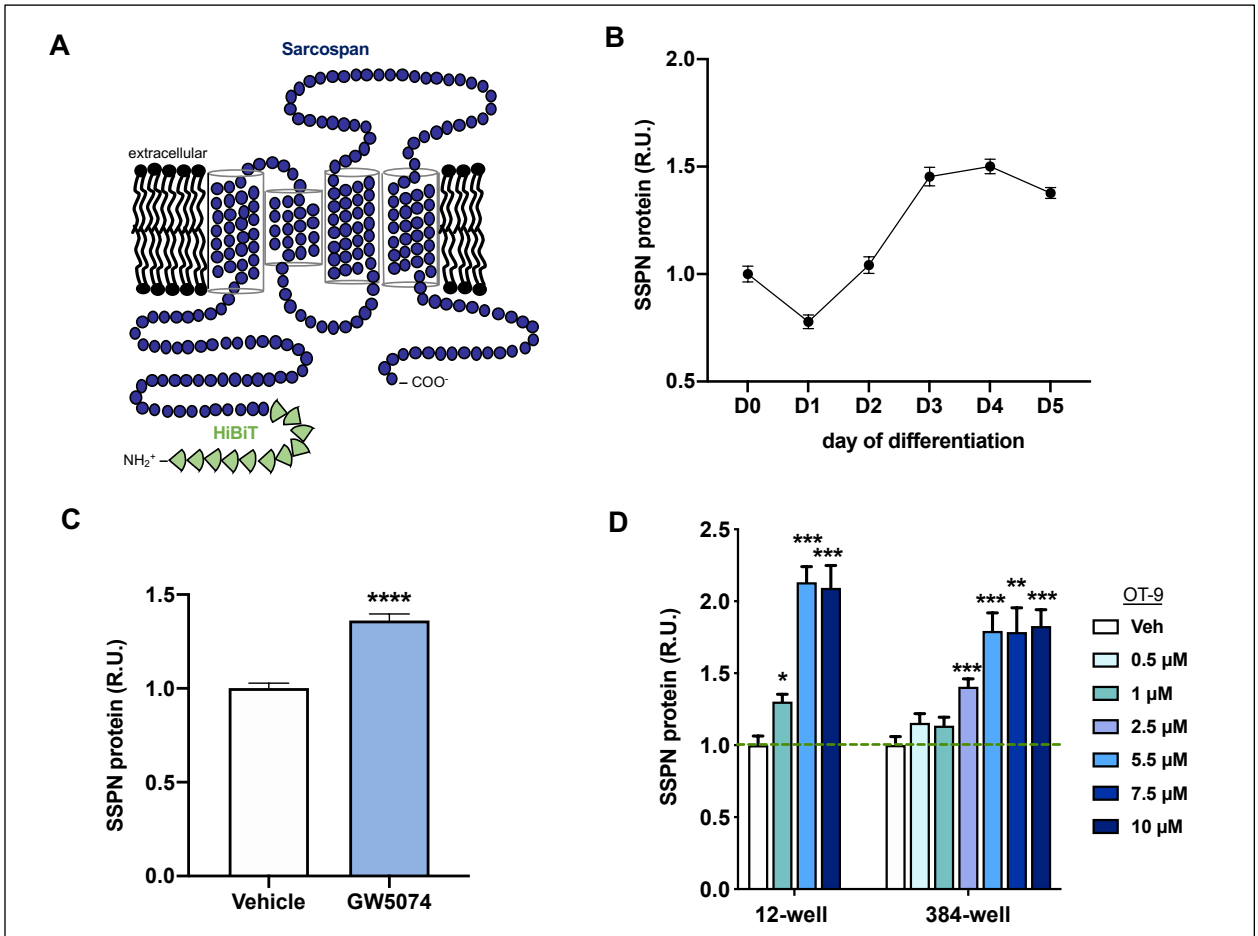

Figure 4-1. Characterization and validation of C2C12 SSPN-HiBiT protein reporter assay. (A) The gene encoding the HiBiT luciferase enzyme subunit was inserted into the endogenous sarcospan gene using CRISPR/Cas9. The 11 amino acid HiBiT is fused to the N-term of sarcospan. (B) SSPN-HiBiT protein levels increase with differentiation. (C) SSPN-HiBiT myotubes are responsive to positive control, GW5074, a c-raf inhibitor. Calculation of plate quality using GW5074 as a positive control using robust strictly standardized mean deviation (SSMD*) results in an SSMD* of 2.48, indicating it is an excellent moderate control. (D) The SSPN-HiBiT 12-well and 384-well format assays detect increases in reporter expression after treatment with OT-9. SSPN-HiBiT cells were treated on day 2 and harvested on day 4 of differentiation. R.U. = relative units normalized to vehicle control (DMSO), protein concentration for the 12-well assay, or nuclear count for the 384-well assay. Data shown represents the mean ± SEM values. n=6. *p<0.05, **p<0.01, ***p<0.001, ****p<0.0001.

and to catalyze the formation of luminescent signal. The C2C12 SSPN-HiBiT cells express reporter protein at increasing levels throughout differentiation, which is supported by our previous finding that SSPN mRNA increases with differentiation (Fig. 4-1B).[19] We identified GW5074, a c-raf inhibitor, for use as a positive control for the assay. SSPN-HiBiT C2C12 myotubes treated with 5 µM of GW5074 exhibit a 1.35-fold increase in SSPN-HiBiT levels (Fig. 4-1C). Plate

quality control was calculated using robust strictly standardized mean deviation (SSMD)*, which takes into account the difference between the negative and positive controls and the variation within each control group. The *SSMD of the SSPN-HiBiT assay using GW5074 as a positive control was 2.69, indicating it was an excellent moderate control. We developed a 12-well plate and 384-well plate format for the assay. A summary of the standard operating procedures for each assay can be found in Supplementary Table 4-3.

To validate the ability of the reporter to detect changes in SSPN protein levels after treatment with our lead compounds, we treated SSPN-HiBiT cells in both the 12-well and 384-well plate formats with 0.5-10 μM of OT-9. The assays detected dose-sensitive increases in SSPN protein levels after 48 hours of treatment (Fig. 4-1D). These results demonstrate that the SSPN HiBiT C2C12 assays are useful tools in the SAR analysis of our lead compounds.

SAR series 1: determining the activity of moieties within lead compounds

The goal of SAR series 1 was to determine the necessity of specific moieties within each of the lead compounds. Moiety X, a potentially hepatotoxic structure, in OT-9 was altered to create OT-9a and OT-9b. Moiety Y, a potentially destabilizing structure, in PC1-36 was altered to create PC1-36a and PC1-36b. We tested both parent compounds and analogues in the same experiment to determine if the substitutions affected the ability of the compounds to increase SSPN protein levels. Using the murine SSPN-HiBiT C2C12 384-well microplate assay, we found that OT-9, OT-9a, and OT-9b increased SSPN protein levels relative to the vehicle control and that OT-9a and OT-9b did not have reduced activity relative to OT-9 (Fig. 4-2A). To determine the effect of the drugs on SSPN expression in a dystrophin-deficient cells, we tested the compounds at 5 μM in human DMD myotubes and *mdx* murine myotubes and assessed protein and transcript

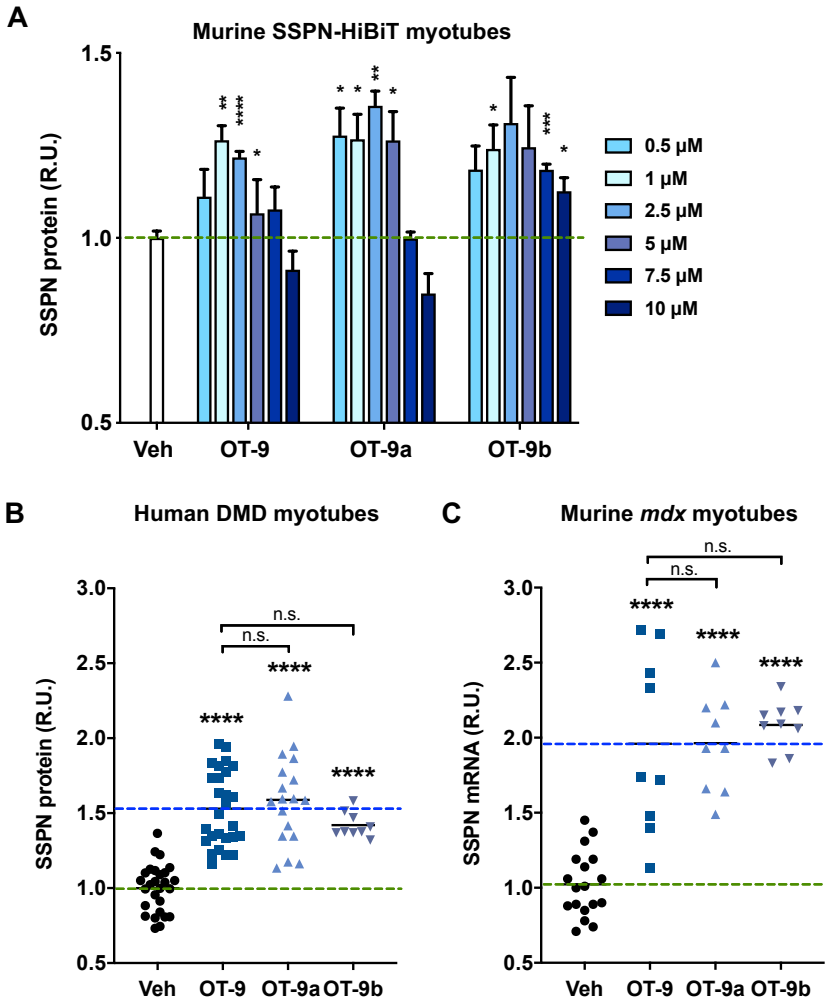

Figure 4-2. OT-9 SAR series 1 demonstrates that substitution of moiety X does not affect activity of OT-9. (A) The parent compound and analogues were tested at 6 doses ranging from 0.5-10 µM in murine SSPN-HiBiT C2C12 cells using the 384-well format assay. The compounds were further validated at 5 µM in (B) human DMD myotubes with ELISA readout and (C) murine *mdx* myotubes with qPCR readout. In all assays, OT-9, OT-9a, and OT-9b increase SSPN levels relative to the vehicle control and the activity of the analogues was not significantly changed relative to OT-9. All cell lines were treated on day 2 and harvested on day 4 of differentiation. The green dashed line denotes average vehicle values. The blue dashed line denotes average parent compound values. R.U. = relative units normalized to vehicle control and nuclear count for SSPN-HiBiT 384-well microplate assay, protein concentration for the ELISA, or housekeeping gene for qPCR. n=9-16. *p<0.05, **p<0.01, ***p<0.001,

levels, respectively. In human DMD myotubes, OT-9, OT-9a, and OT-9b induced a 1.5, 1.6, and 1.3-fold increase in SSPN protein levels, respectively (Fig. 4-2B). In murine *mdx* myotubes, OT-9, OT-9a, and OT-9b induced a 2, 2, and 2.2-fold increase in SSPN gene expression, respectively (Fig. 4-2C). In both the DMD and *mdx* myotubes, the activity of OT-9 and the analogues did not

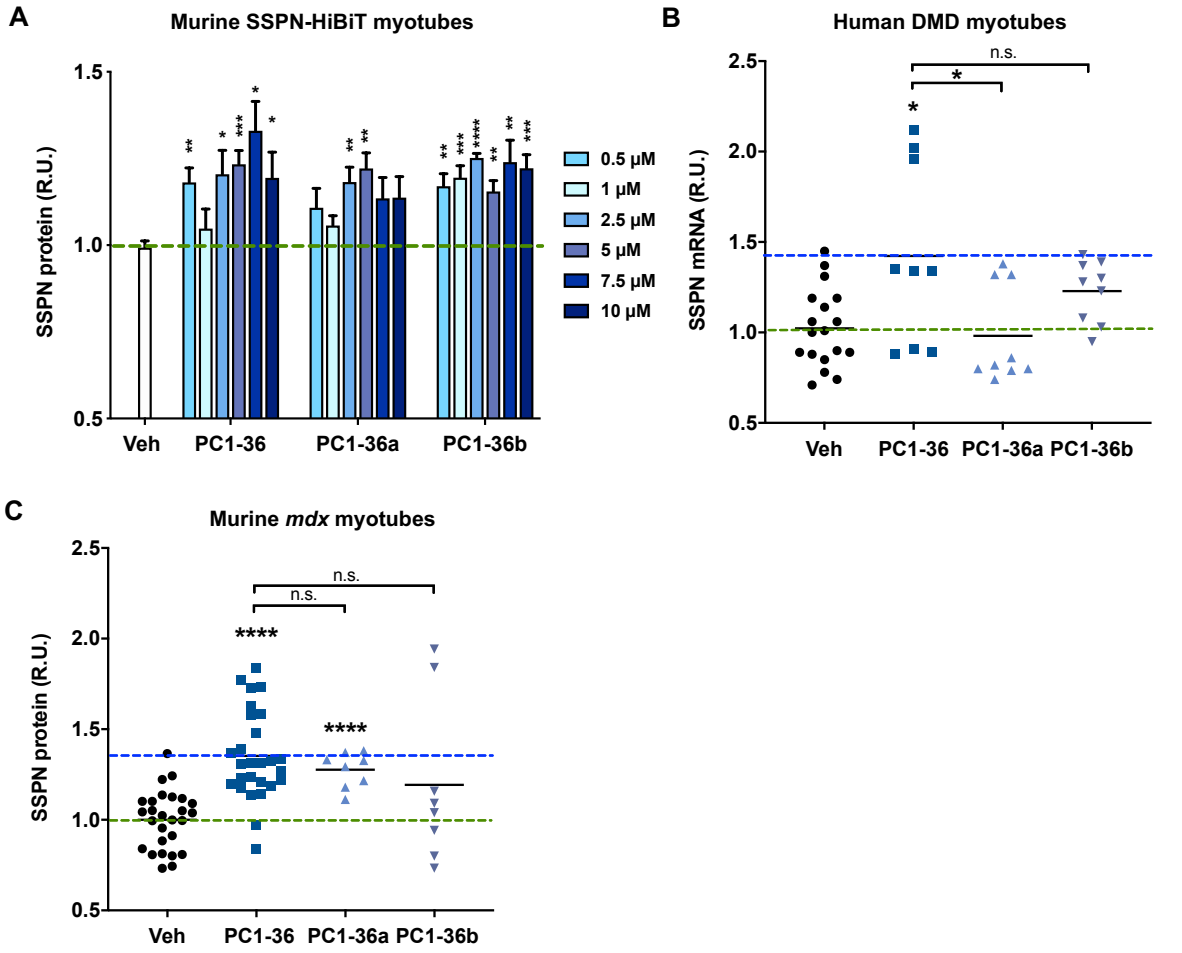

Figure 4-3. SAR series 1 demonstrates that substitution of moiety Y does not affect activity of PC1-36. (A) The parent compound and analogues were tested at 6 doses ranging from 0.5-10 µM in murine SSPN-HiBiT C2C12 cells using the 384-well format assay. PC1-36a and PC1-36b do not have diminished activity relative to PC1-36. (B) Assessment of the compounds at 5 µM in human DMD myotubes with ELISA readout demonstrate that only PC1-36 and PC1-36a increase SSPN protein levels and that the activity of PC1-36a is retained relative to PC1-36. (C) Assessment of the compounds at 5 µM in murine *mdx* myotubes with qPCR readout suggest that both PC1-36a and PC1-36b had reduced activity relative to PC1-36. All cell lines were treated on day 2 and harvested on day 4 of differentiation. The green dashed line denotes average vehicle values. The blue dashed line denotes average parent compound values. R.U. = relative units normalized to vehicle control and nuclear count for SSPN-HiBiT 384-well microplate assay, protein concentration for the ELISA, or housekeeping gene for qPCR. n=9-12. *p<0.05, **p<0.01, ***p<0.001, ****p<0.0001.

differ significantly. The results of the three assays demonstrate that substitution of moiety X in OT-9 does not affect its ability to increase SSPN levels and can therefore be replaced to reduce potential hepatotoxicity. Both OT-9a and OT-9b retained activity and were therefore used as backbones for following SAR analyses.

Using the same workflow, we assessed the activity of PC1-36 SAR series 1 analogues. In the SSPN-HiBiT 384-well assay, PC1-36a and PC1-36b increased SSPN protein levels relative to the vehicle control and their activity was similar to that of PC1-36 (Fig. 4-3A). In DMD myotubes, PC1-36 and PC1-36a induced a 1.4 and 1.3-fold increase in SSPN protein levels, respectively, while PC1-36b did not possess any activity (Fig. 4-3B). The activity of PC1-36 and PC1-36a were not statistically different, indicating PC1-36a retained the activity of PC1-36. Assessment of activity in *mdx* myotubes demonstrated that PC1-36 increased SSPN gene expression by 1.4-fold, while PC1-36a and PC1-36b lacked activity (Fig. 4-3C). These results indicate that in SSPN-HiBiT C2C12 and DMD myotubes, substitution of the potentially unstable moiety Y in PC1-36 does not affect the activity of the analogue PC1-36a. PC1-36a was therefore chosen as a backbone for the following SAR analyses.

SAR series 2: improving the solubility of lead compounds

One of the challenges in drug development is achieving optimal solubility, which is a major determinant of oral bioavailability. OT-9 and PC1-36 exhibit poor solubility characteristics (<0.8 μM), which renders them sub-optimal for pre-clinical studies. To address these solubility issues, we created SAR series 2 analogues with the goal of improving solubility while retaining or improving activity. Using OT-9a and OT-9b as backbones, we designed and synthesized five new analogues predicted through *in silico* analysis to have improved solubility: OT-9c, OT-9d, OT-9e, OT-9f, and OT-9g. Solubility testing revealed that OT-9c, OT-9d, OT-9e, and OT-9f were more soluble than OT-9, but still had relatively low solubility (Fig. 4-4A). To assess the activity of the

A

Compound	Aqueous solubility (μM)
OT-9	<0.8
OT-9a	<0.8
OT-9b	<0.8
OT-9c	1.1
OT-9d	2.1
OT-9e	2.4
OT-9f	1.9
OT-9g	≈0.8

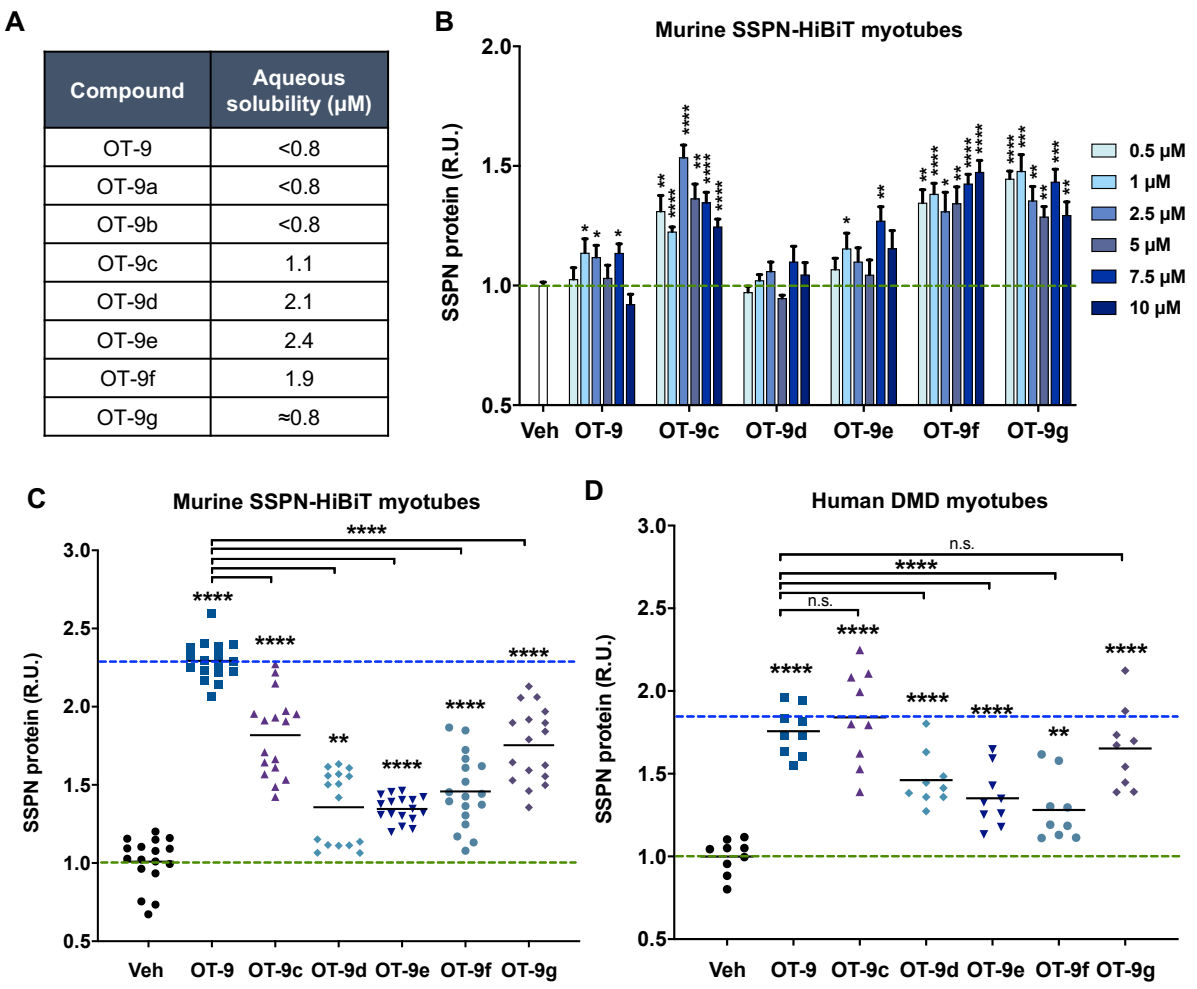

Figure 4-4. Modifications in the OT-9 SAR series 2 analogues result in improved solubility and retention of activity. (A) Four OT-9 analogues have improved aqueous solubility relative to the parent compound. (B) Dose testing of the compounds using the murine SSPN-HiBiT C2C12 384-well format assay indicate that OT-9d and OT-9e have reduced activity relative to OT-9. (C) Assessment of 5 μM of compounds using 12-well SSPN-HiBiT assay shows reduced activity in all OT-9 series 2 SAR analogues. (D) Assessment of 5 μM of compounds on human DMD myotubes shows that the analogues do not improve the activity of OT-9 as measured by an ELISA. All cells were treated on day 2 of differentiation and harvested after 48 hrs. The green dashed line denotes average vehicle values. The blue dashed line denotes average parent compound values. R.U. = relative units normalized to vehicle control and nuclear count for SSPN-HiBiT 384-well microplate assay or protein concentration for the SSPN-HiBiT 12-well plate assay and ELISA. n=6-33. *p<0.05, **p<0.01, ***p<0.001, ****p<0.0001.

analogues, we tested the compounds at six doses ranging from 0.5-10 μM and found that activity was retained in OT-9c, OT-9f, and OT-9g, while OT-9d and OT-9e were less active than OT-9 (Fig. 4-4B). Using the SSPN-HiBiT 12-well plate assay, we found that all the analogues increased

A

Compound	Aqueous solubility (μM)
PC1-36	<0.8
PC1-36a	<0.8
PC1-36b	n/a
PC1-36c	<0.8
PC1-36d	n/a
PC1-36e	<0.8

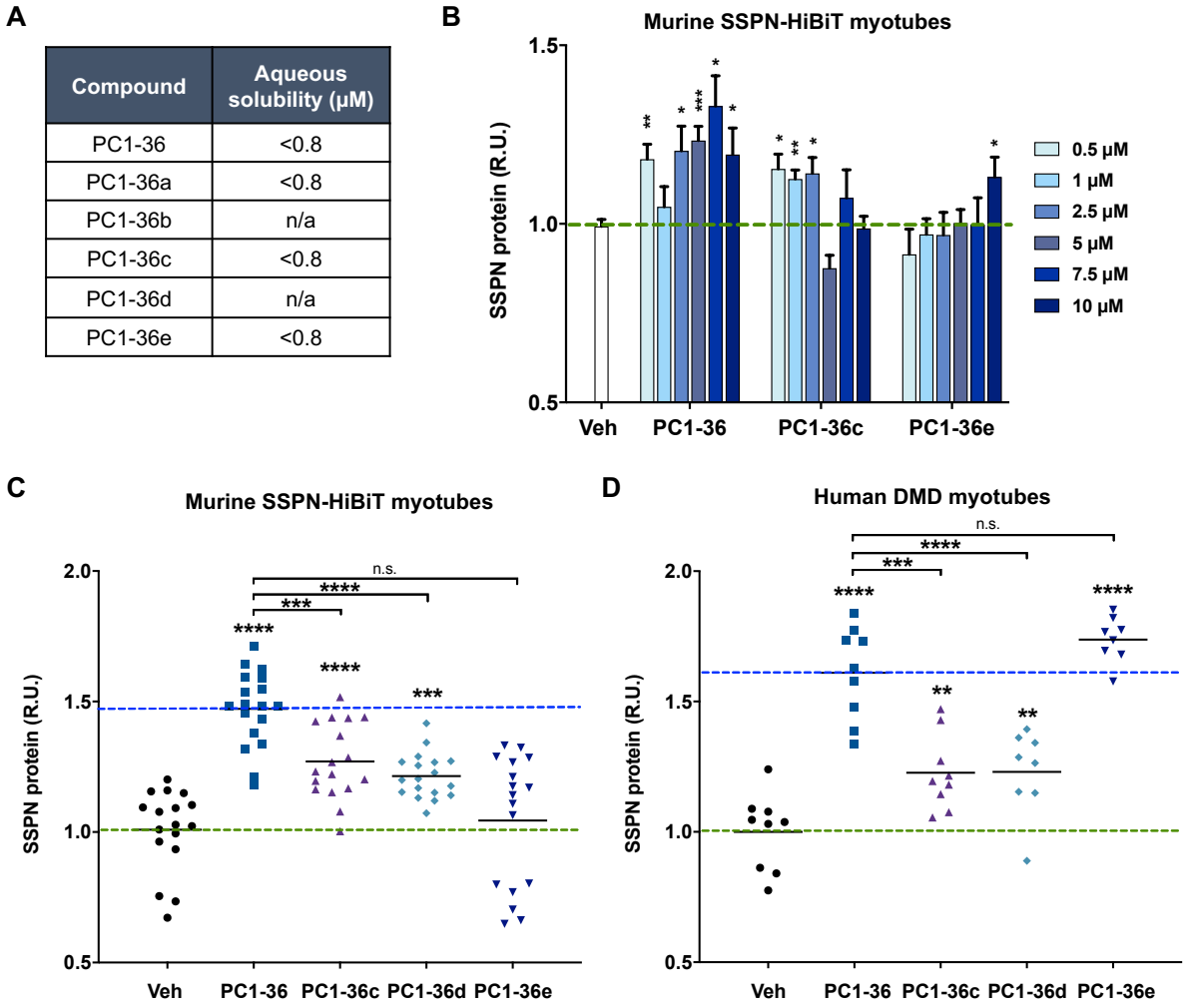

Figure 4-5. PC1-36 SAR series 2 analogues do not improve solubility or activity. (A) The PC1-36 analogues do not have improved aqueous solubility. (B) Dose testing of the compounds using the murine SSPN-HiBiT C2C12 384-well format assay demonstrate that PC1-36c and PC1-36e have reduced activity relative to PC1-36. (C) Assessment of 5 μM of compounds using 12-well SSPN-HiBiT assay indicates all analogues have reduced activity relative to PC1-36. (D) Assessment of 5 μM of compounds in human DMD myotubes suggests that the analogues do not improve the activity of PC1-36 as measured by the SSPN ELISA. All cells were treated on day 2 of differentiation and harvested after 48 hrs. The green dashed line denotes average vehicle values. The blue dashed line denotes average parent compound values. R.U. = relative units normalized to vehicle control and nuclear count for SSPN-HiBiT 384-well microplate assay or protein concentration for the SSPN-HiBiT 12-well plate assay and ELISA. n=9-18. *p<0.05, **p<0.01, ***p<0.001, ****p<0.0001.

SSPN protein levels relative to the vehicle control, but that they all resulted in reduced activity relative to OT-9 (Fig. 4-4C). Validation in DMD myotubes demonstrated that while all the compounds increased SSPN protein levels relative to the vehicle control, OT-9d, OT-9e, and OT-

9f were less active than OT-9 (Fig. 4-4D). Based on these results, we chose OT-9c as a backbone for following SAR analyses.

For the PC1-36 series, we created three analogues using PC1-36a as a backbone and assessed the solubility and activity of the new analogues: PC1-36c, PC1-36d, and PC1-36e. Series 1 and 2 analogues did not exhibit improved solubility (Fig. 4-5A). Using the SSPN-HiBiT 384-well assay, we showed that PC1-36c and PC1-36e were less active than PC1-36 (Fig. 4-5B). This result was reflected in the SSPN-HiBiT 12-well assay, which demonstrated that all analogues had reduced activity over PC1-36 (Fig. 4-5C). We assessed the activity of the compounds in DMD myotubes and found that while all the compounds increased SSPN protein levels relative to the vehicle control, PC1-36c and PC1-36d were less active than PC1-36 (Fig. 4-5D). Based on the results, we chose PC1-36e as a backbone for following SAR analyses because it retained activity in DMD myotubes, which is the most relevant target for our therapy.

SAR series 3: improving the ability of lead compounds to increase sarcospan protein levels

In SAR series 3, we created analogues with the goal of improving activity to 2 to 3-fold overexpression of SSPN, which we previously established is necessary for rescue in *mdx* mice.[5] For the OT-9 series, we created six analogues (OT-9h, OT-9i, OT-9j, OT-9k, OT-9l, OT-9p) using OT-9a as a backbone and three analogues (OT-9m, OT-9n, OT-9o) using OT-9c as a backbone. Assessment of the compounds using the SSPN-HiBiT assay demonstrated that all the analogues increased SSPN expression over the vehicle control, but only OT-9m increased activity relative to OT-9 (Fig. 4-6A). OT-9m induced a 2.4-fold increase in SSPN protein levels, while OT-9 induced a 1.6-fold increase in SSPN. We observed similar results in DMD myotubes with all the analogues increasing SSPN over the vehicle control and OT-9m increasing SSPN by 1.9-fold compared to

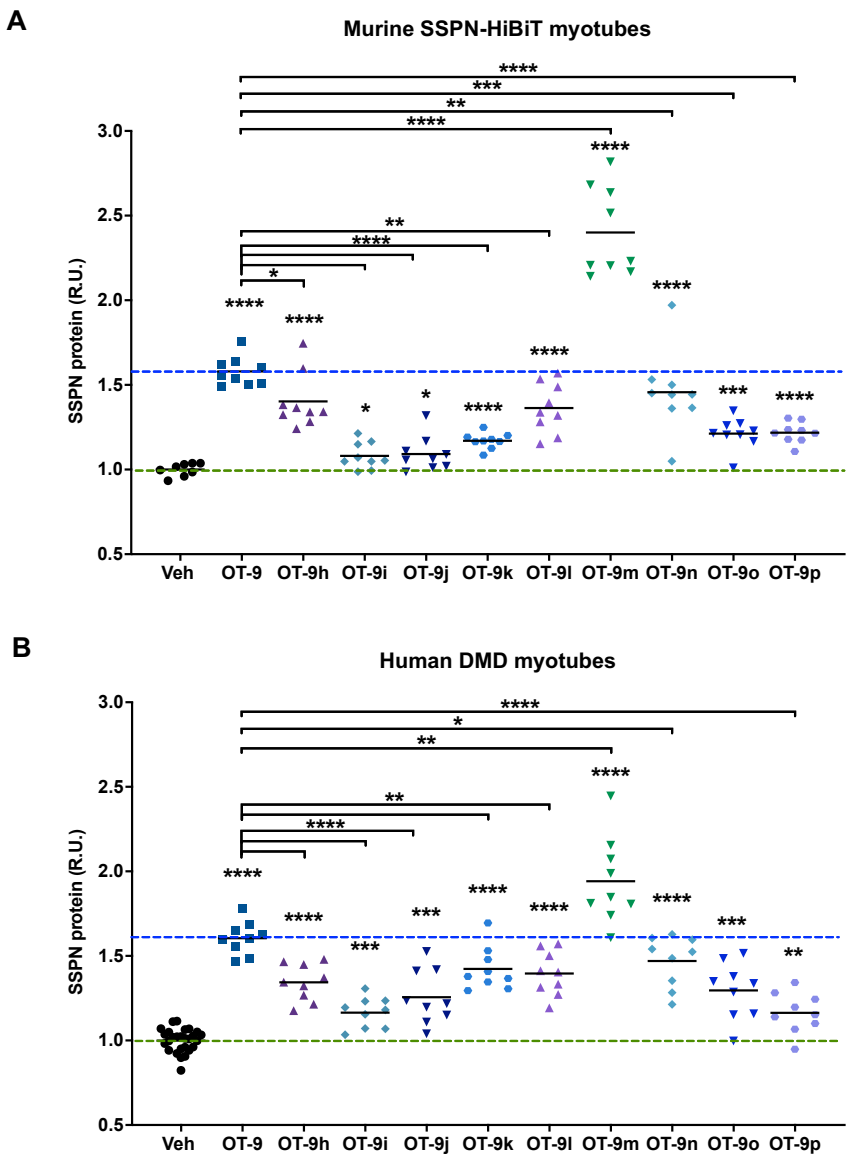

Figure 4-6. OT-9 SAR series 3 analogue testing reveals enhanced activity of OT-9m. (A) Assessment of 5 µM of compounds using 12-well murine SSPN-HiBiT C2C12 assay shows that OT-9m significantly improves activity relative to OT-9. (B) Assessment of 5 µM of compounds on human DMD myotubes shows that OT-9m significantly improves activity relative to OT-9 as measured by the SSPN ELISA. All cells were treated on day 2 of differentiation and harvested after 48 hrs. The green dashed line denotes average vehicle values. The blue dashed line denotes average parent compound values. R.U. = relative units normalized to DMSO and protein concentration. n=9-21. *p<0.05. **p<0.01 ***p<0.001, ****p<0.0001.

OT-9, which increased SSPN by 1.6-fold (Fig. 4-6B). Our findings demonstrate that in both SSPN-HiBiT C2C12 and DMD myotubes, OT-9m outperforms OT-9 by 60% and is able to induce a 1.9 to 2.4-fold increase in SSPN protein levels in mouse and human cells, respectively.

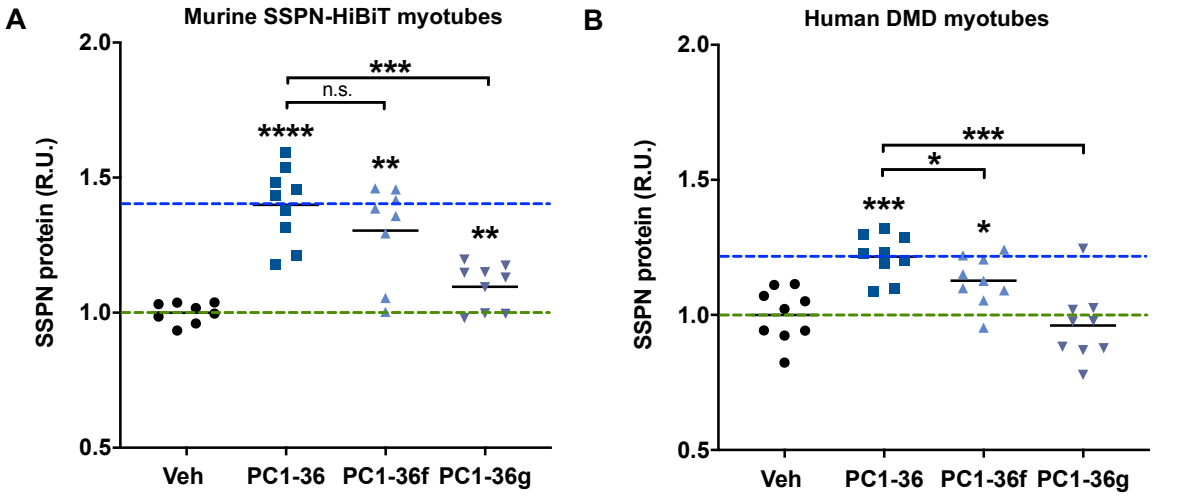

Figure 4-7. PC1-36 SAR series 3 compounds do not improve activity. (A) Assessment of 5 µM of compounds using 12-well murine SSPN-HiBiT C2C12 assay shows that none of the analogues have improved activity relative to PC1-36. (B) Assessment of 5 µM of compounds on human DMD myotubes none of the analogues have improved activity relative to PC1-36 as measured by the SSPN ELISA. All cells were treated on day 2 of differentiation and harvested after 48 hrs. The green dashed line denotes average vehicle values. The blue dashed line denotes average parent compound values. R.U. = relative units normalized to DMSO and protein concentration. n=9-21. *p<0.05. **p<0.01 ***p<0.001, ****p<0.0001.

For the PC1-36 series, we created two analogues (PC1-36f and PC1-36g) using PC1-36e as a backbone as it induced the greatest increase in SSPN protein levels in DMD myotubes. Assessment of the compounds using the SSPN-HiBiT assay revealed that while both analogues increased SSPN protein levels over the vehicle control, neither outperformed PC1-36 (Fig. 4-7A). In DMD myotubes, PC1-36 and PC1-36f increased SSPN levels relative to the vehicle control, while PC1-36g showed no activity and both had reduced activity relative to PC1-36 (Fig. 4-7B).

Discussion

The summary of our lead optimization is presented in Figure 4-8 and shows that through three series of SAR analyses, we developed OT-9m, an analogue of OT-9 with 60% greater activity. Future *in vitro* studies will assess the effect of OT-9m on membrane stability and membrane localization of compensatory adhesion complexes. *In vivo* studies will assess the

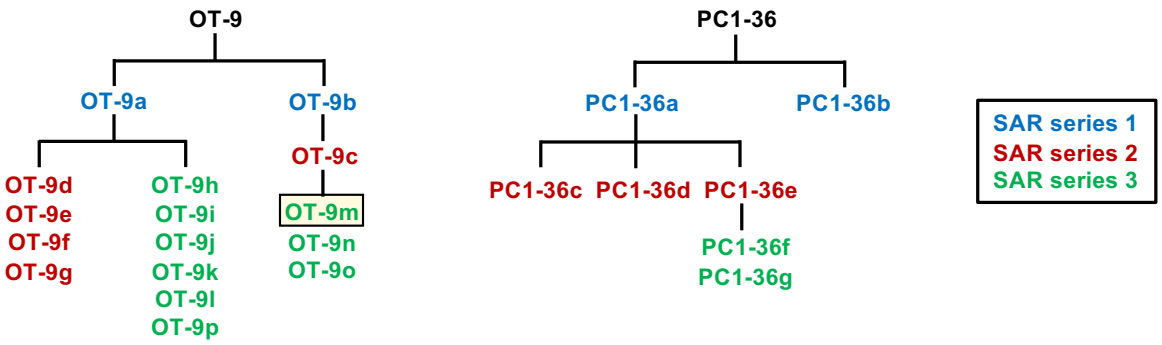

Figure 4-8. Summary of lead optimization. OT-9 and PC1-36 were optimized using an iterative process of structure activity relationship (SAR) analysis by assessing SSPN protein levels in treated SSPN-HiBiT C2C12 murine muscle cells and human DMD myotubes. Following three rounds of SAR analysis, we developed OT-9m, an analogue with improved activity.

pharmacokinetics and efficacy of OT-9m in the *mdx* mouse model. Finally, identification of the biological target is expected to facilitate improving efficacy and proper targeting of OT-9m.

Methods and Materials

C2C12 HiBiT Assay Development

Cas9, gRNA, donor ssDNA, RNP complex formation

Recombinant *Streptococcus pyogenes* Cas9 with a double nuclear localization tag on the C-terminus was obtained as a 40 µM protein solution in 20 mM HEPES-KOH pH 7.5, 150 mM KCl, 10% glycerol, 1 mM DTT (QB3). The Alt-R CRISPR RNA (crRNA) and ssDNA template containing the HiBiT sequence targeting the 5' SSPN locus was designed according the manufacturer's protocols (Promega) and used Blast and Alt-R CRISPR-Cas9 guide RNA design tool (Integrated DNA Technologies) (Supplementary Table 4-1). ssDNA was purchased as single-stranded Ultramer Oligonucleotides (Integrated DNA Technologies) and resuspended to 100 µM in nuclease-free water. To assemble gRNA, Alt-R CRISPR RNA (crRNA) and Alt-R trans-activating crRNA-ATTO™ 550 (tracrRNA) containing fluorescent dye (Integrated DNA

Technologies) were resuspended in Nuclease-Free Duplex Buffer (Integrated DNA Technologies) to a final concentration of 200 µM and combined to reach a 100 µM duplex concentration. The duplex was incubated at 95 °C for 5 min and then cooled down to room temperature. 600 pmol of gRNA and 720 pmol of Cas9 (1:1.2 molar ratio) were mixed in PBS to reach a volume of 25 µL and incubated at room temperature for 20 min to allow for the formation of the ribonucleotide protein (RNP) complex. The mixture was kept on ice until electroporation.

Cell preparation and electroporation with RNP complex

C2C12 immortalized murine myoblasts were cultured in growth media consisting of DMEM (Gibco) with 20% fetal bovine serum (FBS) (Sigma-Aldrich) at 37°C with 5% CO_2. After detachment with Trypsin (Gibco), 1 x 10^7 cells were diluted in PBS to a final volume of 40 ml and centrifuged at 200 x *g* for 5 min at room temperature. The pellet was resuspended in PBS, cells were pelleted down by centrifugation (200 x *g* for 5 min) and resuspended in 750 µL of PBS. 1 x 10^6 cells in 75 µl were aliquoted, kept on ice for at least 5 min, and combined with 20 µl of RNP complex and 5 µl of donor ssDNA. The mixture was transferred into precooled 0.2 cm gap cuvette and electroporated using the Gene Pulsar II Electroporation System (Bio-Rad) set at 1 pulse, 110 V, and a capacitance of 960 µF. After electroporation, the cells were transferred to dishes containing preheated C2C12 growth media and incubated for 24 hr. The efficiency of electroporation was estimated using fluorescent imaging.

gRNA screening

To choose the most effective gRNA, C2C12 myoblasts were electroporated with donor ssDNA and the RNP complexes consisting of unique gRNAs (gRNA1-4) and grown in 100 mm cell

culture dishes. After 48 hours, a portion of the myoblasts were frozen at -80C^{o} and a portion of the myoblasts from each electroporation were differentiated in media consisting of DMEM with 2% horse serum (Sigma-Aldrich) for 4 days, then the media was aspirated, the cells were washed with PBS and frozen at -80^{o}C. The plates with myoblasts and myotubes were thawed and lysed with 500 µl of ice-cold mRIPA buffer (25 Tris HCl pH 8.0, 170 mM NaCl, 1 mM EDTA, 0.5 mM EGTA, 0.05% Triton X-100, 0.005 % SDS, 0.005% DOC). Cells were scratched, transferred into 1.5 ml tubes and centrifuged for 20 min at 16,000 x g, 4^{o} C, then the cell lysates were transferred into the new tubes. 15 µl of protein samples were added into 384-well white, white bottom microplate (Greiner), prefilled with 15 µl of PBS. 30 µl Nano-Glo HiBiT Lytic Detection (Promega) working solution was added and the plate was incubated for 30 min at room temperature with shaking. The luminescence was measured on Envision and the signal was normalized to the protein concentration of corresponding samples detected with DC protein assay. The relative luminescence was calculated as a fold increase relative to non-transfected control cells. Cells transfected with gRNA1 possessed the highest reporter signal and was therefore used to generate single cell clones (Supplementary Fig. 4-1A).

Generation of monoclonal cell line expressing endogenous SSPN with a HiBiT tag

After a 24 hr incubation, electroporated cells were detached, counted, pelleted down as described above and resuspended in cell sorting buffer (1X PBS (Ca/Mg-free), 1 mM EDTA, 25 mM HEPES pH 7, 1% HI-FBS) to reach a final concentration of 0.5 x 10^{6} cells/ml. To label dead cells DAPI (Fisher Scientific) was added to reach a final concentration of 3 µM and incubated for 5 min. Cells were selected as DAPI-negative and RNP positive using FACSAria (BD) and plated using the Automated Cell Deposition Unit (BD) 96-well plate containing C2C12 growth media

(DMEM with 20% FBS). The cells were monitored for 6 weeks and observed for colony formation. Cells from each colony were detached and transferred into 96 and 6-well plates. Upon reaching confluency, the growth media was replaced with differentiation media consisting of DMEM with 2% horse serum (Sigma-Aldrich). At day 4 of differentiation, cells were washed with PBS twice and assayed using the Nano-Glo HiBiT Lytic Detection System (Promega) according to the manufacturer's protocol. After addition of the assay reagent, the cells were incubated for 30 min at room temperature with shaking and transferred to a white 384-well microplate (Greiner) for signal detection. Luminescence was measured using the EnVision plate reader (PerkinElmer) to determine HiBiT-positive clones. Only nine clones developed chemiluminescent signal and were expanded into separate monoclonal cell lines and subjected to detailed analysis.

Confirmation of HiBiT insertion into the SSPN loci

DNA from the nine monoclonal lines was isolated using a genomic DNA isolation kit (Thermo Fisher Scientific). PCR analysis of the clones using MyTaq Mix (Bioline) and primers that anneal to the HiBiT coding sequence and exon 1 of SSPN demonstrate presence of SSPN-HiBiT product in clone 3, but not wild-type C2C12 cells (CTRL) (Supplementary Table 4-2; Supplementary Fig. 4-1B). PCR was also performed using primers generated to target start codon and exon 1 of SSPN and demonstrate the presence of WT SSPN product in CTRL cells, but not clone 3 (Supplementary Fig. 4-1C). After 4 days of differentiation, robust luciferase activity was detected in the SSPN-HiBiT C2C12 clone 3, indicating expression of the SSPN-HiBiT fusion protein. To determine the size of the fusion protein, cell lysates from CTRL and clone 3 were electrophoresed on an SDS-PAGE gel and incubated in NanoGlo blotting assay (Promega) substrate to develop

luminescence signal from SSPN-HiBiT or subjected to immunoblotting. Luminescence signal in clone 3 indicates that the SSPN-HiBiT fusion protein is present, active, and detected at the correct size (23 kDa) (Supplementary Fig. 4-1E, top membrane). Immunoblotting for SSPN and GAPDH as previously described confirmed the presence of SSPN protein in CTRL and clone 3 (middle membrane).[19] GAPDH is shown as a loading control (bottom membrane).

12-well plate format C2C12 SSPN-HiBiT assay

C2C12 SSPN-HiBiT myoblasts were seeded at 25,000 cells per well in 2 ml of growth media in 12 well-plates and incubated for 3 days. Upon reaching confluency, the growth media was replaced with 2 ml of differentiation media. At day 2 of differentiation, the media on the cells was replaced with 2 ml of differentiation media containing compounds at a final concentration of 5.5 µM in 0.06% DMSO. For vehicle control-treated cells, 0.06% DMSO was added to the cells. After 48 hrs the cells were washed with PBS and frozen for 2-24 hrs. The plates containing cells were thawed on ice and 100 µl of ice-cold modified RIPA buffer containing 1% Triton X-100, 0.05% DOC, 0.05% SDS, and Halt Protease Inhibitor was added to each well. Cells were scratched, transferred into 1.5 ml tubes, and centrifuged for 20 min at 16,000 x g at 4^{o} C. The cell lysates were transferred into new tubes. DC assay was performed on cell lysates to determine protein concentration. White walled, white bottom 384-well microplates (Greiner) were prefilled with 15 µl of PBS and 15 µl of cell lysates were added to each well in triplicate. Then 30 µl Nano-Glo HiBiT Lytic Detection working solution was added to each well and incubated for 30 min at RT with shaking. The luminescence was measured on the EnVision plate reader and the signal was normalized to protein concentration and signal from vehicle-treated controls.

384-well microplate format C2C12 SSPN-HiBiT assay

C2C12 SSPN-HiBiT myoblasts were seeded at 500 cells per well in 50 µl of growth media in 384-well white, clear bottom microplates (Greiner) and incubated for 3 days. Upon reaching confluency, the growth media was replaced with 50 µl of differentiation media consisting of phenol-red free DMEM with 2% horse serum (Sigma-Aldrich) using an EL406 combination washer dispenser (Biotek). At day 2 of differentiation, the media on the cells was aspirated, left with a residual volume of 10 µl, and replaced with 30 µl of fresh differentiation media. 0.5 µl of small molecule in DMSO or DMSO alone (for vehicle and positive control wells) were added to each well using a Biomek Fx (Beckman). To ensure proper mixing of the DMSO, 50 µl of additional differentiation media was added to all wells except the positive control treated wells. The final concentration of compound in each treated well was 0.5-10 µM in 0.55% DMSO and 0.55% DMSO only for vehicle. After 48 hrs of incubation, the plate was washed with phenol red-free DMEM, aspirated, and left with a residual volume of 5 µl using EL406 combination washer dispenser. After the wash, 25 µl of differentiation media containing 12 µM DRAQ5 nuclear stain was added to reach a final concentration 10 µM in each well and incubated for 15 min at 37°C with 5% CO_2. The cells were imaged using ImageXpress Micro Confocal High Content Imaging System (Molecular Devices). The nuclei count of imaged cells were determined using a custom module analysis in MetaXpress Analysis software (Molecular Devices). After imaging and analysis, the plate was aspirated, left with a residual volume of 5 µl and placed at -80°C for 2 -24 hrs. The plate was thawed at RT and 25 µl of PBS was added, followed by 30 µl of Nano-Glo HiBiT Lytic Detection working solution prepared according manufacturer recommendations. Luminescence was measured using the EnVision plate reader and the signal of each well was normalized to nuclei count and signal from vehicle-treated controls.

Cell culture

C2C12 cells (American Type Culture Collection) were grown at 37°C with 5% CO_2 in growth media containing DMEM (Gibco) with 20% FBS (Sigma-Aldrich). Upon reaching 90-100% confluency, myoblasts were induced to differentiate by replacing the media with differentiation media consisting of DMEM with 2% horse serum (Sigma-Aldrich). Conditionally immortalized H2K *mdx* myoblasts with a nonsense mutation in exon 23 of dystrophin were a gift from Terrance Partridge, Ph.D. (Children's National Medical Center, Washington, D.C.) [77]. Myoblasts were allowed to proliferate on 0.01% gelatin (Sigma-Aldrich) coated plates at 33°C with 5% CO_2 with growth media containing DMEM, 20% HI-FBS (Invitrogen), 2% L-glutamine (Sigma-Aldrich), 2% chicken embryo extract (Accurate Chemical), 1% penicillin-streptomycin (Sigma-Aldrich), and 20 U/ml of fresh interferon gamma (Gibco). For differentiation, H2K myoblasts were seeded on plates coated with 0.1 mg/ml matrigel (Corning) diluted in DMEM and grown in proliferation conditions. Upon reaching 90-100% confluency, cells were grown at 37°C with 5% CO_2 in differentiation media containing DMEM with 5% horse serum (Sigma-Aldrich), 2% L-glutamine, and 1% penicillin-streptomycin using established protocols.[77] The immortalized human DMD myoblast cell line was grown in Skeletal Muscle Basal Medium (Promocell) containing 20% FBS (Fisher Scientific), Skeletal Muscle Growth Supplement Mix (Promocell), and 1% penicillin-streptomycin at 37°C with 5% CO_2.[82] Upon, reaching 100% confluency, the media was replaced with differentiation media containing Skeletal Muscle Basal Medium, Skeletal Muscle Differentiation Supplement Mix (Promocell), and 1% penicillin-streptomycin.

Compounds

Compounds were designed in house and analyzed *in silico* using StarDrop (Optibrium) for predictions of chemical properties. Synthesis was conducted by the Drug Discovery Lab and Volochem Inc. Structure and purity were confirmed by LC-MS.

Human sarcospan ELISA

DMD myotubes were lysed in modified RIPA buffer containing 1% Triton X-100, 0.05% DOC, 0.05% SDS, and Halt Protease Inhibitor and subjected to 3 rounds of sonication. The lysate was centrifuged at 12000xg for 10 min and the supernatant transferred to new tubes. Protein concentration was determined using DC assay. After measurement of protein concentration, 10mM DTT was added to the samples. A 96-well Nunc MaxiSorp plate (Invitrogen) was coated with 100 µl of 1 µg/ml SSPN antibody (sc-393187, Santa Cruz Biotechnology) per well overnight at 4°C. washed three times with 1X TBS containing 0.05% Tween-20, blocked for 1 hour at RT in 1% BSA in 1X TBS, and washed again. 100 µl of recombinant human SSPN standards (Novus Biologicals) and lysates were added to plate, incubated overnight at 4°C, and washed. 100 µl of 400 ng/ml SSPN antibody (Life Span Biosciences, LS-C747357) was added to each well and incubated for 2 hours at RT and washed. 100 µl of Goat Anti-Rabbit IgG HRP (Abcam, 1:10,000) was added to each well, incubated for 1 hour at RT, and washed. 100 µl of TMB substrate (Fisher Scientific) was added to each well. After signal development, 100 µl of stop solution was added to each well and the plate was measured using a plate reader set to 450 nm. For analysis, protein concentrations of samples were calculated using the standard curve, results were normalized to protein concentration and vehicle-treated controls.

Gene expression analysis

RNA from myotubes treated for 48 hrs was extracted from cells using Trizol-based (Thermo Fisher Scientific) phase separation, as previously described.[76] RNA concentrations were determined using a NanoDrop 1000 (Thermo Fisher Scientific) and 750 ng of RNA in a 20 µl reaction was reverse transcribed using iScript cDNA synthesis (Bio-Rad) with the following cycling conditions: 25°C for 5 mins, 42°C for 30 mins, 85°C for 5 mins. For mouse qPCR, SsoFast EvaGreen Supermix (Bio-Rad), 400 nM of each optimized forward and reverse primer (SSPN F: 5' TGCTAGTCAGAGATACTCCGTTC 3', SSPN R: 5' GTCCTCTCGTCAACTTGGTATG 3', BACT F: 5' GAGCACCCTGTGCTGCTCACCG 3', BACT R: 5' CAATGCCTGTGGTACGACCA 3'), and cDNA corresponding to 37.5 ng RNA were used to amplify cDNA measured by QuantStudio 5 Real-Time PCR System (Thermo Fisher Scientific) with the following reaction conditions: 55°C for 2 mins, 95°C for 2 mins, 40 cycles of 95°C for 10 seconds and 62°C for 30 seconds, and dissociation stage. Each sample was run in triplicate. Data was analyzed using the ddCT method and normalized to reference gene ACTB with vehicle-treated samples serving as the calibrator (relative expression of vehicle control = 1).

Solubility testing

To determine aqueous solubility, 9 mM of compounds dissolved in 100% DMSO was diluted in PBS to 50 µM and placed into HTS–PCF filter plate. The plate was rotated at 300 rpm for 90 min at room temperature. The filtrates were collected into a receiving plate and absorbance was read at 410 nm. The standards were generated using an 8 point serial dilution in DMSO starting at 50 µM.

Statistics

Robust strictly standardized mean difference (SSMD) was used to assess plate quality and for hit selection. SSMD* = $X_P - X_N/1.4826\sqrt{s_P^2 + s_N^2}$, where X_P, X_N, S_P, and S_N are the medians and median absolute deviations of the positive and negative controls, respectively.[68] For plate quality, SSMD* ≥ 1 indicates a good quality moderate positive control. For initial hit selection, a 1.4-fold increase over vehicle and SSMD* > 0.25 was considered a hit. Statistical analysis was performed using Prism version 7.0 (GraphPad Software) for Mac OS X using the two-tailed, non-parametric Kolmogorov-Smirnov test. Data are reported as mean ± SEM. A p-value of <0.05 was considered statistically significant. * p<0.05, ** p<0.01, *** p<0.001, **** p<0.0001.

Author Contributions

C.S. wrote manuscript and consulted on SSPN-HiBiT reporter assay design, assisted with cell line creation, and performed cell culture. L.P. created and conducted SSPN-HiBiT reporter cell line and assay. L.P. and E.M. created and performed SSPN ELISA. J.R.C. assisted with cell line creation. V.J., J.C., and B.J. designed and synthesized all analogues. R.H.C. conceived of the project and consulted on all experiments, data analysis, figures, and manuscript drafting.

Acknowledgments

Support for this work was provided by the Muscle Cell Biology, Pathogenesis, and Therapeutics Training Grant (NIH T32 AR065972), Pilot and Feasibility Seed Grant program (NIH/NIAMS P30 AR057230), UCLA Department of Integrative Biology & Physiology Eureka Scholarship, Muscular Dystrophy Association (MDA 274143; Venture Philanthropy Program), NIH NIAMS (R01 AR048179), and NIH NHLBI (R01 HL126204).

Supplementary Figures

Supplementary Table 4-1. Sequences of Alt-R CRISPR RNA used in the development of the SSPN-HiBiT C2C12 cell line.

Alt-R CRISPR RNA	Sequence (5' → 3')	On-target Score	Off target score
SSPN gRNA1	AGGCACCACCGAGGGAACAT	71	73
SSPN gRNA2	CCAGGCGCAGGCACCACCGA	38	73
SSPN gRNA3	GGCACCACCGAGGGAACATG	68	49
SSPN gRNA4	CAGGCACCACCGAGGGAACA	59	39

Supplementary Table 4-2. Primers used to confirm presence of HiBiT insert into the 5' sarcospan locus.

Primer	Sequence (5' → 3')	Location	Amplicon length
SSPN-HiBiT F	TGGCGGCTGTTCAAGAAGAT	HiBiT-exon 1	504 BP
SSPN-HiBiT R	GGTGGGCCTGCAGTTATCTT	exon 1	
WT SSPN F	GGGAACATGGGGCGCAAG	promotor-exon1	495 BP
WT SSPN R	GAGACAAGGACCAAGCCACA	exon 1	

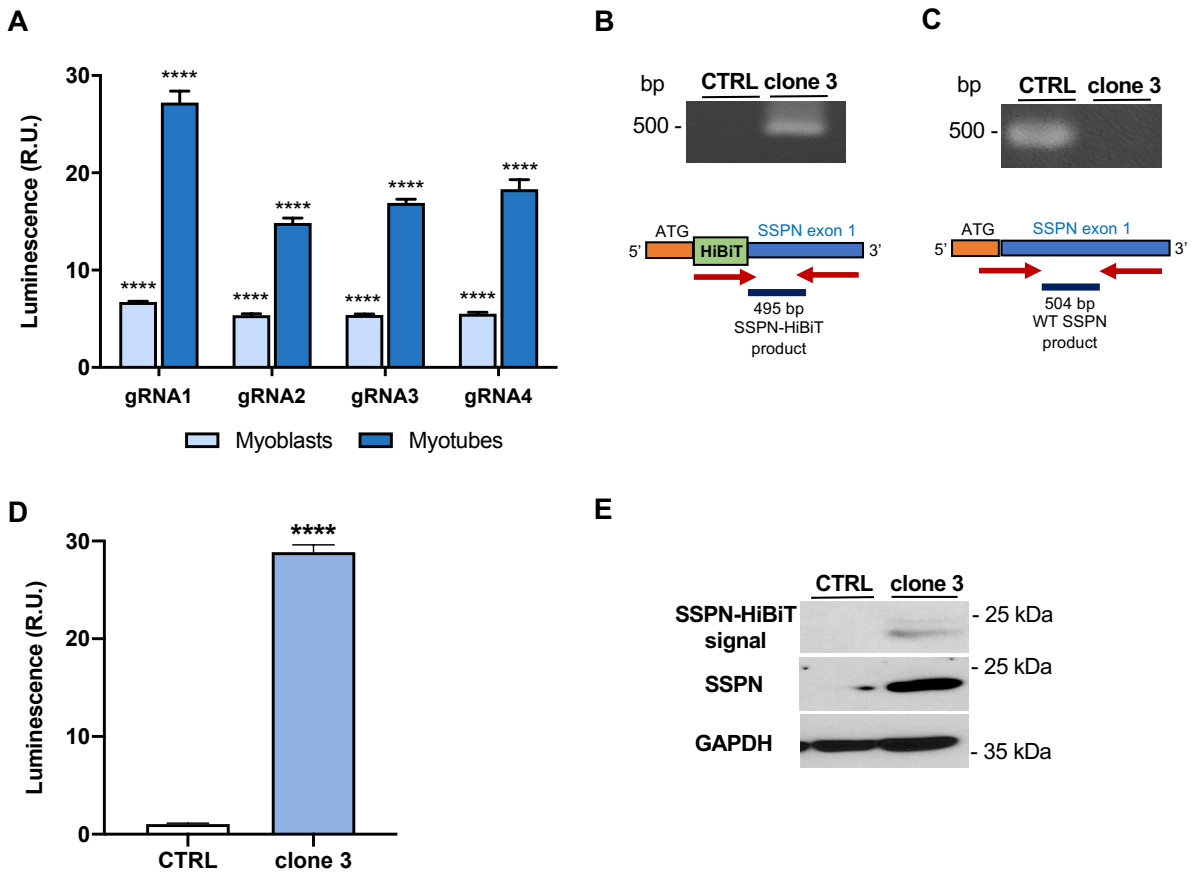

Supplementary Figure 4-1. Generation of monoclonal C2C12 cell line containing HiBiT reporter sequence in the endogenous sarcospan loci. (A) C2C12 myoblasts were transfected with RNP complexes containing one of four guide RNAs (gRNA1-4) and donor ssDNA containing the coding sequence for HiBiT. Transfected myoblasts and myotubes were harvested and assayed for SSPN-HiBiT activity. In all samples, myotubes expressed higher levels of SSPN-HiBiT than myoblasts. gRNA1 produced the most robust luminescence signal and was subjected to signal cell cloning. The luminescence was calculated as the fold change relative to non-transfected control cells. n=3. (B) Evaluation of clone 3 with PCR analysis using primers that anneal to the HiBiT coding sequence and exon 1 of SSPN demonstrate presence of SSPN-HiBiT product in clone 3, but not wild-type C2C12 cells (CTRL). (C) PCR analysis using primers that anneal to the start codon and exon 1 of SSPN demonstrate presence of WT SSPN product in CTRL cells, but not clone 3. (D) After 4 days of differentiation, robust luciferase activity was detected in SSPN-HiBiT C2C12 clone 3. (E) Cell lysates from CTRL and the clone 3 were electrophoresed on an SDS-PAGE gel and incubated in substrate to develop luminescence signal from SSPN-HiBiT or subjected to immunoblotting. Luminescence signal in the clone 3 indicates that the SSPN-HiBiT fusion protein is present, active, and detected at the correct size (23 kDa) (top membrane). Immunoblotting for SSPN confirms the presence of SSPN protein in CTRL and clone 3 (middle membrane). GAPDH is shown as a loading control (bottom membrane). ****p<0.0001.

Supplementary Table 4-3. Summary of standard operating procedures for 12-well and 384-well SSPN-HiBiT reporter assays.

Day	12-well plate assay	384-well microplate assay
-3	Seed 25,000 SSPN-HiBiT cells/well in 12-well plate	Seed 500 SSPN-HiBiT cells/well in white 384-well microplate
0	Switch to differentiation media	Switch to differentiation media
2	Change media and add drugs or positive control	Change media and add drugs or positive control to reach 80 µL/well
4	• Wash cells with PBS • Freeze cells for 2 hours to facilitate cell lysis • Add 100 µL mRIPA buffer/well, lyse the cells • Pellet cell debris by centrifugation, transfer supernatant to new tubes • Apply protein lysates to chemiluminescence assay (Nano-Glo HiBiT Lytic Detection System) • Determine protein concentration using DC protein assay • Normalize chemiluminescence data to protein concentration and vehicle control	• Wash plate twice with phenol red-free DMEM • Add DRAQ5 nuclear stain in phenol red-free differentiation media, image with high-content imager, and run nuclear count analysis • Aspirate media, freeze plate for 2 hours to lyse cells and release SSPN-HiBiT protein • Lyse cells and check chemiluminescence using Nano-Glo HiBiT Lytic Detection System • Normalize data to nuclear count and vehicle control

Chapter 5: Conclusion

The potential and challenges of small molecule modalities for DMD

The pursuit of small molecules therapies for DMD has been the subject of both academic and private-sector interest since the early 2000s. High-throughput screening provides an opportunity for extensive assaying of compounds and has led to the successful development of Translarna for the treatment of DMD in the European Union. As with other modalities, one of the challenges in small molecule development is translating animal studies to clinical studies. Despite undergoing a decade of pre-clinical animal testing, the utrophin modulator Ezutromid failed to meet its phase II trial endpoints. Previously, phase I clinical trials to determine safety and tolerability of multiple doses were conducted on healthy and DMD patients and revealed the drug half-life to be 5 to 10 hours.[83-85] Interestingly, after 11 days of treatment, Ezutromid levels decreased by 56% to 65%, while metabolite levels increased, indicating a shift in the endogenous metabolism of Ezutromid. A subsequent study found hepatic clearance by cytochrome P450 1A (CYP1A) as the main source of Ezutromid metabolism.[86] In rat and mini-pig studies, repeated oral administration of Ezutromid increased biomarkers of CYP1A induction. The metabolites were determined to be less potent than Ezutromid when tested *in vitro*. The development of Ezutromid illustrates the ongoing challenges in the development of small molecule modalities and careful attention that must be paid to address the complex nature of hepatic metabolism during the process of absorption, distribution, metabolism, and elimination (ADME) testing.

Considerations for SSPN as a therapeutic target

Many questions remain about the practical application of SSPN as a therapy. Our preclinical work was performed on *mdx:*SSPN-Tg mice, which overexpress SSPN under control

of the alpha-actin promoter during embryonic development leading to prevention of muscle disease. Currently, it is unknown when SSPN therapies can be applied to prevent or delay disease progression. This question can be addressed through an inducible gene expression system or by testing OT-9 on mice at different stages of the disease. Another consideration is that the *mdx*:SSPN-Tg mice overexpress SSPN under control of the alpha-actin promoter, which is active in muscle and relatively inactive in other tissue types. Therefore, the effect of SSPN overexpression in other tissue types needs to be further investigated for potential detrimental off-target tissue effects. Previously, our group showed that a 3-fold overexpression of SSPN is necessary to induce a rescue effect in *mdx* mice. Although the work presented in this thesis shows that a 1.8-fold increase in SSPN by OT-9 improves membrane stability, it is unknown if this 3-fold minimum will translate to human studies.

Although there is extensive evidence that SSPN overexpression rescues *mdx* mice by increasing compensatory adhesion complexes, there remains a gap in our knowledge of other pathways and mechanisms that may contribute to the rescue effect. Current and future studies are focused on developing a deeper understanding of the pathways that contribute to SSPN-mediated rescue of DMD. This includes a multi-omics analysis of skeletal muscle from mice that overexpression transgenic SSPN and characterization of ECM properties that define and contribute to the rescue effect. We are also investigating the necessity of SSPN for utrophin and GALGT2-mediated rescue of DMD.

Prospective studies on small molecule modulators of SSPN

In this thesis, I describe the creation and validation of cell-based assays for the identification of SSPN modulators. High-throughput screening using the assays resulted in

identification of compounds capable of increasing SSPN expression in dystrophin-deficient murine and human myotubes. The lead compound, OT-9, is a promising candidate that increased cell surface associated α-dystroglycan and utrophin, members of laminin-binding adhesion complexes. Restoration of the critical cell-to-ECM connection is a well-documented approach to rescue muscle pathology in animal models. Using osmotic shock assays, we demonstrated that OT-9 increased the membrane stability of dystrophin-deficient murine and human myotubes, presumably by increasing sarcolemmal adhesion complexes. The full membrane stabilizing effect was dependent on SSPN, indicating that OT-9 indirectly/directly targets SSPN to confer protection to the membrane. The ability of OT-9 to improve membrane stability by increasing laminin-binding adhesion complexes is supported by our *in vivo* studies on *mdx*:SSPN-Tg mice, which demonstrated SSPN-mediated rescue through upregulation of compensatory adhesion complexes.[4, 5, 7]

Future studies will focus on target identification and continued structure activity relationship (SAR) analysis, which may provide insight needed to increase the specificity and potency of the OT-9 and its analogues. Using chemical proteomics, the target of the utrophin modulator Ezutromid was found to be the aryl hydrocarbon receptor.[50] This revealed a previously unknown pathway in utrophin modulation that can be exploited in the development of DMD therapies. Although the target of OT-9 is currently unknown, previous studies in our lab established that activation of the protein kinase B (Akt) pathway is necessary for rescue of *mdx* mice by SSPN.[7] Of the numerous predicted transcription factor binding motifs in the promoter of SSPN, the transcription factor Nkx2-5 was recently found to interact genetically with SSPN in murine cardiac development.[87] These studies provide insight into the potential targets of OT-9, which will be further investigated to improve upon the modulators identified in this thesis.

Through three iterations of SAR analysis, we determined structural moieties of the lead compounds that were necessary and beneficial to activity and solubility. In the first SAR analysis, we excluded the necessity of moieties that were potential liabilities due to hepatoxicity and stability. OT-9, the original compound identified in the screen, increased SSPN protein levels by 1.9-fold. OT-9, the analogue developed in this thesis work, was found to be more soluble and increased SSPN protein levels by 2.4-fold, bringing us closer to a more effective therapy. OT-9m is evidence that we can further improve upon the activity and properties of lead compounds. We will also pursue further characterization of OT-9m to assess functional and *in vivo* efficacy. Although OT-9 increased SSPN gene expression in muscles of dystrophin-deficient mice, further studies must be performed to understand the ADME, pharmacokinetics, pharmacodynamics, and efficacy of OT-9. In closing, the work presented in this thesis describes the identification and early development of an urgently needed treatment for DMD.

References

1. Kendall, G. C., Mokhonova, E. I., Moran, M., Sejbuk, N. E., Wang, D. W., Silva, O., Wang, R. T., Martinez, L., Lu, Q. L., Damoiseaux, R., et al. (2012). Dantrolene enhances antisense-mediated exon skipping in human and mouse models of Duchenne muscular dystrophy. Sci Transl Med. *4*, 164ra160.

2. Cabrera, P. V., Pang, M., Marshall, J. L., Kung, R., Nelson, S. F., Stalnaker, S. H., Wells, L., Crosbie-Watson, R. H., and Baum, L. G. (2012). High throughput screening for compounds that alter muscle cell glycosylation identifies new role for N-glycans in regulating sarcolemmal protein abundance and laminin binding. J Biol Chem. *287*, 22759-22770.

3. Sun, C., Choi, I. Y., Rovira Gonzalez, Y. I., Andersen, P., Talbot, C. C., Jr., Iyer, S. R., Lovering, R. M., Wagner, K. R., and Lee, G. (2020). Duchenne muscular dystrophy hiPSC-derived myoblast drug screen identifies compounds that ameliorate disease in mdx mice. JCI Insight.

4. Gibbs, E. M., Marshall, J. L., Ma, E., Nguyen, T. M., Hong, G., Lam, J. S., Spencer, M. J., and Crosbie-Watson, R. H. (2016). High levels of sarcospan are well tolerated and act as a sarcolemmal stabilizer to address skeletal muscle and pulmonary dysfunction in DMD. Hum Mol Genet. *25*, 5395-5406.

5. Peter, A. K., Marshall, J. L., and Crosbie, R. H. (2008). Sarcospan reduces dystrophic pathology: stabilization of the utrophin-glycoprotein complex. J Cell Biol. *183*, 419-427.

6. Parvatiyar, M. S., Marshall, J. L., Nguyen, R. T., Jordan, M. C., Richardson, V. A., Roos, K. P., and Crosbie-Watson, R. H. (2015). Sarcospan Regulates Cardiac Isoproterenol Response and Prevents Duchenne Muscular Dystrophy-Associated Cardiomyopathy. J Am Heart Assoc. *4*,

7. Marshall, J. L., Holmberg, J., Chou, E., Ocampo, A. C., Oh, J., Lee, J., Peter, A. K., Martin, P. T., and Crosbie-Watson, R. H. (2012). Sarcospan-dependent Akt activation is required for utrophin expression and muscle regeneration. J Cell Biol. *197*, 1009-1027.

8. Peter, A. K., Miller, G., and Crosbie, R. H. (2007). Disrupted mechanical stability of the dystrophin-glycoprotein complex causes severe muscular dystrophy in sarcospan transgenic mice. J Cell Sci. *120*, 996-1008.

9. Sarathy, A., Wuebbles, R. D., Fontelonga, T. M., Tarchione, A. R., Mathews Griner, L. A., Heredia, D. J., Nunes, A. M., Duan, S., Brewer, P. D., Van Ry, T., et al. (2017). SU9516 Increases alpha7beta1 Integrin and Ameliorates Disease Progression in the mdx Mouse Model of Duchenne Muscular Dystrophy. Mol Ther. *25*, 1395-1407.

10. Shahnoor, N., Siebers, E. M., Brown, K. J., and Lawlor, M. W. (2019). Pathological Issues in Dystrophinopathy in the Age of Genetic Therapies. Annu Rev Pathol. *14*, 105-126.

11. Pestronk, A. (2019). Neuromuscular Disease Center. neuromuscular.wustl.edu.

12. Welch, E. M., Barton, E. R., Zhuo, J., Tomizawa, Y., Friesen, W. J., Trifillis, P., Paushkin, S., Patel, M., Trotta, C. R., Hwang, S., et al. (2007). PTC124 targets genetic disorders caused by nonsense mutations. Nature. *447*, 87-91.

13. Lim, K. R., Maruyama, R., and Yokota, T. (2017). Eteplirsen in the treatment of Duchenne muscular dystrophy. Drug Des Devel Ther. *11*, 533-545.

14. Khan, N., Eliopoulos, H., Han, L., Kinane, T. B., Lowes, L. P., Mendell, J. R., Gordish-Dressman, H., Henricson, E. K., McDonald, C. M., Eteplirsen, I., et al. (2019). Eteplirsen Treatment Attenuates Respiratory Decline in Ambulatory and Non-Ambulatory Patients with Duchenne Muscular Dystrophy. J Neuromuscul Dis. *6*, 213-225.

15. Moxley, R. T., Pandya, S., Ciafaloni, E., Fox, D. J., and Campbell, K. (2010). Change in natural history of Duchenne muscular dystrophy with long-term corticosteroid treatment: implications for management. J Child Neurol. *25*, 1116-1129.

16. Marshall, J. L., Chou, E., Oh, J., Kwok, A., Burkin, D. J., and Crosbie-Watson, R. H. (2012). Dystrophin and utrophin expression require sarcospan: loss of α7 integrin exacerbates a newly discovered muscle phenotype in sarcospan-null mice. Hum Mol Genet. *21*, 4378-4393.

17. Frank, D. E., Schnell, F. J., Akana, C., El-Husayni, S. H., Desjardins, C. A., Morgan, J., Charleston, J. S., Sardone, V., Domingos, J., Dickson, G., et al. (2020). Increased dystrophin production with golodirsen in patients with Duchenne muscular dystrophy. Neurology.

18. Kawahara, G., and Kunkel, L. M. (2013). Zebrafish based small molecule screens for novel DMD drugs. Drug Discov Today Technol. *10*, e91-96.

19. Shu, C., Kaxon-Rupp, A. N., Collado, J. R., Damoiseaux, R., and Crosbie, R. H. (2019). Development of a high-throughput screen to identify small molecule enhancers of sarcospan for the treatment of Duchenne muscular dystrophy. Skelet Muscle. *9*, 32.

20. Tinsley, J. M., Fairclough, R. J., Storer, R., Wilkes, F. J., Potter, A. C., Squire, S. E., Powell, D. S., Cozzoli, A., Capogrosso, R. F., Lambert, A., et al. (2011). Daily treatment with SMTC1100, a novel small molecule utrophin upregulator, dramatically reduces the dystrophic symptoms in the mdx mouse. PLoS One. *6*, e19189.

21. Crosbie, R. H., Heighway, J., Venzke, D. P., Lee, J. C., and Campbell, K. P. (1997). Sarcospan, the 25-kDa transmembrane component of the dystrophin-glycoprotein complex. J Biol Chem. *272*, 31221-31224.

22. Péladeau, C., Adam, N., Bronicki, L. M., Coriati, A., Thabet, M., Al-Rewashdy, H., Vanstone, J., Mears, A., Renaud, J. M., Holcik, M., & Jasmin, B. J. . (2020). Identification of therapeutics that target eEF1A2 and upregulate utrophin A translation in dystrophic muscles. Nature communications. *11*, 1990.

23. Loro, E., Sengupta, K., Bogdanovich, S., Whig, K., Schultz, D. C., Huryn, D. M., and Khurana, T. S. (2020). High-throughput identification of post-transcriptional utrophin up-regulators for Duchenne muscle dystrophy (DMD) therapy. Sci Rep. *10*, 2132.

24. Ryder, S., Leadley, R. M., Armstrong, N., Westwood, M., de Kock, S., Butt, T., Jain, M., and Kleijnen, J. (2017). The burden, epidemiology, costs and treatment for Duchenne muscular dystrophy: an evidence review. Orphanet J Rare Dis. *12*, 79.

25. Nigro, G., Comi, L. I., Politano, L., and Bain, R. J. (1990). The incidence and evolution of cardiomyopathy in Duchenne muscular dystrophy. Int J Cardiol. *26*, 271-277.

26. Hoffman, E. P., Brown, R. H., and Kunkel, L. M. (1987). Dystrophin: the protein product of the Duchenne muscular dystrophy locus. Cell. *51*, 919-928.

27. Farup, J., Madaro, L., Puri, P. L., and Mikkelsen, U. R. (2015). Interactions between muscle stem cells, mesenchymal-derived cells and immune cells in muscle homeostasis, regeneration and disease. Cell Death Dis. *6*, e1830.

28. Kunkel, L. M., Monaco, A. P., Middlesworth, W., Ochs, H. D., and Latt, S. A. (1985). Specific cloning of DNA fragments absent from the DNA of a male patient with an X chromosome deletion. Proc Natl Acad Sci U S A. *82*, 4778-4782.

29. Campbell, K. P., and Kahl, S. D. (1989). Association of dystrophin and an integral membrane glycoprotein. Nature. *338*, 259-262.

30. Yoshida, M., and Ozawa, E. (1990). Glycoprotein complex anchoring dystrophin to sarcolemma. J Biochem. *108*, 748-752.

31. Petrof, B. J., Shrager, J. B., Stedman, H. H., Kelly, A. M., and Sweeney, H. L. (1993). Dystrophin protects the sarcolemma from stresses developed during muscle contraction. Proc Natl Acad Sci U S A. *90*, 3710-3714.

32. Ervasti, J. M. (2007). Dystrophin, its interactions with other proteins, and implications for muscular dystrophy. Biochim Biophys Acta. *1772*, 108-117.

33. Crosbie, R. H., Lebakken, C. S., Holt, K. H., Venzke, D. P., Straub, V., Lee, J. C., Grady, R. M., Chamberlain, J. S., Sanes, J. R., and Campbell, K. P. (1999). Membrane targeting and stabilization of sarcospan is mediated by the sarcoglycan subcomplex. J Cell Biol. *145*, 153-165.

34. Sandona, D., and Betto, R. (2009). Sarcoglycanopathies: molecular pathogenesis and therapeutic prospects. Expert Rev Mol Med. *11*, e28.

35. Song, W. K., Wang, W., Foster, R. F., Bielser, D. A., and Kaufman, S. J. (1992). H36-alpha 7 is a novel integrin alpha chain that is developmentally regulated during skeletal myogenesis. J Cell Biol. *117*, 643-657.

36. Tinsley, J. M., Blake, D. J., Roche, A., Fairbrother, U., Riss, J., Byth, B. C., Knight, A. E., Kendrick-Jones, J., Suthers, G. K., Love, D. R., et al. (1992). Primary structure of dystrophin-related protein. Nature. *360*, 591-593.

37. Tinsley, J., Deconinck, N., Fisher, R., Kahn, D., Phelps, S., Gillis, J. M., and Davies, K. (1998). Expression of full-length utrophin prevents muscular dystrophy in mdx mice. Nat Med. *4*, 1441-1444.

38. Takemitsu, M., Ishiura, S., Koga, R., Kamakura, K., Arahata, K., Nonaka, I., and Sugita, H. (1991). Dystrophin-related protein in the fetal and denervated skeletal muscles of normal and mdx mice. Biochem Biophys Res Commun. *180*, 1179-1186.

39. Helliwell, T. R., Man, N. T., Morris, G. E., and Davies, K. E. (1992). The dystrophin-related protein, utrophin, is expressed on the sarcolemma of regenerating human skeletal muscle fibres in dystrophies and inflammatory myopathies. Neuromuscul Disord. *2*, 177-184.

40. Hodges, B. L., Hayashi, Y. K., Nonaka, I., Wang, W., Arahata, K., and Kaufman, S. J. (1997). Altered expression of the alpha7beta1 integrin in human and murine muscular dystrophies. J Cell Sci. *110 (Pt 22)*, 2873-2881.

41. Burkin, D. J., Wallace, G. Q., Milner, D. J., Chaney, E. J., Mulligan, J. A., and Kaufman, S. J. (2005). Transgenic expression of {alpha}7{beta}1 integrin maintains muscle integrity, increases regenerative capacity, promotes hypertrophy, and reduces cardiomyopathy in dystrophic mice. Am J Pathol. *166*, 253-263.

42. Miller, G., Wang, E. L., Nassar, K. L., Peter, A. K., and Crosbie, R. H. (2007). Structural and functional analysis of the sarcoglycan-sarcospan subcomplex. Exp Cell Res. *313*, 639-651.

43. Marshall, J. L., Oh, J., Chou, E., Lee, J. A., Holmberg, J., Burkin, D. J., and Crosbie-Watson, R. H. (2015). Sarcospan integration into laminin-binding adhesion complexes that ameliorate muscular dystrophy requires utrophin and α7 integrin. Hum Mol Genet. *24*, 2011-2022.

44. Parvatiyar, M. S., Brownstein, A. J., Kanashiro-Takeuchi, R. M., Collado, J. R., Dieseldorff Jones, K. M., Gopal, J., Hammond, K. G., Marshall, J. L., Ferrel, A., Beedle, A. M., et al. (2019). Stabilization of the cardiac sarcolemma by sarcospan rescues DMD-associated cardiomyopathy. JCI Insight. *4*, e123855.

45. Mendell, J. R., Goemans, N., Lowes, L. P., Alfano, L. N., Berry, K., Shao, J., Kaye, E. M., Mercuri, E., and Network, E. S. G. a. T. F. D. I. (2016). Longitudinal effect of eteplirsen versus historical control on ambulation in Duchenne muscular dystrophy. Ann Neurol. *79*, 257-271.

46. Rodino-Klapac, L. (2019). Clinical Update: Micro-dystrophin Study-101. Sarepta Therapeutics.

47. Sun, C., Serra, C., Lee, G., and Wagner, K. R. (2020). Stem cell-based therapies for Duchenne muscular dystrophy. Exp Neurol. *323*, 113086.

48. Santos, R., Ursu, O., Gaulton, A., Bento, A. P., Donadi, R. S., Bologa, C. G., Karlsson, A., Al-Lazikani, B., Hersey, A., Oprea, T. I., et al. (2017). A comprehensive map of molecular drug targets. Nat Rev Drug Discov. *16*, 19-34.

49. Auld, D. S., Lovell, S., Thorne, N., Lea, W. A., Maloney, D. J., Shen, M., Rai, G., Battaile, K. P., Thomas, C. J., Simeonov, A., et al. (2010). Molecular basis for the high-affinity binding and stabilization of firefly luciferase by PTC124. Proc Natl Acad Sci U S A. *107*, 4878-4883.

50. Wilkinson, I. V. L., Perkins, K. J., Dugdale, H., Moir, L., Vuorinen, A., Chatzopoulou, M., Squire, S. E., Monecke, S., Lomow, A., Geese, M., et al. (2020). Chemical Proteomics and Phenotypic Profiling Identifies the Aryl Hydrocarbon Receptor as a Molecular Target of the Utrophin Modulator Ezutromid. Angew Chem Int Ed Engl. *59*, 2420-2428.

51. Guiraud, S., Squire, S. E., Edwards, B., Chen, H., Burns, D. T., Shah, N., Babbs, A., Davies, S. G., Wynne, G. M., Russell, A. J., et al. (2015). Second-generation compound for the modulation of utrophin in the therapy of DMD. Hum Mol Genet. *24*, 4212-4224.

52. Koeks, Z., Bladen, C. L., Salgado, D., van Zwet, E., Pogoryelova, O., McMacken, G., Monges, S., Foncuberta, M. E., Kekou, K., Kosma, K., et al. (2017). Clinical Outcomes in Duchenne Muscular Dystrophy: A Study of 5345 Patients from the TREAT-NMD DMD Global Database. J Neuromuscul Dis. *4*, 293-306.

53. Ervasti, J. M., Ohlendieck, K., Kahl, S. D., Gaver, M. G., and Campbell, K. P. (1990). Deficiency of a glycoprotein component of the dystrophin complex in dystrophic muscle. Nature. *345*, 315-319.

54. Ohlendieck, K., Ervasti, J. M., Matsumura, K., Kahl, S. D., Leveille, C. J., and Campbell, K. P. (1991). Dystrophin-related protein is localized to neuromuscular junctions of adult skeletal muscle. Neuron. *7*, 499-508.

55. Ervasti, J. M., Kahl, S. D., and Campbell, K. P. (1991). Purification of dystrophin from skeletal muscle. J Biol Chem. *266*, 9161-9165.

56. Bonilla, E., Samitt, C. E., Miranda, A. F., Hays, A. P., Salviati, G., DiMauro, S., Kunkel, L. M., Hoffman, E. P., and Rowland, L. P. (1988). Duchenne muscular dystrophy: deficiency of dystrophin at the muscle cell surface. Cell. *54*, 447-452.

57. Karpati, G., Carpenter, S., Morris, G. E., Davies, K. E., Guerin, C., and Holland, P. (1993). Localization and quantitation of the chromosome 6-encoded dystrophin-related protein in normal and pathological human muscle. J Neuropathol Exp Neurol. *52*, 119-128.

58. Burkin, D. J., and Kaufman, S. J. (1999). The alpha7beta1 integrin in muscle development and disease. Cell Tissue Res. *296*, 183-190.

59. Matsumura, K., Ervasti, J. M., Ohlendieck, K., Kahl, S. D., and Campbell, K. P. (1992). Association of dystrophin-related protein with dystrophin-associated proteins in mdx mouse muscle. Nature. *360*, 588-591.

60. Squire, S., Raymackers, J. M., Vandebrouck, C., Potter, A., Tinsley, J., Fisher, R., Gillis, J. M., and Davies, K. E. (2002). Prevention of pathology in mdx mice by expression of utrophin: analysis using an inducible transgenic expression system. Hum Mol Genet. *11*, 3333-3344.

61. Bao, Z. Z., Lakonishok, M., Kaufman, S., and Horwitz, A. F. (1993). Alpha 7 beta 1 integrin is a component of the myotendinous junction on skeletal muscle. J Cell Sci. *106 (Pt 2)*, 579-589.

62. Lebakken, C. S., Venzke, D. P., Hrstka, R. F., Consolino, C. M., Faulkner, J. A., Williamson, R. A., and Campbell, K. P. (2000). Sarcospan-deficient mice maintain normal muscle function. Mol Cell Biol. *20*, 1669-1677.

63. Marshall, J. L., and Crosbie-Watson, R. H. (2013). Sarcospan: a small protein with large potential for Duchenne muscular dystrophy. Skelet Muscle. *3*, 1.

64. Marshall, J. L., Kwok, Y., McMorran, B. J., Baum, L. G., and Crosbie-Watson, R. H. (2013). The potential of sarcospan in adhesion complex replacement therapeutics for the treatment of muscular dystrophy. FEBS J. *280*, 4210-4229.

65. Schnell, F., Donoghue, C., Dworzak, J., Charleston, J., Frank, D., Wilton, S., Lewis, S., Mendell, J., Rodino-Klapac, L., and Sahenk, Z. (2017). Development of a validated Western blot method for quantification of human dystrophin protein used in Phase II and III clinical trials of

eteplirsen for the treatment of Duchenne muscular dystrophy (DMD) (P5.105). Neurology. *88*, P5.105.

66. Dedieu, S., Dourdin, N., Dargelos, E., Poussard, S., Veschambre, P., Cottin, P., and Brustis, J. J. (2002). Calpain and myogenesis: development of a convenient cell culture model. Biol Cell. *94*, 65-76.

67. Rudnicki, M. A., Schnegelsberg, P. N., Stead, R. H., Braun, T., Arnold, H. H., and Jaenisch, R. (1993). MyoD or Myf-5 is required for the formation of skeletal muscle. Cell. *75*, 1351-1359.

68. Zhang, X. D. (2011). Illustration of SSMD, z score, SSMD*, z* score, and t statistic for hit selection in RNAi high-throughput screens. J Biomol Screen. *16*, 775-785.

69. Capote, J., DiFranco, M., and Vergara, J. L. (2010). Excitation-contraction coupling alterations in mdx and utrophin/dystrophin double knockout mice: a comparative study. Am J Physiol Cell Physiol. *298*, C1077-1086.

70. Vallejo-Illarramendi, A., Toral-Ojeda, I., Aldanondo, G., and López de Munain, A. (2014). Dysregulation of calcium homeostasis in muscular dystrophies. Expert Rev Mol Med. *16*, e16.

71. Arias-Calderón, M., Almarza, G., Díaz-Vegas, A., Contreras-Ferrat, A., Valladares, D., Casas, M., Toledo, H., Jaimovich, E., and Buvinic, S. (2016). Characterization of a multiprotein complex involved in excitation-transcription coupling of skeletal muscle. Skelet Muscle. *6*, 15.

72. Johnson, P. L., and Bhattacharya, S. K. (1993). Regulation of membrane-mediated chronic muscle degeneration in dystrophic hamsters by calcium-channel blockers: diltiazem, nifedipine and verapamil. J Neurol Sci. *115*, 76-90.

73. Altamirano, F., Valladares, D., Henríquez-Olguín, C., Casas, M., López, J. R., Allen, P. D., and Jaimovich, E. (2013). Nifedipine treatment reduces resting calcium concentration, oxidative and apoptotic gene expression, and improves muscle function in dystrophic mdx mice. PLoS One. *8*, e81222.

74. Phillips, M. F., and Quinlivan, R. (2008). Calcium antagonists for Duchenne muscular dystrophy. Cochrane Database Syst Rev. CD004571.

75. Leyva-Leyva, M., Sandoval, A., Felix, R., and González-Ramírez, R., Biochemical and Functional Interplay Between Ion Channelsand the Components of the Dystrophin-Associated Glycoprotein Complex The Journal of Membrane Biology: Vol. 252, pp 1-16.

76. Chomczynski, P. (1993). A reagent for the single-step simultaneous isolation of RNA, DNA and proteins from cell and tissue samples. Biotechniques. *15*, 532-534, 536-537.

77. Morgan, J. E., Beauchamp, J. R., Pagel, C. N., Peckham, M., Ataliotis, P., Jat, P. S., Noble, M. D., Farmer, K., and Partridge, T. A. (1994). Myogenic cell lines derived from transgenic mice carrying a thermolabile T antigen: a model system for the derivation of tissue-specific and mutation-specific cell lines. Dev Biol. *162*, 486-498.

78. Schneider, C. A., Rasband, W. S., and Eliceiri, K. W. (2012). NIH Image to ImageJ: 25 years of image analysis. Nat Methods. *9*, 671-675.

79. Teijeira, S., Teijeiro, A., Fernández, R., and Navarro, C. (1998). Subsarcolemmal expression of utrophin in neuromuscular disorders: an immunohistochemical study of 80 cases. Acta Neuropathol. *96*, 481-486.

80. Damoiseaux, R. (2014). UCLA's Molecular Screening Shared Resource: enhancing small molecule discovery with functional genomics and new technology. Comb Chem High Throughput Screen. *17*, 356-368.

81. Young, C. S., Hicks, M. R., Ermolova, N. V., Nakano, H., Jan, M., Younesi, S., Karumbayaram, S., Kumagai-Cresse, C., Wang, D., Zack, J. A., et al. (2016). A Single CRISPR-Cas9 Deletion Strategy that Targets the Majority of DMD Patients Restores Dystrophin Function in hiPSC-Derived Muscle Cells. Cell Stem Cell. *18*, 533-540.

82. Mamchaoui, K., Trollet, C., Bigot, A., Negroni, E., Chaouch, S., Wolff, A., Kandalla, P. K., Marie, S., Di Santo, J., St Guily, J. L., et al. (2011). Immortalized pathological human myoblasts: towards a universal tool for the study of neuromuscular disorders. Skelet Muscle. *1*, 34.

83. Tinsley, J., Robinson, N., and Davies, K. E. (2015). Safety, tolerability, and pharmacokinetics of SMT C1100, a 2-arylbenzoxazole utrophin modulator, following single- and multiple-dose administration to healthy male adult volunteers. J Clin Pharmacol. *55*, 698-707.

84. Muntoni, F., Tejura, B., Spinty, S., Roper, H., Hughes, I., Layton, G., Davies, K. E., Harriman, S., and Tinsley, J. (2019). A Phase 1b Trial to Assess the Pharmacokinetics of Ezutromid in Pediatric Duchenne Muscular Dystrophy Patients on a Balanced Diet. Clin Pharmacol Drug Dev. *8*, 922-933.

85. Ricotti, V., Spinty, S., Roper, H., Hughes, I., Tejura, B., Robinson, N., Layton, G., Davies, K., Muntoni, F., and Tinsley, J. (2016). Safety, Tolerability, and Pharmacokinetics of SMT C1100, a 2-Arylbenzoxazole Utrophin Modulator, following Single- and Multiple-Dose Administration to Pediatric Patients with Duchenne Muscular Dystrophy. PLoS One. *11*, e0152840.

86. Chatzopoulou, M., Claridge, T. D. W., Davies, K. E., Davies, S. G., Elsey, D. J., Emer, E., Fletcher, A. M., Harriman, S., Robinson, N., Rowley, J. A., et al. (2020). Isolation, Structural Identification, Synthesis, and Pharmacological Profiling of 1,2-trans-Dihydro-1,2-diol Metabolites of the Utrophin Modulator Ezutromid. J Med Chem. *63*, 2547-2556.

87. Panzer, A. A., Regmi, S. D., Cormier, D., Danzo, M. T., Chen, I. D., Winston, J. B., Hutchinson, A. K., Salm, D., Schulkey, C. E., Cochran, R. S., et al. (2017). Nkx2-5 and Sarcospan genetically interact in the development of the muscular ventricular septum of the heart. Sci Rep. *7*, 46438.